

*Masters Directed Project*

*Final Report for IT 598*



# **Cyclic Potentiodynamic Survey of Medical Materials**

Submitted to the Department of Manufacturing & Construction Engineering Technology and Interior Design

College of Engineering, Technology and Computer Science

Purdue University Fort Wayne Campus

As partial fulfillment of the requirements for the

Degree of [Master of Science in Technology](#)

By

**Lawrence E. Kay**

December 2010

This Masters Directed Project is submitted to the College of Engineering Technology and Computer Science in partial fulfillment of the requirements for the degree of Master of Science in Technology, specialization Industrial Technology/Manufacturing.

**Committee Approval:**

Barry Dupen,  
M.S. Directed Project Chair

Signature:

Date:

\_\_\_\_\_

\_\_\_\_\_

Ramesh V. Narang

Signature:

Date:

\_\_\_\_\_

\_\_\_\_\_

Paul I. Lin

Signature:

Date:

\_\_\_\_\_

\_\_\_\_\_

## TABLE OF CONTENTS

LIST OF FIGURES .....	v
LIST OF TABLES .....	vii
NOMENCLATURE .....	viii
SYMBOLS .....	xiv
ABSTRACT .....	xvi
1 INTRODUCTION .....	1
1.1 Background .....	1
1.2 Gaps in Previous Knowledge .....	2
1.3 Implications/Significance of the Study.....	2
1.4 General Limitations and Assumptions .....	3
2 MATERIALS AND METHODS .....	3
2.1 Sample Design and Plan .....	3
2.2 Experimental Design .....	3
2.3 Sample Description .....	5
2.3.1 Stainless Steel .....	5
2.3.2 Cobalt Based Alloys .....	6
2.3.3 Nitinol Material Conditions .....	6
2.3.4 Titanium Alloys .....	7
2.3.5 DFT® Composite .....	7
2.3.6 Mechanical Properties Summary .....	8
2.4 Equipment and Setup .....	10
2.5 Test Procedure .....	11
3 RESULTS AND DISCUSSION .....	12
3.1 Summary of Main Findings .....	12
3.1.1 Individual Alloy Charts .....	12
3.1.1.1 302 Alloy Stainless Steel .....	13

3.1.1.2	304V Alloy Stainless Steel .....	16
3.1.1.3	316LVM Stainless Steel .....	18
3.1.1.4	420 Alloy Stainless Steel .....	20
3.1.1.5	Custom 455® Alloy Stainless Steel .....	22
3.1.1.6	Micro Melt® Biodur® Custom 470® Stainless Steel .....	24
3.1.1.7	FWM1058® Alloy .....	26
3.1.1.8	MP35N® Alloy .....	28
3.1.1.9	35N LT® Alloy .....	30
3.1.1.10	L605 Alloy .....	32
3.1.1.11	Nitinol Light Oxide Finish .....	34
3.1.1.12	Nitinol Dark Oxide Finish .....	36
3.1.1.13	Nitinol Etched Finish .....	39
3.1.1.14	Nitinol Etched, Polished Finish .....	42
3.1.1.15	Commercially Pure Titanium Grade 1 .....	45
3.1.1.16	Titanium 6Aluminum 4Vanadium ELI Alloy .....	47
3.1.1.17	35N LT®-DFT®-41Ag Composite – Masked .....	49
3.1.1.18	35N LT®-DFT®-41Ag Composite – Unmasked .....	51
3.2	Findings: Converging and Conflicting Evidence .....	54
3.3	Further Directions and Experiments .....	56
3.4	Discussion and Summary .....	56
3.5	Conclusions and Key Points .....	68
REFERENCES .....		73
ACKNOWLEDGEMENTS .....		75
APPENDICES .....		76
A.	Complete Data Table of Corrosion Measurements .....	76
B.	Wire Mechanical Properties (Imperial Units) .....	79
C.	Wire Mechanical Properties (SI Units) .....	81
D.	Nitinol Wire Mechanical Properties (Imperial Units).....	83
E.	Nitinol Wire Mechanical Properties (SI Units) .....	84

## LIST OF FIGURES

	Page
Figure 1. DFT Cross Section (ref image of 28% Ag core material) .....	8
Figure 2. Sample Preparation.....	10
Figure 3. Corrosion Cell .....	11
Figure 4. Cathodic and Anodic Polarization Plots cyclic potentiodynamic analysis .....	12
Figure 5. Alloy 302 As Drawn Surface .....	13
Figure 6. Alloy 302 Surface After Corrosion Test .....	13
Figure 7. Alloy 302 Cyclic Polarization Curve .....	14
Figure 8. Alloy 304V As Drawn Surface.....	16
Figure 9. Alloy 304V Surface After Corrosion Test.....	16
Figure 10. Alloy 304V Cyclic Polarization Curve.....	17
Figure 11. Alloy 316LVM As Drawn Surface.....	18
Figure 12. Alloy 316LVM Surface After Corrosion Test.....	18
Figure 13. Alloy 316LVM Cyclic Polarization Curve.....	19
Figure 14. Alloy 420 As Drawn Surface .....	20
Figure 15. Alloy 420 Surface After Corrosion Test .....	20
Figure 16. Alloy 420 Cyclic Polarization Curve .....	21
Figure 17. Custom 455® Alloy As Drawn Surface.....	22
Figure 18. Custom 455® Alloy Surface After Corrosion Test.....	22
Figure 19. Custom 455® Alloy Cyclic Polarization Curve.....	23
Figure 20. Micro Melt® Biodur® Custom 470® Alloy As Drawn Surface .....	24
Figure 21. Micro Melt® Biodur® Custom 470® Alloy Surface After Corrosion Test .....	24
Figure 22. Micro Melt® Biodur® Custom 470® Alloy Cyclic Polarization Curve .....	25
Figure 23. FWM1058® Alloy As Drawn Surface.....	26
Figure 24. FWM1058® Alloy Surface After Corrosion Test.....	26
Figure 25. FWM1058® Alloy Cyclic Polarization Curve.....	27
Figure 26. MP35N® Alloy As Drawn Surface.....	28
Figure 27. MP35N® Alloy Surface After Corrosion Test.....	28
Figure 28. MP35N® Alloy Cyclic Polarization Curve.....	29
Figure 29. 35N LT® Alloy As Drawn Surface.....	30
Figure 30. 35N LT® Alloy Surface After Corrosion Test.....	30
Figure 31. 35N LT® Alloy Cyclic Polarization Curve.....	31
Figure 32. L605 Alloy As Drawn Surface .....	32
Figure 33. L605 Alloy Surface After Corrosion Test.....	32
Figure 34. L605 Alloy Cyclic Polarization Curve .....	33
Figure 35. Nitinol Light Oxide As Drawn Surface.....	34
Figure 36. Nitinol Light Oxide Surface After Corrosion Test.....	34

Figure 37. Nitinol Light Oxide Cyclic Polarization Curve.....	35
Figure 38. Nitinol Dark Oxide As Drawn Surface .....	36
Figure 39. Nitinol Dark Oxide Surface After Corrosion Test .....	37
Figure 40. Nitinol Dark Oxide Cyclic Polarization Curve .....	37
Figure 41. Nitinol Etched As Drawn Surface .....	39
Figure 42. Nitinol Etched Surface After Corrosion Test .....	39
Figure 43. Nitinol Etched Cyclic Polarization Curve .....	40
Figure 44. Nitinol Etched, Mechanically Polished As Drawn Surface.....	42
Figure 45. Nitinol Etched, Mechanically Polished Surface After Corrosion Test.....	42
Figure 46. Nitinol Etched, Mechanically Polished Cyclic Polarization Curve.....	43
Figure 47. Commercially Pure Titanium Grade 1 As Drawn Surface .....	45
Figure 48. Commercially Pure Titanium Grade 1 Surface After Corrosion Test.....	45
Figure 49. Commercially Pure Titanium Grade 1 Cyclic Polarization Curve.....	46
Figure 50. Titanium 6Aluminum 4Vanadium ELI As Drawn Surface.....	47
Figure 51. Titanium 6Aluminum 4Vanadium ELI Surface After Corrosion Test.....	47
Figure 52. Titanium 6Aluminum 4Vanadium ELI Cyclic Polarization Curve.....	48
Figure 53. 35N LT® DFT®-41Ag Masked As Drawn Surface .....	49
Figure 54. 35N LT® DFT®-41Ag Masked Surface After Corrosion Test .....	50
Figure 55. 35N LT® DFT®-41Ag Masked Cyclic Polarization Curve .....	50
Figure 56. 35N LT® DFT®-41Ag Unmasked As Drawn Surface.....	51
Figure 57. 35N LT® DFT®-41Ag Unmasked Surface After Corrosion Test.....	52
Figure 58. 35N LT® DFT®-41Ag Unmasked Cyclic Polarization Curve.....	52
Figure 59. 35N LT® DFT®-41Ag Cut End PRIOR TO Corrosion Test .....	54
Figure 60. 35N LT® DFT®-41Ag Cut End AFTER Corrosion Test.....	55
Figure 61. 35N LT® DFT®-41Ag Combined (Masked and Unmasked) Cyclic Polarization Curve.....	55
Figure 62. Interval Plot of $E_r$ , Rest Potential .....	57
Figure 63. Interval Plot of Uniform Corrosion Rate .....	58
Figure 64. Interval Plot of $E_b$ , Breakdown Potential .....	59
Figure 65. Interval Plot of $E_p$ , Protection Potential .....	60
Figure 66. ASTM G82 Galvanic Series .....	62
Figure 67. Galvanic Series of Data Generated in this Study .....	64
Figure 68. Current Study $E_{corr}$ Series vs. ASTM G82 Galvanic Series .....	66
Figure 69. Interval Plot of $E_{corr}$ , Corrosion Potential.....	67
Figure 70. Interval Plot of $E_b$ - $E_r$ .....	70
Figure 71. Study $E_{corr}$ Series vs. Breakdown Potentials .....	72
Figure 72. Scatterplot of $E_{corr}$ vs $E_b$ .....	72

## LIST OF TABLES

	Page
Table 1. Corrosion Evaluation Criteria.....	4
Table 2. Stainless Steel Alloys.....	5
Table 3. Cobalt Alloys .....	6
Table 4. Nitinol Surface Conditions .....	7
Table 5. Titanium Alloys .....	7
Table 6. Wire Mechanical Properties.....	9
Table 7. Nitinol Wire Mechanical Properties .....	9
Table 8. Alloy 302 Cyclic Polarization Results.....	15
Table 9 Alloy 304V Cyclic Polarization Results.....	17
Table 10. Alloy 316LVM Cyclic Polarization Results.....	19
Table 11. Alloy 420 Cyclic Polarization Results.....	21
Table 12. Custom 455® Alloy Cyclic Polarization Results .....	23
Table 13. Micro Melt® Biodur® Custom 470® Alloy Cyclic Polarization Results.....	25
Table 14. FWM1058® Alloy Cyclic Polarization Results .....	27
Table 15. MP35N® Alloy Cyclic Polarization Results .....	29
Table 16. 35N LT® Alloy Cyclic Polarization Results.....	31
Table 17. L605 Alloy Cyclic Polarization Results .....	33
Table 18. Nitinol Light Oxide Cyclic Polarization Results .....	35
Table 19. Nitinol Dark Oxide Cyclic Polarization Results.....	38
Table 20. Nitinol Etched Cyclic Polarization Results .....	40
Table 21. Nitinol Etched, Mechanically Polished Cyclic Polarization Results.....	43
Table 22. Commercially Pure Titanium Grade 1 Cyclic Polarization Results .....	46
Table 23. Titanium 6Aluminum 4Vanadium ELI Cyclic Polarization Results.....	48
Table 24. 35N LT® DFT®-41Ag Masked Cyclic Polarization Results.....	51
Table 25. 35N LT® DFT®-41Ag Unmasked Cyclic Polarization Results .....	53
Table 26. Corrosion Potential, E <sub>corr</sub> , Results.....	63
Table 27. Evaluation of Breakdown Potential Results .....	68
Table 28. Evaluation of E <sub>b</sub> -E <sub>r</sub> .....	69
Table 29. Corrosion Testing Results Summary .....	71

## NOMENCLATURE<sup>1</sup>

**active**—negative direction of electrode potential. (Also used to describe corrosion and its associated potential range when an electrode potential is more negative than an adjacent depressed corrosion rate [passive] range.)

**anion**—negatively charged ion.

**anode**—electrode of an electrolytic cell at which oxidation is the principal reaction. (Electrons flow away from the anode in the external circuit. It is usually the electrode where corrosion occurs and metal ions enter solution.)

**anode corrosion efficiency**—ratio of the actual corrosion (weight loss) of an anode to the theoretical corrosion (weight loss) calculated by Faraday's law from the quantity of electricity that has passed.

**anodic inhibitor**—corrosion inhibitor whose primary action is to slow the kinetics of the anodic reaction, producing a positive shift in corrosion potential.

**anodic polarization**—change of the electrode potential in the noble (positive) direction due to current flow. (See **polarization**.)

**anodic protection**—technique to reduce the corrosion rate of a metal by polarizing it into its passive region where dissolution rates are low.

**breakdown potential**—least noble potential where pitting or crevice corrosion, or both, will initiate and propagate.

**cathode**—electrode of an electrolytic cell at which reduction is the principal reaction. (Electrons flow toward the cathode in the external circuit.)

---

<sup>1</sup> Nomenclature from [1], [19] and [28]



**cathodic protection**—technique to reduce the corrosion rate of a metal surface by making it the cathode of an electrochemical cell.

**cation**—positively charged ion.

**corrosion**—chemical or electrochemical reaction between a material, usually a metal, and its environment that produces a deterioration of the material and its properties.

**corrosion potential**—potential of a corroding surface in an electrolyte relative to a reference electrode measured under open-circuit conditions.

**corrosion rate**—amount of corrosion occurring in unit time. (For example, mass change per unit area per unit time; penetration per unit time.)

**counter electrode**—electrode in an electrochemical cell that is used to transfer current to or from a test electrode.

**coupon**—specimen, usually flat, but occasionally curved or cylindrical.

**critical anodic current density**—maximum anodic current density observed in the active region for a metal or alloy electrode that exhibits active-passive behavior in an environment.

**critical pitting potential**—least noble potential where pitting corrosion will initiate and propagate. (See breakdown potential.)

**current density**—electric current to or from a unit area of an electrode surface.

**current efficiency**—ratio of the electrochemical equivalent current density for a specific reaction to the total applied current density.

**electrochemical cell**—electrochemical system consisting of an anode and a cathode in metallic contact and immersed in an electrolyte. (The anode and cathode may be different metals or dissimilar areas on the same metal surface.)

**electrochemical potential (electrochemical tension)**—partial derivative of the total electrochemical free energy of the system with respect to the number of moles of the constituent in a solution when all other factors are constant. (Analogous to the chemical potential of the constituent except that it includes the electrical as well as the chemical contributions to the free energy.)

**electrode potential**—potential of an electrode in an electrolyte as measured against a reference electrode. (The electrode potential does not include any resistance losses in potential in either the solution or external circuit. It represents the reversible work to move a unit charge from the electrode surface through the solution to the reference electrode.)

**electrolysis**—production of chemical changes of the electrolyte by the passage of current through an electrochemical cell.

**Electromotive Force Series (EMF Series)**—list of elements arranged according to their standard electrode potentials, with “noble” metals such as gold being positive and “active” metals such as zinc being negative.

**equilibrium (reversible) potential**—potential of an electrode in an electrolytic solution when the forward rate of a given reaction is exactly equal to the reverse rate. (The equilibrium potential can only be defined with respect to a specific electrochemical reaction.)

**external circuit**—wires, connectors, measuring devices, current sources, and so forth, that are used to bring about or measure the desired electrical conditions within the test cell.

**galvanic corrosion**—accelerated corrosion of a metal because of an electrical contact with a more noble metal or nonmetallic conductor in a corrosive electrolyte.

**galvanic couple**—pair of dissimilar conductors, commonly metals, in electrical contact. (See **galvanic corrosion**.)

**galvanic current**—electric current between metals or conductive nonmetals in a galvanic couple.

**galvanic series**—list of metals and alloys arranged according to their relative corrosion potentials in a given environment.

**local corrosion cell**—electrochemical cell created on a metal surface because of a difference in potential between adjacent areas on that surface.

**localized corrosion**—corrosion at discrete sites, for example, pitting, crevice corrosion, and stress corrosion cracking

**mixed potential**—potential of a specimen (or specimens in a galvanic couple) when two or more electrochemical reactions are occurring simultaneously.

**noble**—positive (increasingly oxidizing) direction of electrode potential.

**noble metal**—metal with a standard electrode potential that is more noble (positive) than that of hydrogen.

**open-circuit potential**—potential of an electrode measured with respect to a reference electrode or another electrode when no current flows to or from it.

**oxidation**—loss of electrons by a constituent of a chemical reaction. (Also refers to the corrosion of a metal that is exposed to an oxidizing gas at elevated temperatures.)

**passivation**—process in metal corrosion by which metals become passive. (See **passive**.)

**passive**—state of the metal surface characterized by low corrosion rates in a potential region that is strongly oxidizing for the metal.

**patina**—corrosion product film, usually green, that forms on the surface of copper and copper alloys exposed to the atmosphere. (Also used to describe a weathered surface of any metal.)

**pitting**—corrosion of a metal surface, confined to a point or small area, that takes the form of cavities.

**polarization**—change from the open-circuit electrode potential as the result of the passage of current.

**potentiodynamic**—refers to a technique wherein the potential of an electrode with respect to a reference electrode is varied at a selected rate by application of a current through the electrolyte.

**potentiodynamic cyclic polarization (forward and reverse polarization)**—a technique in which the potential of the test specimen is controlled and the corrosion current measured by a potentiostat. The potential is scanned in the positive or noble (forward) direction as defined in Practice G 3. The potential scan is continued until a predetermined potential or current density is reached. Typically, the scan is run until the transpassive region is reached, and the specimen no longer demonstrates passivity, as defined in Practice G 3. The potential scan direction then is reversed until the specimen repassivates or the potential reaches a preset value.

**potentiostat**—instrument for automatically maintaining an electrode in an electrolyte at a constant potential or controlled potentials with respect to a suitable reference electrode.

**potentiostatic**—technique for maintaining a constant electrode potential.

**primary passive potential (passivation potential)**—potential corresponding to the maximum active current density (critical anodic current density) of an electrode that exhibits active-passive corrosion behavior.

**protection potential**—most noble potential where pitting and crevice corrosion will not propagate.

**reduction**—gain of electrons by a constituent of a chemical reaction.

**reference electrode**—electrode having a stable and reproducible potential, which is used in the measurement of other electrode potentials.

**rest potential**—See **open-circuit potential**.

**sample**—portion of material taken from a larger quantity and representative of the whole, to be used for test purposes.

**scan rate**—the rate at which the controlling voltage is changed.

**specimen**—prepared portion of a sample upon which a test is intended to be performed

**Tafel slope**—slope of the straight line portion of a polarization curve, usually occurring at more than 50 mV from the open-circuit potential, when presented in a semi-logarithmic plot in terms of volts per logarithmic cycle of current density (commonly referred to as volts per decade).

**transpassive region**—region of an anodic polarization curve, noble to and above the passive potential range, in which there is a significant increase in current density (increased metal dissolution) as the potential becomes more positive (noble).

**uniform corrosion**—corrosion that proceeds at about the same rate over a metal surface.

**working electrode**—test or specimen electrode in an electrochemical cell.

## SYMBOLS<sup>2</sup>

**AOD = Argon Oxygen Decarburization**—metal refining technique to reduce the carbon content to a desired level in the molten metal.

**EAF = Electric Arc Furnace**—a primary melting technique for steel and other metals.

**E<sub>b</sub> = Breakdown or Critical Pitting Potential**—the least noble potential at which pitting or crevice corrosion or both will initiate and propagate as defined in Terminology G 15. An increase in the resistance to pitting corrosion is associated with an increase in E<sub>b</sub>.

**E<sub>corr</sub> = Corrosion Potential**—the potential of a corroding surface in an electrolyte, relative to a reference electrode. Also called rest potential, open circuit potential, or freely corroding potential.

**E<sub>f</sub> = Final Potential**—a preset potential at which the scan is stopped.

**E<sub>i</sub> = Initial Potential**—the potential at which the potentiostat begins the controlled potentiodynamic scan.

**E<sub>p</sub> = Protection Potential**—the potential at which the reverse scan intersects the forward scan at a value that is less noble than E<sub>b</sub>. E<sub>p</sub> cannot be determined if there is no breakdown. Whereas, pitting will occur on a pit-free surface above E<sub>b</sub>, it will occur only in the range of potentials between E<sub>p</sub> and E<sub>b</sub> if the surface is already pitted. The severity of crevice corrosion susceptibility increases with increasing hysteresis of the polarization curve, the difference between E<sub>b</sub> and E<sub>p</sub>.

**E<sub>r</sub> = Rest Potential**—the potential of the working electrode relative to the reference electrode measured under virtual open-circuit conditions (working electrode is not polarized).

**E<sub>v</sub> = Vertex Potential**—a preset potential, at which the scan direction is reversed.

---

<sup>2</sup> Symbols from [1]

**Ezc = Zero Current Potential**—the potential at which the current reaches a minimum during the forward scan.

**Mpsi = one million pounds per square inch** ( $1 \times 10^6$  psi)-unit of pressure for Modulus.

**mpy = mils per year**-the unit of measure of uniform corrosion, where one mpy = 0.001” per year.

**mV = millivolt**-unit of electrical potential.

**psi = pounds per square inch**-unit of pressure for measurements of Ultimate Tensile Strength and Yield Strength.

**SCE = Saturated Calomel Electrode**-the reference electrode in the corrosion cell.

**VAR = Vacuum Arc Remelt**-a metal refining melting technique to remove impurities and non-metallic inclusions from the primary melt.

## ABSTRACT

The aim of this study is to provide a comprehensive examination of the electrochemical behavior of various biomedical materials in a common form with similar processing methods. Wire products comprising seventeen alloys and conditions at 0.762mm (0.030”) diameter have been tested per the ASTM International Standard F 2129 – Standard Test Method for Conducting Cyclic Potentiodynamic Polarization Measurements to Determine the Corrosion Susceptibility of Small Implant Devices. Tests were conducted in phosphate buffered saline solution at 37°C. Materials tested include: Alloy 302, Alloy 304V, Alloy 316LVM, Alloy 420, Custom 455<sup>3</sup>, MicroMelt® Biodur® Custom 470<sup>4</sup>, FWM1058<sup>5</sup>, MP35N<sup>6</sup>, 35N LT<sup>7</sup>, L-605, Nitinol (four surface finish conditions), Commercially Pure Titanium Grade 1 (Cp Ti Gr 1), Titanium 6 Aluminum 4 Vanadium (Ti-6Al-4V ELI), and the composite wire 35N LT®-DFT®-41Ag<sup>8</sup>. Comparative results, graphs, and tabular summaries are provided to serve as a reference for the medical device designer.

---

<sup>3</sup> Custom 455 is a registered trademark of CRS Holdings, Inc. a subsidiary of Carpenter Technology Corporation, Wilmington DE, USA

<sup>4</sup> MicroMelt, Biodur, and Custom 470 are registered trademarks of CRS Holdings, Inc. a subsidiary of Carpenter Technology Corporation, Wilmington DE, USA

<sup>5</sup> FWM1058 is a registered trademark of Fort Wayne Metals Research Products Corp., Fort Wayne, IN, USA

<sup>6</sup> MP35N is a registered trademark of SPS Technologies, Inc., Jenkintown, PA, USA

<sup>7</sup> 35N LT is a registered trademark of Fort Wayne Metals Research Products Corp., Fort Wayne, IN, USA

<sup>8</sup> DFT (Drawn Filled Tube) is a registered trademark of Fort Wayne Metals Research Products Corp., Fort Wayne, IN, USA



## 1. INTRODUCTION

### 1.1. Background

Corrosion properties of materials used in biomedical applications have been studied for years due to the aggressive in vivo environment. While many studies have looked at materials individually, no comprehensive study has been conducted and published in the format of the in vitro study techniques prescribed in ASTM F2129, Standard Test Method for Conducting Cyclic Potentiodynamic Polarization Measurements to Determine the Corrosion Susceptibility of Small Implant Devices [1].

Galvanic Series in Saltwater are well known and published in both ASTM G82 and Army Missile Command Report RS-TR-67-11 [2]. Clarke & Hickman, published a “Galvanic Series in Equine Serum” in J. Bone Joint Surg. [3].

Rosenbloom and Corbett [4] reviewed specific issues related to the test methodology of ASTM F2129. Clerc, Jedwab, Mayer, Thompson & Stinson conducted a study specifically examining the ASTM F1058 alloy [5]. Ornberg, Pan, Herstedt and Leygraf observed no significant difference in corrosion resistance between 35N LT® and MP35N® alloys, despite certain differences in their chemical composition [6]. Bruce Pound examined the corrosion response of Nitinol in phosphate buffered solution [7].

Nitinol is a shape memory material developed at the Naval Ordnance Laboratory. The Nickel-Titanium (NICKEL TITANIUM NAVAL ORDNANCE LABORATORY = NITINOL) binary alloy produces strain induced martensite under cold working conditions. At specific temperatures the martensitic transformation can be reversed, converting the material back to an austenitic phase. The material has gained in popularity in medical applications due to this ability to recover its original shape after undergoing up to 8 percent strain deformation. This allows for the

development of self-expanding stents and other medical devices. The material can also provide ‘whip free’ torque transfer which allows a doctor to accurately control a guide wire within the arterial system. Unfortunately, the material has had inconsistent corrosion performance. Perez, Gracia-Villa, Puertolas, Arruebo, Irusta and Santamaria [8] examined different passivation treatments to enhance the TiO<sub>2</sub> surface film to aid in corrosion resistance. Shabalovskaya reviewed the corrosion studies conducted on wrought Nitinol alloys commenting that, “Neither standard surface treatment procedures, nor standard surface regulations have been developed for Nitinol.” [9].

### 1.2. Gaps in Previous Knowledge

As previously noted, many studies of individual materials commonly used in medical applications have been completed; however, virtually no comprehensive series information under similar conditions in a body simulated fluid is available in the public record. One of the issues involved is the selection of the analysis fluid. The ASTM F2129 test method prescribes the use of phosphate buffered saline (PBS) as the standard test solution, but describes a total of seven possible solutions: three simulated physiological solutions (including PBS), two bile solutions and two urine formulations.

### 1.3. Implications/Significance of the Study

The results of this research will be useful to the medical device designer when selecting alloys for consideration. The data will also be included in Master Device Files of materials to be registered with the Food and Drug Administration (FDA) by Fort Wayne Metals Research Products Corp. This study will provide a comprehensive, single format, multiple alloy study of materials currently used in medical devices to allow the direct comparison of the results. The data will be compiled into a Galvanic Series format for use in the medical device industry.

#### 1.4. General Limitations and Assumptions

This study only examined material in the as-drawn condition. This should be considered an active surface. Passivation treatments were not applied to any of the materials, which could affect the cyclic potentiodynamic test results.

This study only used a single solution (phosphate buffered saline) as specified in ASTM F2129.

Each test consisted of a single metal alloy exposed to the electrolyte solution. Other than the Un-masked DFT, no examination of galvanic interactions in the corrosion cell were examined.

## 2. MATERIALS AND METHODS

### 2.1. Sample Design and Plan

All wires used in the study were produced by Fort Wayne Metals Research Products Corporation, Ft. Wayne, IN, USA. The wires are in the mechanically cold worked condition (strain hardened). Wire specimens were prepared using single crystal natural diamond dies in standard mineral oil based lubricant, or a sodium based powder lubricant followed by a hot alkaline cleaning step to remove the powder. The study used “Spring Temper” materials with cold work reductions ranging from 37% to 75%. Appendix A provides the complete mechanical properties of the samples

### 2.2. Experimental Design

A sample size of 5 was selected for this study as recommended by Corbett [10]. Although this is the recommended number of samples, the author does caution:

“How many replicates constitute acceptable confidence in the results depends on the number of variables, known and unknown that are integrated into the manufacture of the device. Ideally one wants to have a high confidence that a breakdown potential falls between a narrow range of potentials. In other words, it would be better to report that there is 95% confidence that the breakdown

potential is between +600 and +800 mV than to be 99% confident that it is between +200 and +900mV.”

Acceptance criteria for corrosion data have not been established either by the FDA or the ASTM International organization in any of the applicable standards. Corbett recommends the criteria in Table 1 to evaluate cyclic potentiodynamic tests [10].

*Table 1. Corrosion Evaluation Criteria*

Breakdown Potential, $E_b$ (mV vs SCE)	Corrosion Resistant Condition
> +600	Optimum
+300 to +600	Marginal
< +300	Not Optimum

Corbett suggests in his evaluation of various curves that if the data falls in the “Marginal” range that a large number of samples is needed for acceptance to increase the strength of the confidence interval, although no specific sample quantity is mentioned. He also recommends in addition to the absolute values of the Breakdown Potential, that the scatter of the  $E_r$  and  $E_b$  values be considered as part of the evaluation due to the wide range associated with the confidence intervals in this type of data set. For these reasons, an examination of the confidence intervals of the corrosion parameters is included in the summary data.

Corlett [11 p. 26] suggests that an examination of  $E_b$  and  $E_r$  individually are not adequate. He proposes the measure of  $E_b - E_r$  is a more accurate measure of pitting resistance. The larger this value, the greater the resistance to pitting corrosion. For those alloys that experience breakdown, this parameter is also evaluated.

## 2.3. Sample Description

### 2.3.1. Stainless Steels Alloys

Stainless steels, iron based alloys with greater than 10.5% Chromium, have been well accepted as medically relevant materials since 1926 [10] due to their improved corrosion resistance. The 302 and 304V alloys are common austenitic stainless steels, referred to as 18-8 grade of stainless steel (18 % nominal Chromium, 8% nickel nominal). The 302 alloy is a single melt, Electric Arc Furnace/Argon Oxygen Decarburization (EAF/AOD) material. The 304V alloy has an added Vacuum Arc Remelt (VAR) step to reduce metallurgical impurities. The 316LVM alloy was developed with a low carbon content and an addition of Molybdenum to improve pitting corrosion resistance [11, pp. 24,25]. The 400 series alloys are precipitation hardening materials made from chromium-nickel grades that can be hardened by an aging treatment and are often selected for suture needles [11, p. 25]. These alloys all develop an invisible and adherent chromium rich oxide layer on the surface. This oxide forms and heals itself in the presence of oxygen [11, p. 22]. The alloys studied are listed in various standards, particularly the ASTM F899, Standard Specification for Wrought Stainless Steels for Surgical Instruments. The alloys are listed with their major alloying elements in Table 2 [13] [14] [15].

*Table 2. Stainless Steel Alloys*

Grade	Spec	UNS	% C	%Cr	Alloying Elements
302	ASTM F899	S30200	.15 max	17-19	Ni Mn
304V	ASTM F899	S30400	.07 max	17-19	Ni Mn
316LVM	ASTM F138	S31673	.03 max	17-19	Ni Mo Mn
420	ASTM F899	S42000	.23-.27	12-14	
Custom 455® Micro-Melt®	ASTM A564	S45500	.03max	11-12.5	Ni Cu Ti
BioDur® Custom 470®	--	--	.02max	11-12.5	Ni Ti Mo

### 2.3.2. Cobalt Based Alloys

Cobalt based alloys were first developed for the aerospace industry due to their excellent corrosion resistance at high service temperature. Medical implant designers understood that the high level of corrosion resistance made them suitable materials for permanent implants, first employing them for orthopedic implants in the 1940's [11, p. 31]. The ASTM F1058 alloy was first developed as a corrosion resistant material for watch springs. The MP35N® alloy and 35N LT®, the low Titanium version developed by Fort Wayne Metals, are commonly used as pacemaker leads. L605 is used in both orthopedic applications and as a material for cardiovascular stents. The alloys are listed with their major alloying elements in Table 2 [16] [17] [18].

*Table 3. Cobalt Alloys*

Grade	Spec	UNS	% Co	Alloying Elements
FWM1058®	ASTM F1058	R30008	40.5	Cr Ni Fe Mo
MP35N®	ASTM F562	R30035	35	Ni Cr Mo
35N LT®	ASTM F562	R30035	35	Ni Cr Mo
L605	ASTM F90	R30605	20	W Ni

### 2.3.3. Nitinol Material Conditions

Nitinol wire materials are cold drawn with an oxide layer to provide a barrier between the 'sticky' surface of the material and the diamond dies. The oxide layer can be controlled by the temperature, dwell time, and oxygen content in the atmosphere during annealing operations. Two levels of oxide are commonly specified. Two methods of oxide removal are also offered. In both cases, the oxide surface is completely removed by chemical etching. A secondary surface condition is created by mechanically polishing the surface. The surface conditions are identified in Table 4 [19].

*Table 4. Nitinol Surface Conditions*

Nitinol Alloy	Spec	UNS	Surface Finish
Nitinol #1, Binary	ASTM F2063	--	Dark Oxide Light Oxide Etched Etched, Mechanically Polished

#### 2.3.4. Titanium Alloys

Titanium was originally selected as a medical alloy due to its low modulus and excellent biocompatibility. The material develops a stable oxide film that forms on its surface [11, p. 38]. The Commercially Pure (CP) Titanium Grade 1 has a low oxygen content, and the resulting ultimate tensile strength is also low. However, the material is often used as a permanent staple when closing an endoscopic procedure, as well as bone screws [11, pp. 38-41]. The stronger alloy, Ti 6Al 4V ELI, is a common choice for orthopedic implants. Table 5 lists these two materials and their alloying elements [20] [21].

*Table 5. Titanium Alloys*

Grade	Spec	UNS	Alloying Elements
CP Ti Gr 1	ASTM F67 Gr 1	R50250	O – 0.18% max
Ti 6Al 4V ELI	ASTM F136	R56401	Al V O

#### 2.3.5. DFT® Composite

DFT® (Drawn Filled Tube) is a composite material produced by Fort Wayne Metals. The mixture chosen for this test is an outer sheath of 35N LT® with an interior core of silver (Ag). The material has a silver fill ratio of 41% measured as the cross section area of the wire at the final diameter. Medical electrodes require high mechanical strength and fatigue resistance [11, p.

49]. DFT provides a sheath combining these requirements and a silver core providing high conductivity. The material is chosen as a lead material for Implantable Cardio Defibrillators (ICD's) due to its low resistance when transmitting a high voltage shock to an arrhythmic heart.

Figure 1 is a cross section of this material.

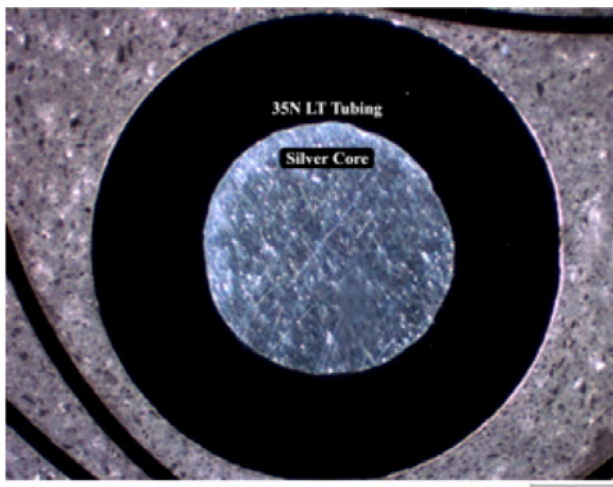


*Figure 1. DFT Cross Section (ref image of 28% Ag core material)*

The DFT was analyzed in two methods. The first technique masked the end of the wire in the electrolyte solution to eliminate any possible galvanic reaction between the two materials. The second method exposed both of the materials to the electrolyte. The results were examined to determine if any difference was observed.

#### 2.3.6. Mechanical Properties Summary

The following table summarizes the average mechanical properties of the wires tested. The average values are from n=3 sampling. The complete table of mechanical properties for these alloys is provided in Appendices A and B.



*Table 6. Wire Mechanical Properties*

Alloy	Ultimate Tensile Strength (psi)	Yield Strength (psi)	Elongation (%)	Modulus (Mpsi)
302	300,039	245,774	2.6	20.6612
304V	313,262	257,827	2.9	20.4022
316LVM	262,698	218,401	3.1	20.4054
420	153,349	139,098	3.3	20.9159
Custom 455®	207,611	187,979	2.9	21.0796
MicroMelt® Biodur® Custom 470®	217,978	201,069	2.4	20.0706
FWM 1058®	314,365	247,048	3.5	20.1297
35N LT®	305,307	261,942	2.9	22.2026
MP35N®	308,358	262,226	2.9	23.3831
L605	309,364	242,475	4.4	23.4040
CP Ti Gr1	110,005	85,638	5.5	11.5259
Ti-6Al-4V ELI	186,537	139,448	4.0	12.0532
35NLT®-DFT®-41%Ag	186,693	165,641	2.2	16.4829

The following table summarizes the average mechanical properties of the Nitinol wires tested. The average values are from n=3 sampling. The complete table of mechanical properties for these alloys is provided in Appendices C and D.

*Table 7. Nitinol Wire Mechanical Properties*

Alloy	Ultimate Tensile Strength (psi)	Upper Plateau Strength (psi)	Lower Plateau Strength (psi)	Elongation (%)	Modulus (Mpsi)
NiTi#1 Light Oxide	212,456	81,642	24,759	15.5	8.567
NiTi#1 Dark Oxide	219,644	83,492	27,004	16.2	7.002
NiTi#1 Etched	216,194	83,699	27,576	15.9	7.854
NiTi#1 Etched, Polished	220,599	82,138	25,138	16.2	7.526

## 2.4. Equipment and Setup

The corrosion test cell was a Gamry Model 992-73 Multiport Corrosion Cell. The cell contains three electrodes:

### **Reference Electrode**

The Reference Electrode is a saturated calomel electrode (SCE) supplied by Gamry. Model Number 930-03.

### **Counter Electrode**

The Counter electrode is a graphite electrode supplied by Gamry. Model Number 935-3.

### **Sample Electrode**

Samples were prepared with a .305mm (12 inch) piece of .762 mm (0.030") diameter wire within an 8 mm PTFE tube set with epoxy per Figure 2. Surface areas ranged from 1.71 cm<sup>2</sup> to 2.01 cm<sup>2</sup>.

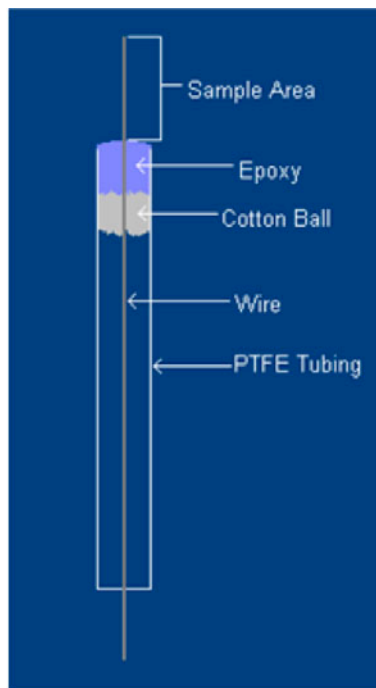


*Figure 2. Sample Preparation*

## 2.5. Test Procedure

Samples were cleaned for two minutes in Reverse Osmosis (RO) water with ultrasonic agitation. A water bath was used to heat the corrosion cell, see Figure 3, containing one liter of phosphate buffered saline, pH = 7.14 nominal, to 37°C +/-1°C. High purity nitrogen, 99.99% pure, was bubbled through the saline to eliminate oxygen in the corrosion cell at a rate of 150cm<sup>3</sup>/min. The system was purged for a minimum of one hour before a test began. A pretest pH measurement was recorded. The sample was placed in the cell. The open circuit potential (Er) was monitored for 1 hour. A potentiodynamic scan began in the positive or noble (forward) direction with an initial potential (Ei) at 100 mV negative or active to Er. The unit reverses the direction back to +1 V (vs Er) at a rate of 0.167 mV/s. Each wire type was tested five times.

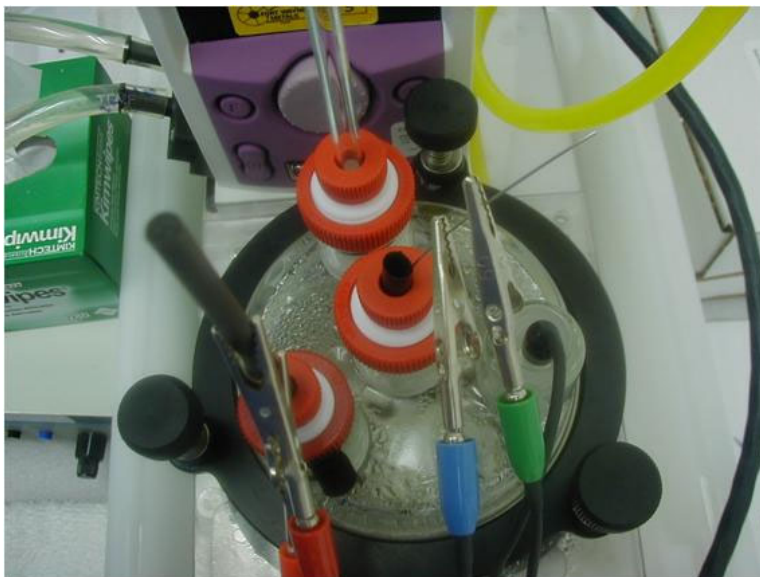


*Figure 3. Corrosion Cell*

The software controls the applied voltage between the sample and the reference electrode and measures the resulting current as the dependent variable. A plot similar to the one in Figure 4 [15] is produced. For this study, the primary value of interest is the E<sub>corr</sub>, Corrosion Potential, as

this is the value specified in ASTM G82 for the creation of a Galvanic Series. The  $E_{corr}$  corrosion potential value can additionally give a fundamental indication of the thermodynamic corrosion risk [16].

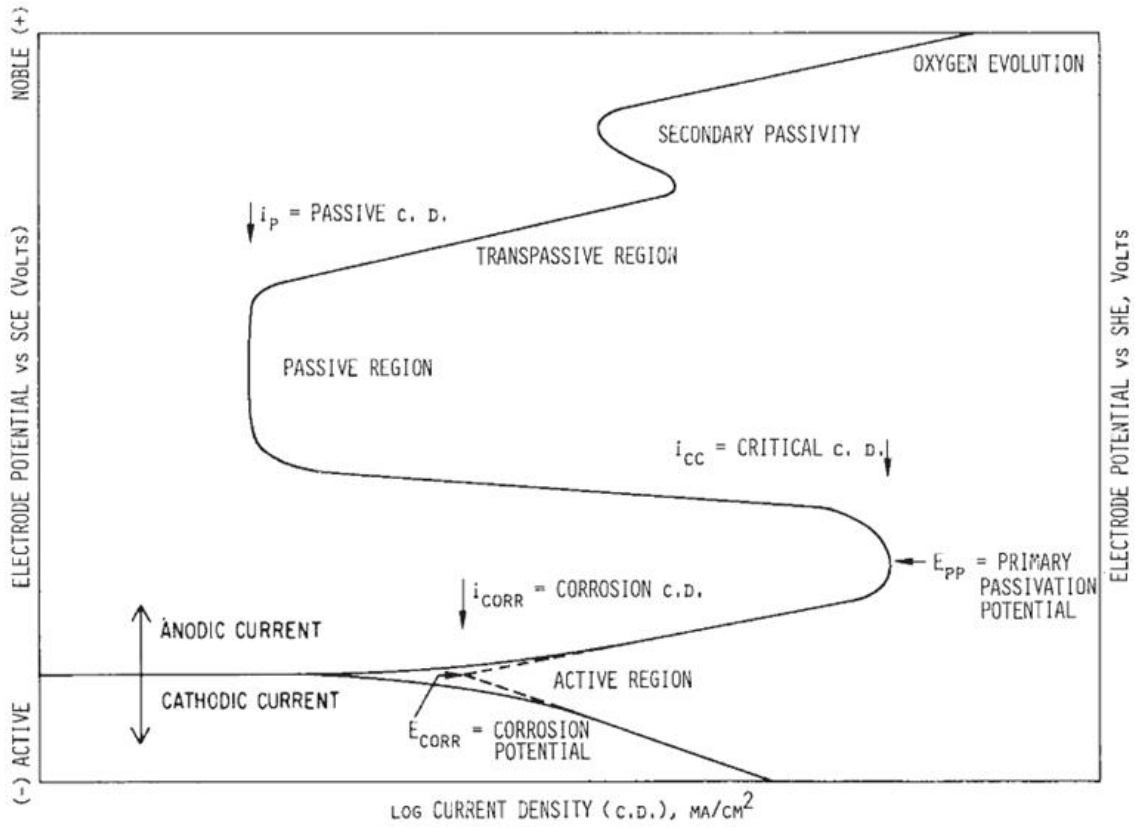


Figure 4. Cathodic and Anodic Polarization Plots cyclic potentiodynamic analysis

### 3. RESEARCH RESULTS

#### 3.1. Summary of Main Findings

##### 3.1.1. Individual Alloy Charts

### 3.1.1.1. Alloy 302 Results

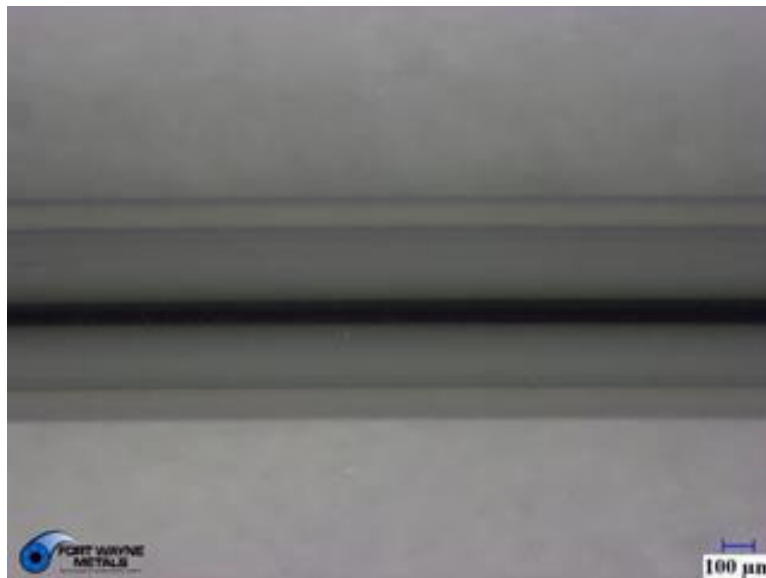


*Figure 5. Alloy 302 As Drawn Surface*

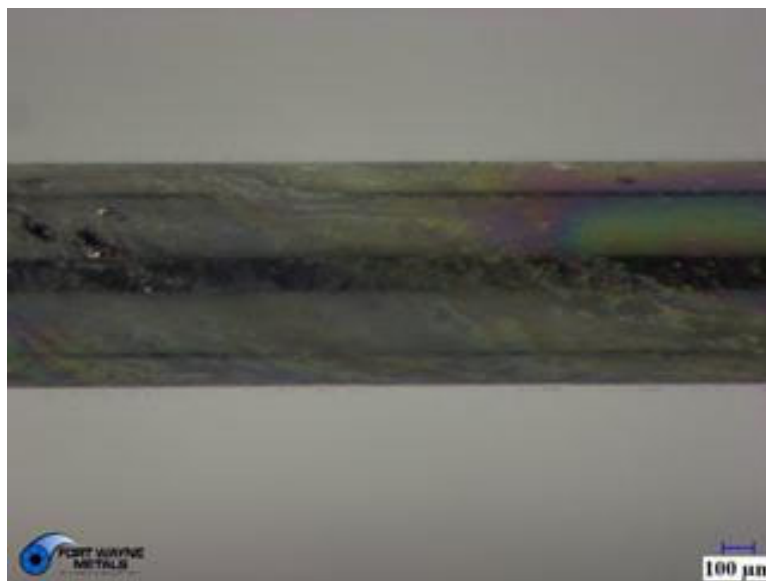


*Figure 6. Alloy 302 Surface After Corrosion Test*

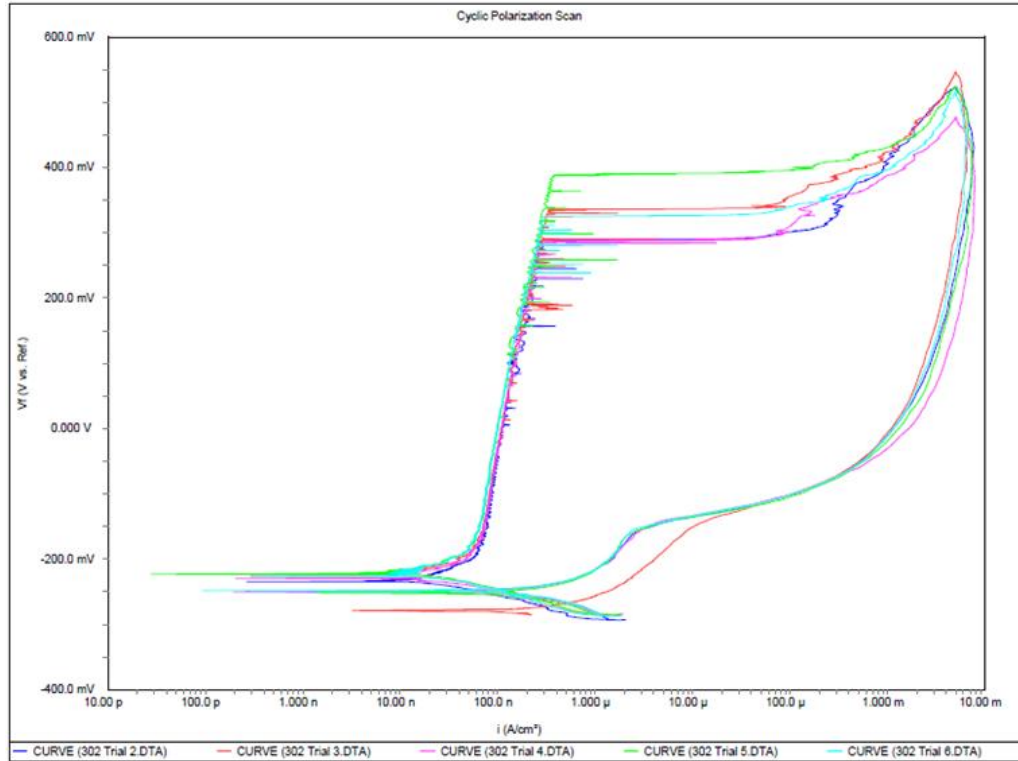


*Figure 7. Alloy 302 Cyclic Polarization Curve*

The wire surface after being subjected to the corrosion test was discolored and had small pits upon removal from the cell. The saline solution appeared cloudy with particles in it at the end of the test.

The material did show a breakdown potential with an average value of 324 mV vs. SCE. The surface evaluation complies by showing a difference between the appearances of the “as received” and the tested samples in pitting and discoloration. The average corrosion rate was found to be 0.025205 mpy.

*Table 8. Alloy 302 Cyclic Polarization Results*

Trial	Surface Area (cm <sup>2</sup> )	Average pH Before Testing	Average pH After Testing	Final Open Circuit Potential E <sub>r</sub> (mV vs. SCE)	Corrosion Rate (mpy)	Breakdown Potential E <sub>b</sub> (mV vs. SCE)	Protection Potential E <sub>p</sub> (mV vs. SCE)	E <sub>b</sub> -E <sub>r</sub> (mV vs SCE)
<b>2</b>	1.8442	7.19	7.20	-193	0.026669	288	-247	481
<b>3</b>	1.9248	7.20	7.22	-185	0.025492	336	-271	521
<b>4</b>	1.8637	7.20	7.21	-187	0.026583	284	-248	471
<b>5</b>	1.9631	7.18	7.19	-186	0.023306	388	-248	574
<b>6</b>	1.8603	7.19	7.19	-188	0.023975	325	-246	513
<b>Average</b>	<b>1.8912</b>	<b>7.19</b>	<b>7.20</b>	<b>-188</b>	<b>0.025205</b>	<b>324</b>	<b>-252</b>	<b>521</b>

Trial 1 did not go to completion due to complications in the apparatus; therefore there is no data for Trial 1.

3.1.1.2. 304V Results

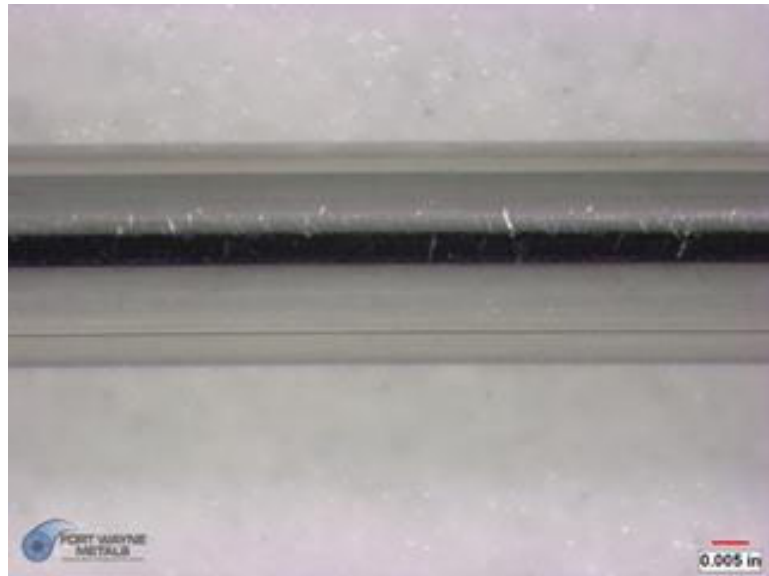


*Figure 8. Alloy 304V As Drawn Surface*

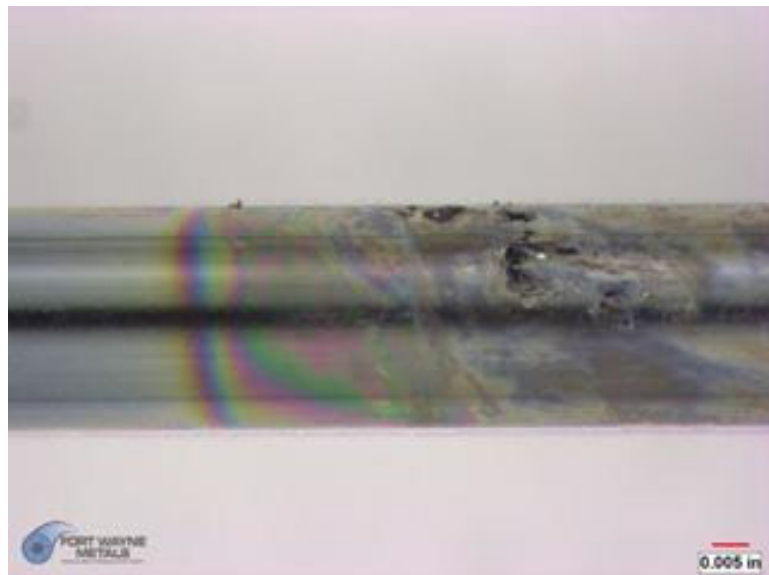


*Figure 9. Alloy 304V Surface After Corrosion Test*



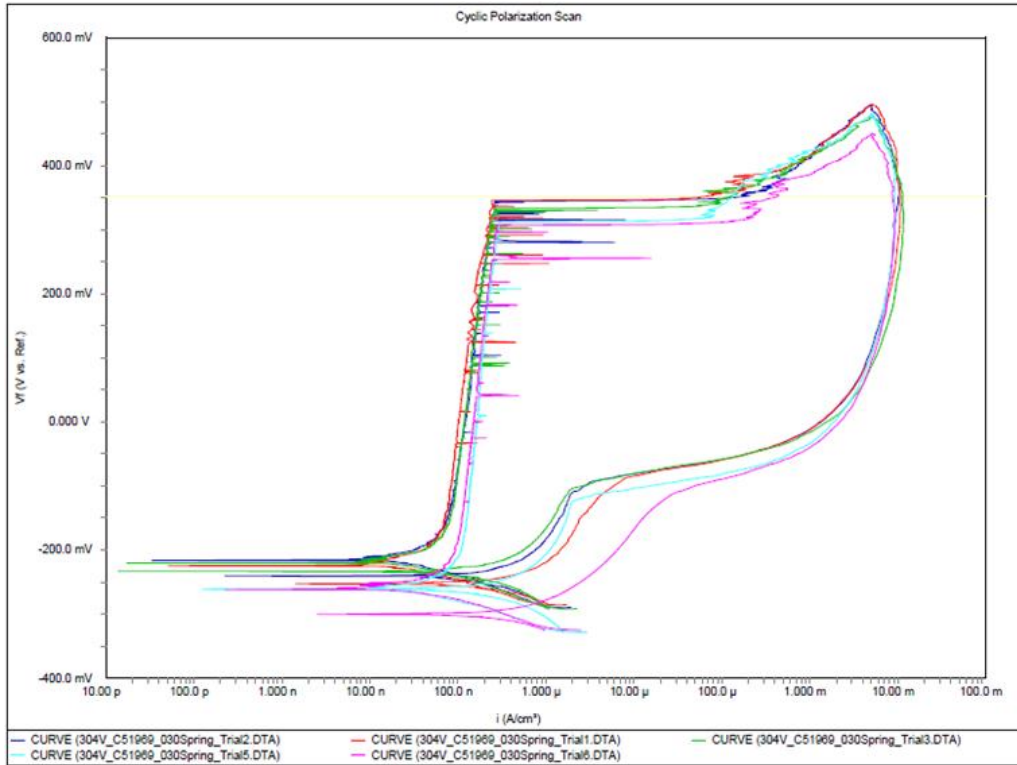


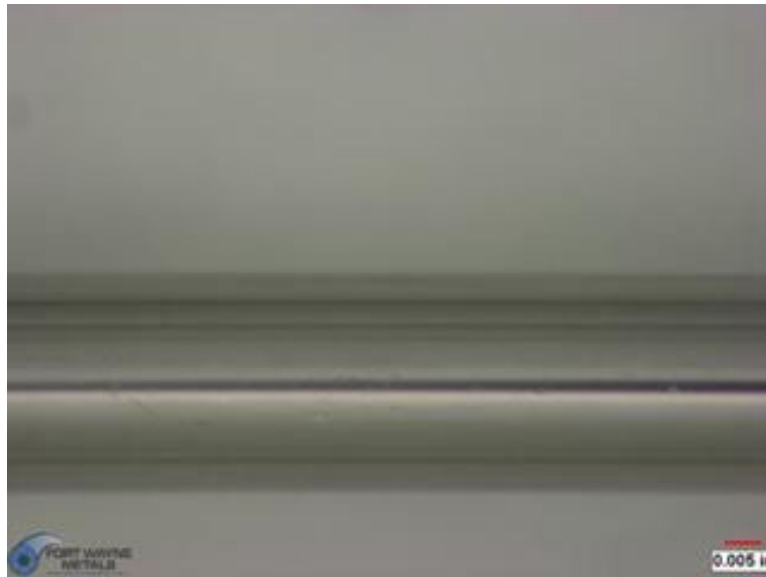
Figure 10. Alloy 304V Cyclic Polarization Curve

Table 9 Alloy 304V Cyclic Polarization Results

Trial	Surface Area (cm <sup>2</sup> )	Average pH Before Testing	Average pH After Testing	Final Open Circuit Potential E <sub>r</sub> (mV vs SCE)	Corrosion Rate (mpy)	Breakdown Potential E <sub>b</sub> (mV vs SCE)	Protection Potential E <sub>p</sub> (mV vs SCE)	E <sub>b</sub> -E <sub>r</sub> (mV vs SCE)
1	1.9752	7.15	7.19	-186	0.024830	346	-249	532
2	1.8117	7.18	7.21	-190	0.035090	345	-237	535
3	1.8351	7.12	7.14	-192	0.032710	333	-231	525
5	1.9439	7.08	7.10	-228	0.040770	312	-260	540
6	1.9591	7.06	7.08	-225	0.032960	307	-295	532
<b>Average</b>	<b>1.9050</b>	<b>7.12</b>	<b>7.14</b>	<b>-204</b>	<b>0.033272</b>	<b>329</b>	<b>-254</b>	<b>533</b>

The material did show a breakdown potential with an average value of 329 mV. The surface evaluation maintained this conclusion by showing a difference between the appearances of the “as received” and the tested samples, in pitting and discoloration. The average corrosion rate was found to be 0.033272 mpy.

### 3.1.1.3. 316LVM Results



*Figure 11. Alloy 316LVM As Drawn Surface*

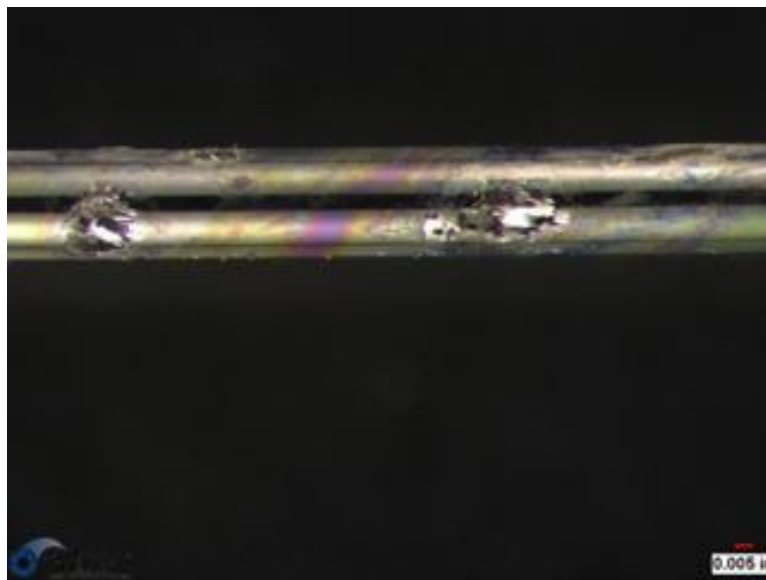


*Figure 12. Alloy 316LVM Surface After Corrosion Test*

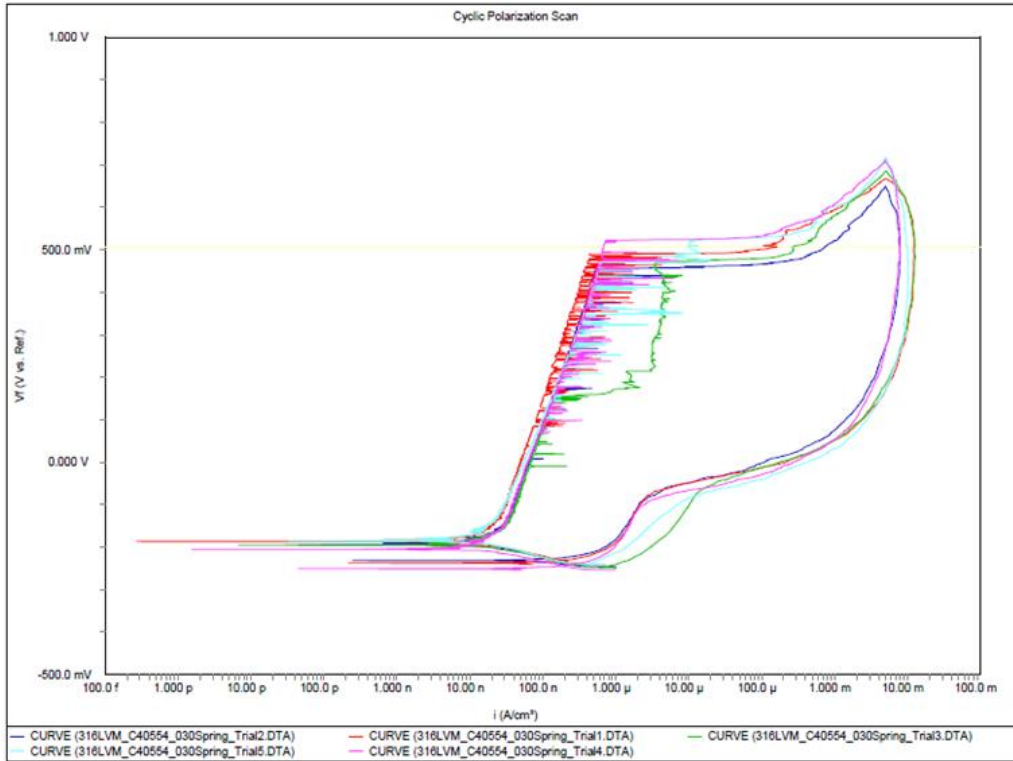


Figure 13. Alloy 316LVM Cyclic Polarization Curve

Table 10. Alloy 316LVM Cyclic Polarization Results

Trial	Surface Area (cm <sup>2</sup> )	Average pH Before Testing	Average pH After Testing	Final Open Circuit Potential E <sub>r</sub> (mV vs SCE)	Corrosion Rate (mpy)	Breakdown Potential E <sub>b</sub> (mV vs SCE)	Protection Potential E <sub>p</sub> (mV vs SCE)	E <sub>b</sub> -E <sub>r</sub> (mV vs SCE)
1	1.8968	7.10	7.15	-141	0.009484	490	-231	631
2	1.9442	7.13	7.14	-146	0.013920	457	-227	603
3	1.9205	7.14	7.19	-148	0.014460	470	-284	618
4	1.8863	7.08	7.12	-154	0.012860	523	-244	677
5	1.8217	7.07	7.11	-141	0.012030	470	-240	611
<b>Average</b>	<b>1.8939</b>	<b>7.10</b>	<b>7.14</b>	<b>-146</b>	<b>0.012551</b>	<b>482</b>	<b>-245</b>	<b>628</b>

The material did show a breakdown potential with an average value of 482 mV. The surface evaluation maintained this conclusion by showing a difference between the appearances of the “as received” and the tested samples, in pitting and discoloration. The average corrosion rate was found to be 0.012551 mpy.

#### 3.1.1.4. Alloy 420 Results



*Figure 14. Alloy 420 As Drawn Surface*

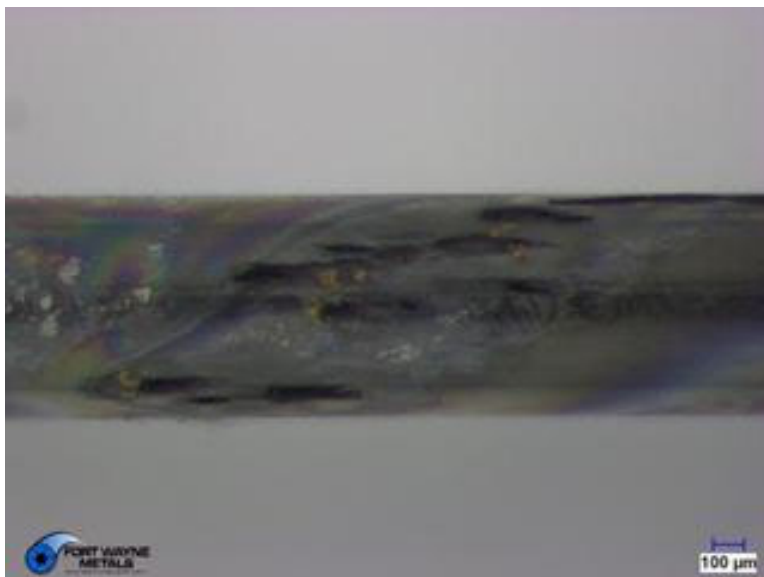


*Figure 15. Alloy 420 Surface After Corrosion Test*

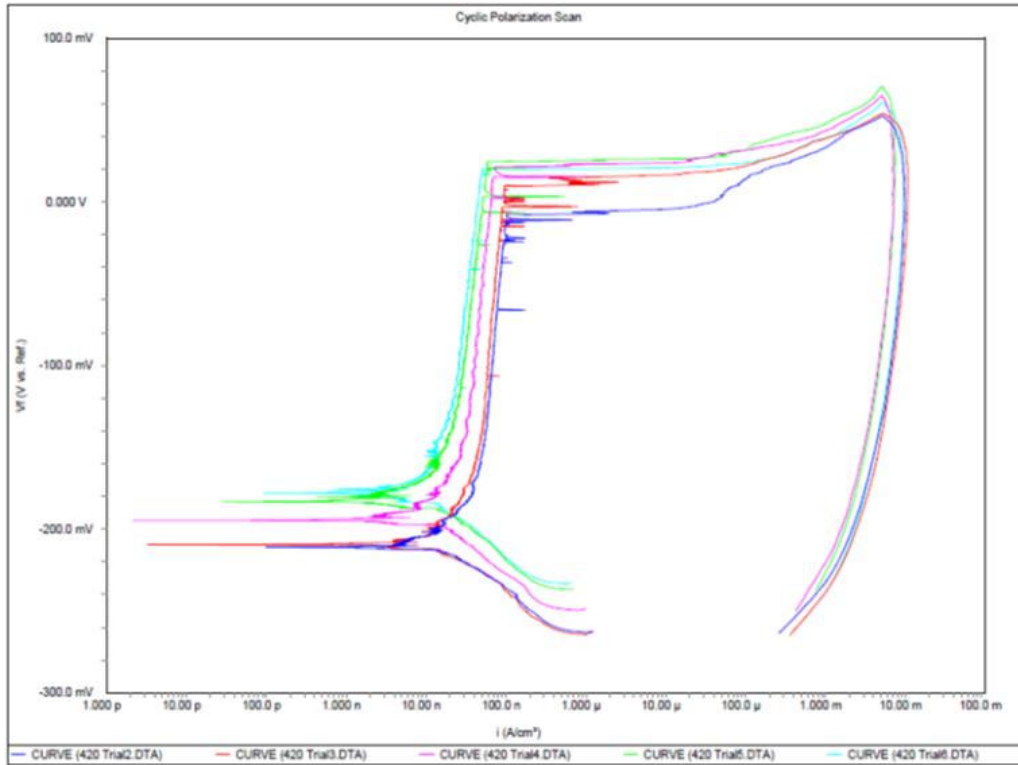


Figure 16. Alloy 420 Cyclic Polarization Curve

Table 11. Alloy 420 Cyclic Polarization Results

Trial	Surface Area (cm <sup>2</sup> )	Average pH Before Testing	Average pH After Testing	Final Open Circuit Potential $E_r$ (mV vs. SCE)	Corrosion Rate (mpy)	Breakdown Potential $E_b$ (mV vs. SCE)	Protection Potential $E_p$ (mV vs. SCE)	$E_b - E_r$ (mV vs. SCE)
2	1.8828	7.18	7.18	-163	0.018525	-8	N/A	155
3	1.9111	7.19	7.20	-165	0.017004	10	N/A	175
4	1.9132	7.22	7.21	-150	0.013456	21	N/A	171
5	1.8618	7.19	7.18	-137	0.011694	25	N/A	162
6	1.9561	7.15	7.17	-134	0.010638	20	N/A	154
<b>Average</b>	<b>1.8922</b>	<b>7.19</b>	<b>7.19</b>	<b>-150</b>	<b>0.015170</b>	<b>14</b>	<b>N/A</b>	<b>163</b>

Trial 1 did not go to completion due to complications in the apparatus; therefore there is no data for Trial 1. The wire surface after being subjected to the corrosion test was discolored and had small pits upon removal from the cell. The saline solution appeared cloudy with particles in it at the end of the test. The material did show a breakdown potential with an average value of 14 mV vs. SCE. The surface evaluation complies by showing a difference between the

appearances of the “as received” and the tested samples in pitting and discoloration. The average corrosion rate was found to be 0.015170 mpy.

### 3.1.1.5. Custom 455® Alloy Results

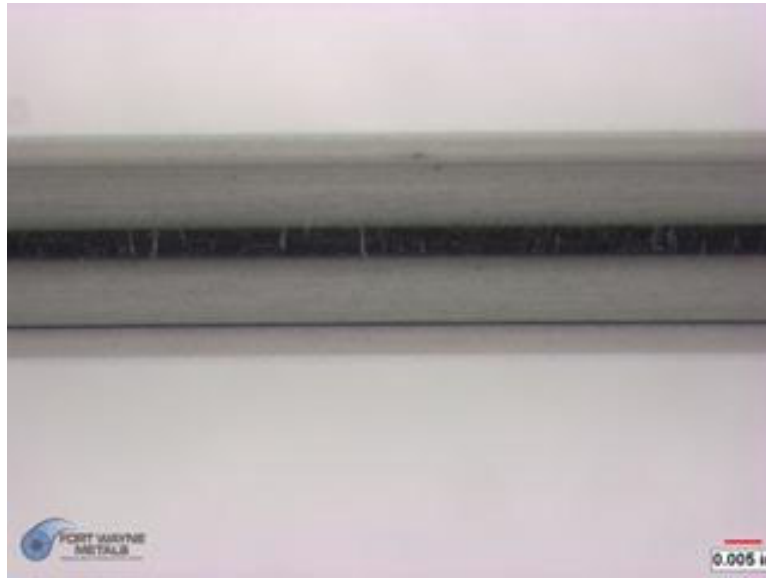


*Figure 17. Custom 455® Alloy As Drawn Surface*

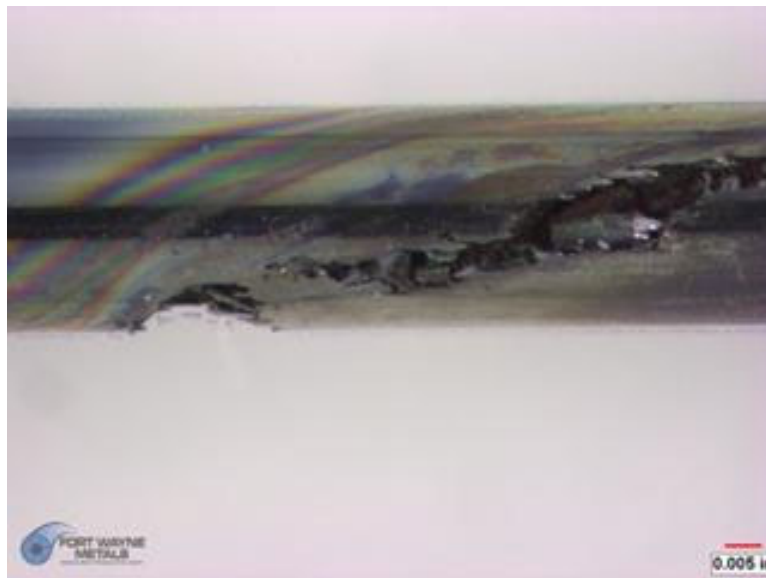


*Figure 18. Custom 455® Alloy Surface After Corrosion Test*

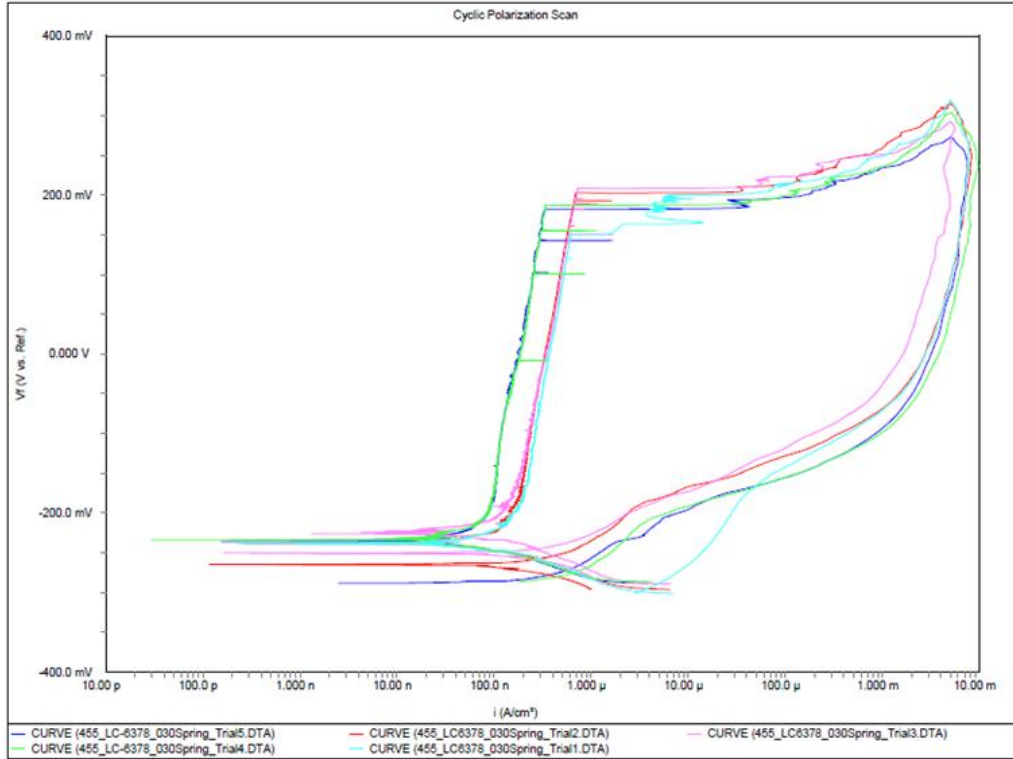


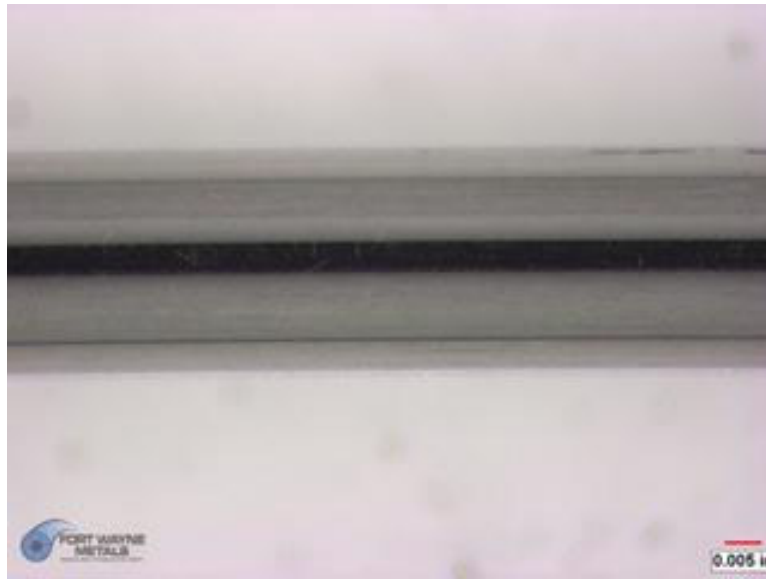
Figure 19. Custom 455® Alloy Cyclic Polarization Curve

Table 12. Custom 455® Alloy Cyclic Polarization Results

Trial	Surface Area (cm <sup>2</sup> )	Average pH Before Testing	Average pH After Testing	Final Open Circuit Potential $E_r$ (mV vs SCE)	Corrosion Rate (mpy)	Breakdown Potential $E_b$ (mV vs SCE)	Protection Potential $E_p$ (mV vs SCE)	$E_b - E_{vr}$ (mV vs SCE)
1	1.9941	7.11	7.13	-201	0.089020	150	-299	351
2	2.0038	7.10	7.15	-196	0.101600	203	-258	399
3	1.9765	7.12	7.12	-189	0.089960	209	-245	398
4	1.9330	7.10	7.12	-185	0.045380	187	-275	372
5	1.9021	7.11	7.12	-187	0.060380	181	-272	368
<b>Average</b>	<b>1.9619</b>	<b>7.11</b>	<b>7.13</b>	<b>-192</b>	<b>0.077268</b>	<b>186</b>	<b>-270</b>	<b>378</b>

Wire surface after being subjected to the corrosion test was discolored and pitted. The saline solution had particles in it at the end of the test. The material did show a breakdown potential with an average value of 186 mV. The surface evaluation maintained this conclusion by showing a difference between the appearances of the “as received” and the tested samples, in pitting and discoloration. The average corrosion rate was found to be 0.077268 mpy.

### 3.1.1.6. Micro Melt® Biodur® Custom 470® Alloy Results



*Figure 20. Micro Melt® Biodur® Custom 470® Alloy As Drawn Surface*

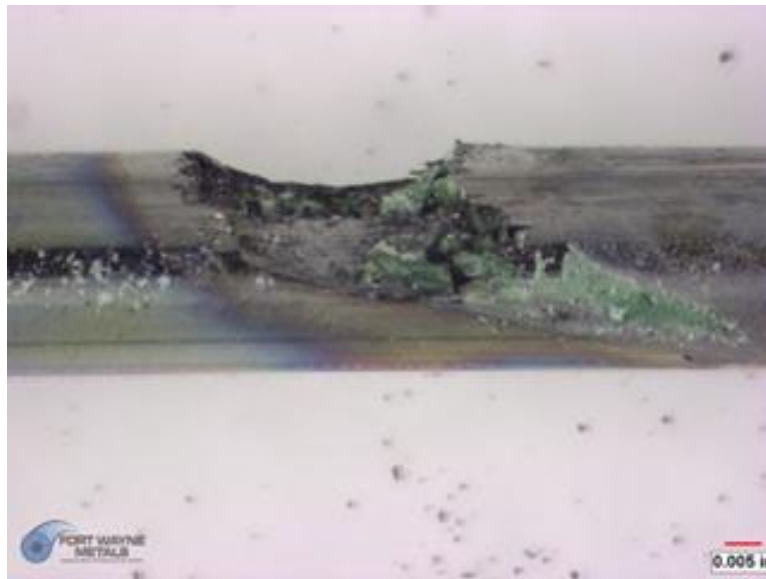


*Figure 21. Micro Melt® Biodur® Custom 470® Alloy Surface After Corrosion Test*



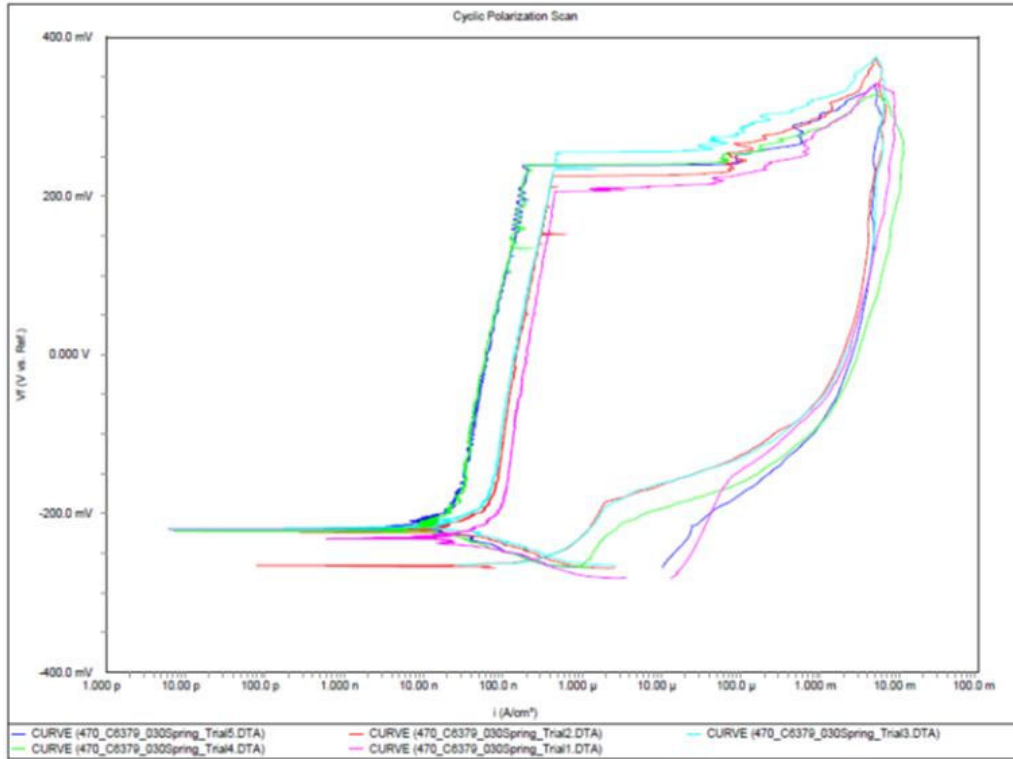


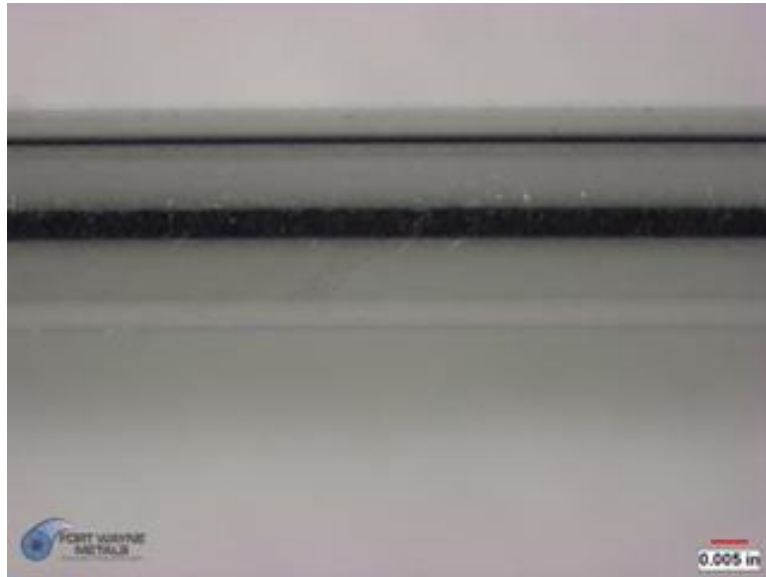
Figure 22. Micro Melt® Biodur® Custom 470® Alloy Cyclic Polarization Curve

Table 13. Micro Melt® Biodur® Custom 470® Alloy Cyclic Polarization Results

Trial	Surface Area (cm <sup>2</sup> )	Average pH Before Testing	Average pH After Testing	Final Open Circuit Potential E <sub>r</sub> (mV vs SCE)	Corrosion Rate (mpy)	Breakdown Potential E <sub>b</sub> (mV vs SCE)	Protection Potential E <sub>p</sub> (mV vs SCE)	E <sub>b</sub> -E <sub>r</sub> (mV vs SCE)
1	1.8637	7.07	7.09	-181	0.035280	206	N/A	387
2	1.9895	7.06	7.12	-169	0.031540	225	-255	394
3	1.9485	7.10	7.12	-165	0.030050	255	-253	420
4	1.9643	7.07	7.10	-167	0.019160	340	-267	507
5	1.9257	7.13	7.14	-168	0.016310	239	N/A	407
<b>Avg</b>	<b>1.9383</b>	<b>7.09</b>	<b>7.11</b>	<b>-170</b>	<b>0.026468</b>	<b>253</b>	<b>-258</b>	<b>423</b>

Wire surface area after being subjected to the corrosion test was discolored and pitted. The saline solution had particles in it at the end of the test. The material did show a breakdown potential with an average value of 253 mV. The surface evaluation maintained this conclusion by showing a difference between the appearances of the “as received” and the tested samples, in pitting and discoloration. The average corrosion rate was found to be 0.026468 mpy.

### 3.1.1.7. FWM1058® Alloy Results



*Figure 23. FWM1058® Alloy As Drawn Surface*

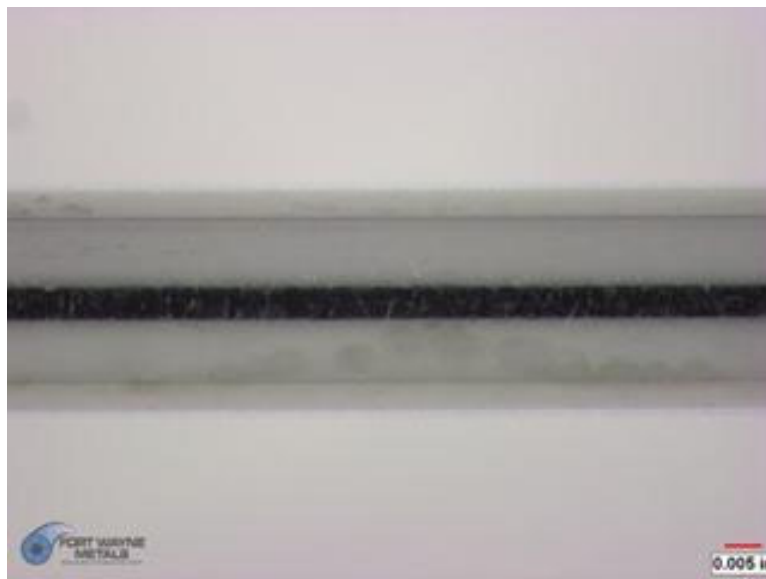


*Figure 24. FWM1058® Alloy Surface After Corrosion Test*

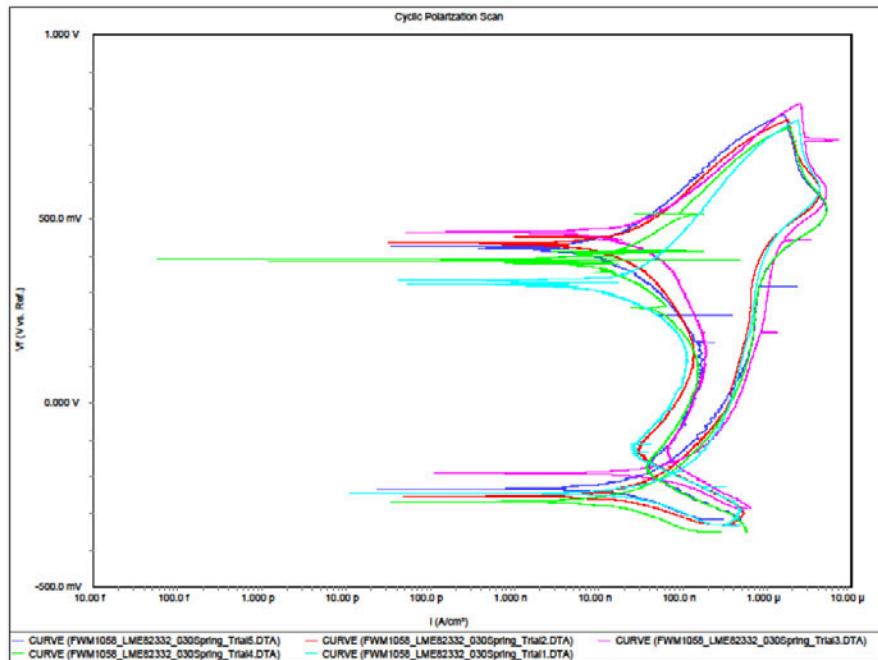


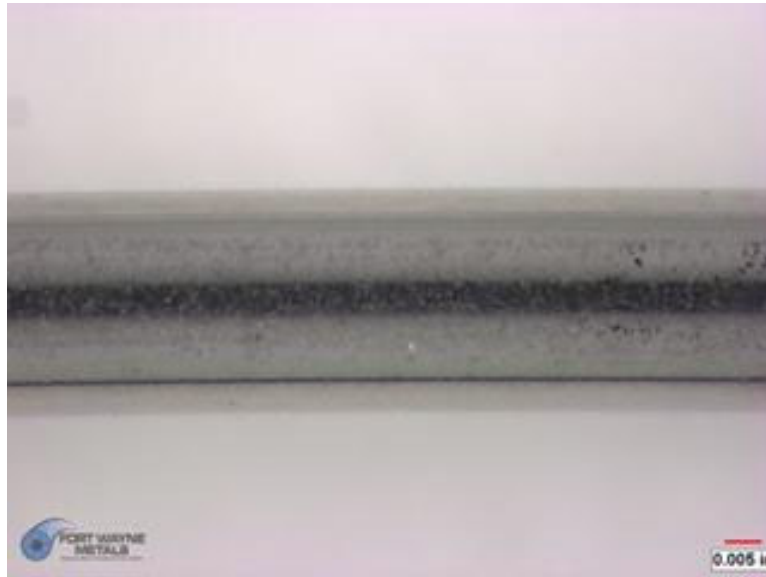
Figure 25. FWM1058® Alloy Cyclic Polarization Curve

Table 14. FWM1058® Alloy Cyclic Polarization Results

Trial	Surface Area (cm <sup>2</sup> )	Average pH Before Testing	Average pH After Testing	Final Open Circuit Potential E <sub>r</sub> (mV vs SCE)	Corrosion Rate (mpy)	Breakdown Potential E <sub>b</sub> (mV vs. SCE)	Protection Potential E <sub>p</sub> (mV vs. SCE)	E <sub>b</sub> -E <sub>r</sub> (mV vs SCE)
1	1.9467	7.18	7.18	-232	0.024110	N/A	N/A	N/A
2	1.9409	7.12	7.19	-231	0.012600	N/A	N/A	N/A
3	1.8512	7.11	7.11	-185	0.051900	N/A	N/A	N/A
4	1.9105	7.11	7.09	-250	0.012280	N/A	N/A	N/A
5	1.9713	7.13	7.12	-216	0.013150	N/A	N/A	N/A
<b>Average</b>	<b>1.9241</b>	<b>7.13</b>	<b>7.14</b>	<b>-223</b>	<b>0.022808</b>	<b>N/A</b>	<b>N/A</b>	<b>N/A</b>

Wire appeared the same before and after the test. There was no pitting. The saline solution looked clear as it did before the test. The material did not show a breakdown potential. The surface evaluation maintained this conclusion by showing no difference between the appearances of the “as received” and the tested samples, in either pitting or discoloration. The average corrosion rate was found to be 0.022808 mpy.

### 3.1.1.8. MP35N® Alloy Results



*Figure 26. MP35N® Alloy As Drawn Surface*

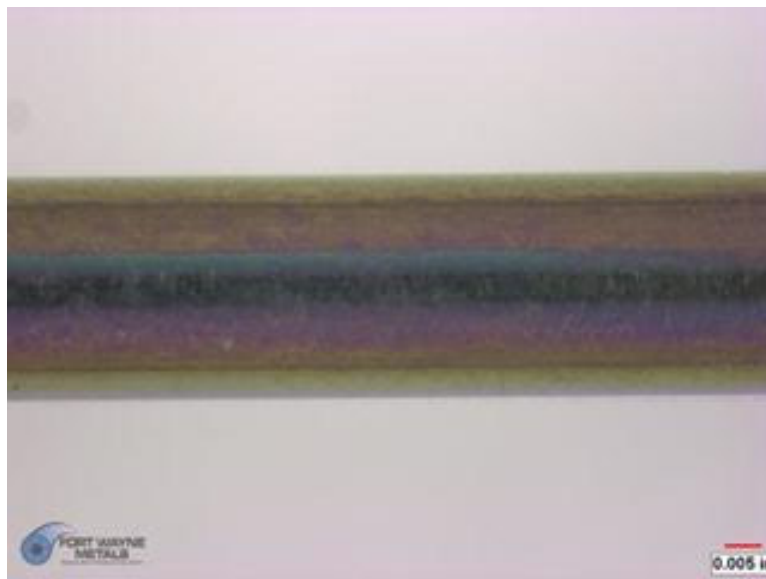


*Figure 27. MP35N® Alloy Surface After Corrosion Test*

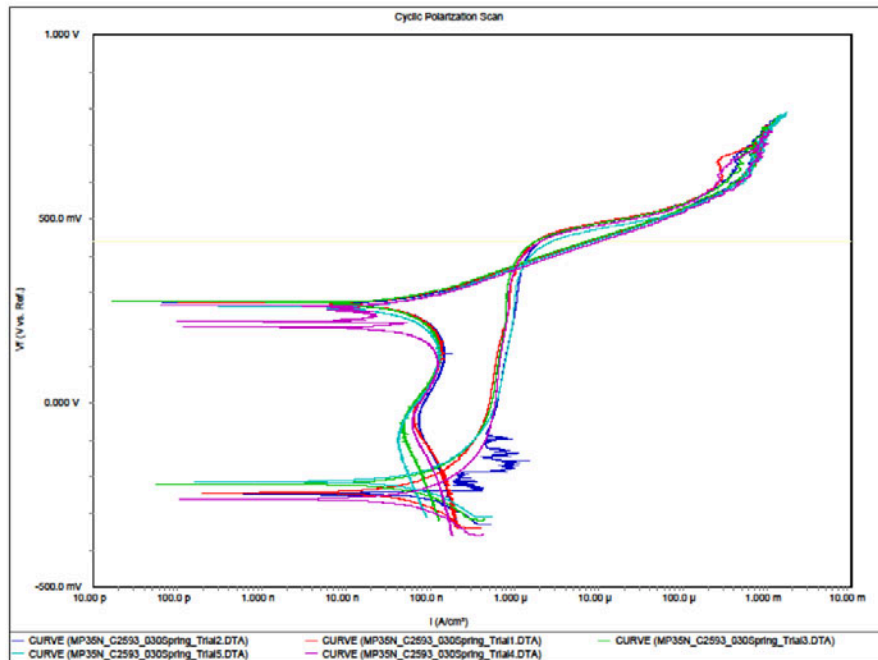


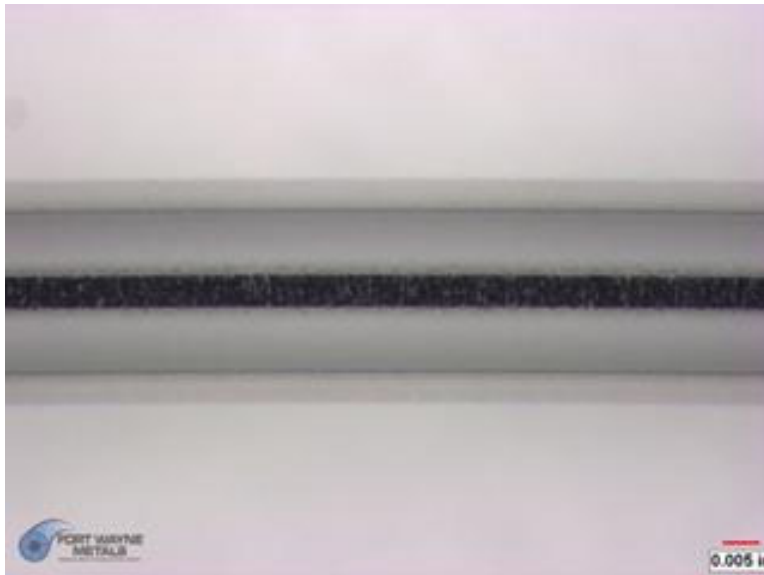
Figure 28. MP35N® Alloy Cyclic Polarization Curve

Table 15. MP35N® Alloy Cyclic Polarization Results

Trial	Surface Area (cm <sup>2</sup> )	Average pH Before Testing	Average pH After Testing	Final Open Circuit Potential E <sub>r</sub> (mV vs SCE)	Corrosion Rate (mpy)	Breakdown Potential E <sub>b</sub> (mV vs. SCE)	Protection Potential E <sub>p</sub> (mV vs. SCE)	E <sub>b</sub> -E <sub>r</sub> (mV vs SCE)
1	1.9470	7.07	7.08	-240	0.089070	N/A	N/A	N/A
2	1.9138	7.10	7.10	-231	0.252500	N/A	N/A	N/A
3	1.9960	7.09	7.13	-218	0.100700	N/A	N/A	N/A
4	2.0199	7.07	7.10	-259	0.142000	N/A	N/A	N/A
5	2.1765	7.07	7.06	-210	0.081970	N/A	N/A	N/A
<b>Average</b>	<b>2.0106</b>	<b>7.08</b>	<b>7.09</b>	<b>-232</b>	<b>0.133248</b>	<b>N/A</b>	<b>N/A</b>	<b>N/A</b>

The material did not show a breakdown potential, although, the surface evaluation showed a difference between the appearances of the “as received” and the tested samples in discoloration. The average corrosion rate was found to be 0.133248 mpy.

### 3.1.1.9. 35N LT® Alloy Results



*Figure 29. 35N LT® Alloy As Drawn Surface*

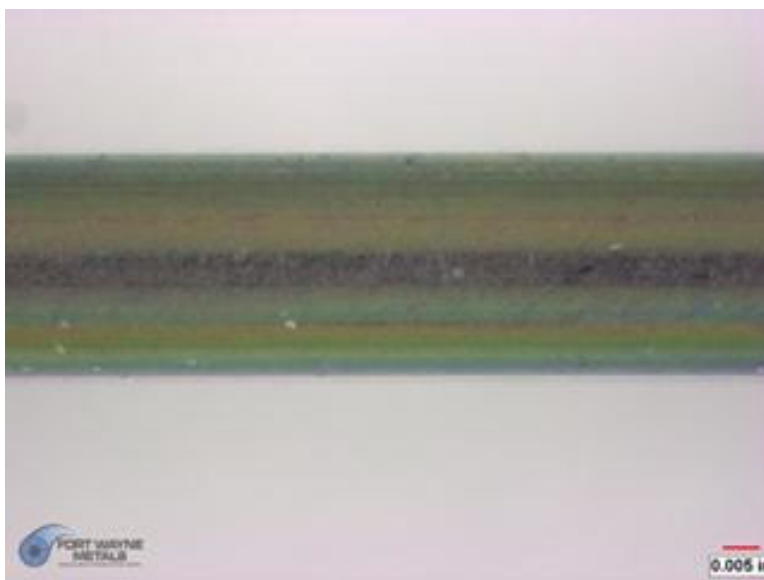


*Figure 30. 35N LT® Alloy Surface After Corrosion Test*

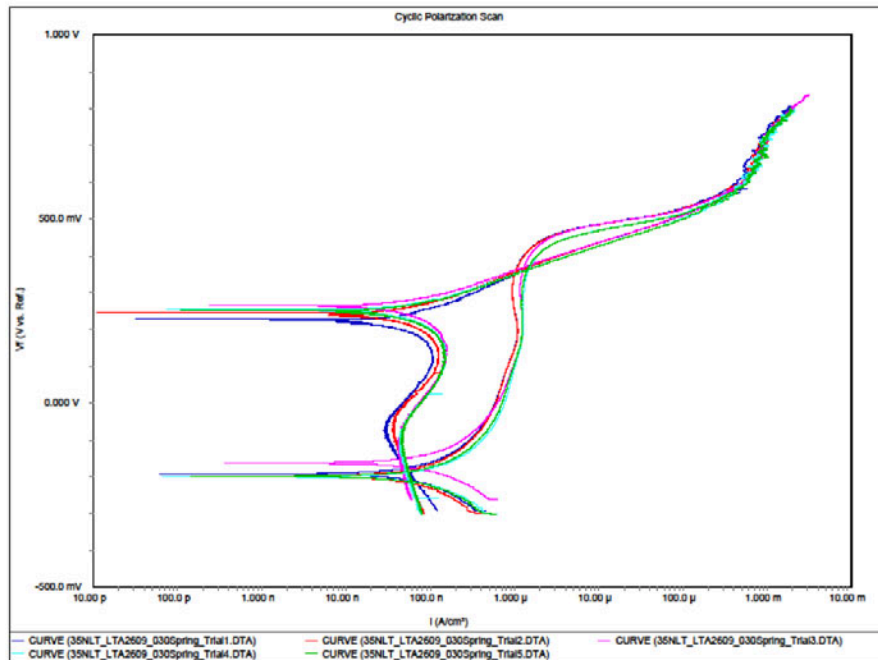


Figure 31. 35N LT® Alloy Cyclic Polarization Curve

Table 16. 35N LT® Alloy Cyclic Polarization Results

Trial	Surface Area (cm <sup>2</sup> )	Average pH Before Testing	Average pH After Testing	Final Open Circuit Potential E <sub>r</sub> (mV vs SCE)	Corrosion Rate (mpy)	Breakdown Potential E <sub>b</sub> (mV vs. SCE)	Protection Potential E <sub>p</sub> (mV vs. SCE)	E <sub>b</sub> -E <sub>r</sub> (mV vs SCE)
1	1.8664	7.09	7.09	-192	0.125200	N/A	N/A	N/A
2	1.9284	7.07	7.09	-199	0.182900	N/A	N/A	N/A
3	1.9172	7.03	7.05	-162	0.139100	N/A	N/A	N/A
4	1.9296	7.06	7.05	-202	0.322800	N/A	N/A	N/A
5	1.9190	7.05	7.09	-201	0.319100	N/A	N/A	N/A
<b>Average</b>	<b>1.9121</b>	<b>7.06</b>	<b>7.07</b>	<b>-191</b>	<b>0.217820</b>	<b>N/A</b>	<b>N/A</b>	<b>N/A</b>

Wire was discolored with no pitting. The saline solution looked clear as it did before the test. The material did not show a breakdown potential, although the surface evaluation shows a difference between the appearances of the “as received” and the tested samples in discoloration. The average corrosion rate was found to be 0.217820 mpy.

### 3.1.1.10. L605 Alloy Results



*Figure 32. L605 Alloy As Drawn Surface*

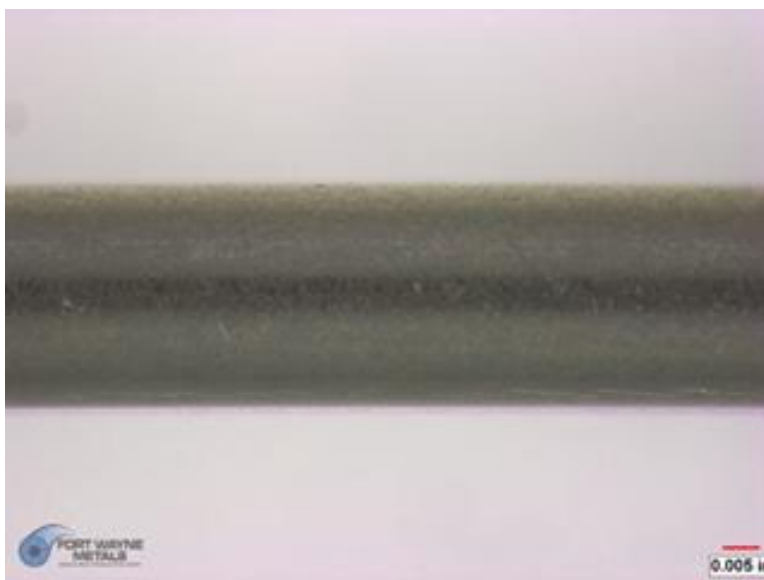


*Figure 33. L605 Alloy Surface After Corrosion Test*



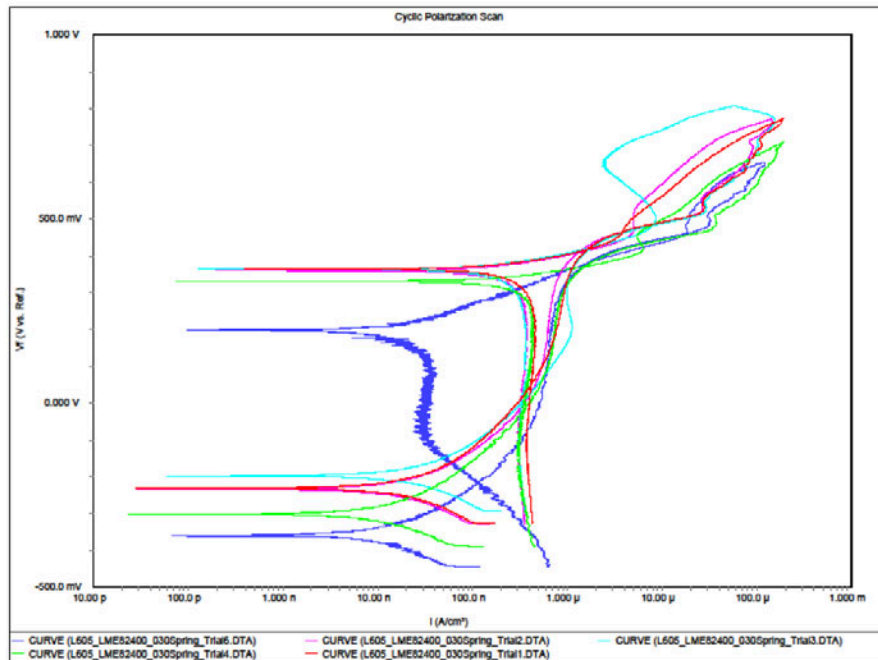


Figure 34. L605 Alloy Cyclic Polarization Curve

Table 17. L605 Alloy Cyclic Polarization Results

Trial	Surface Area (cm <sup>2</sup> )	Average pH Before Testing	Average pH After Testing	Final Open Circuit Potential E <sub>r</sub> (mV vs SCE)	Corrosion Rate (mpy)	Breakdown Potential E <sub>b</sub> (mV vs. SCE)	Protection Potential E <sub>p</sub> (mV vs. SCE)	E <sub>b</sub> -E <sub>r</sub> (mV vs SCE)
1	1.9762	7.08	7.08	-228	0.014840	N/A	N/A	N/A
2	1.8974	7.09	7.12	-229	0.012410	N/A	N/A	N/A
3	1.9278	7.11	7.11	-193	0.016510	N/A	N/A	N/A
4	1.8941	7.14	7.12	-299	0.005992	N/A	N/A	N/A
6	2.0178	7.13	7.11	-345	0.006302	N/A	N/A	N/A
<b>Average</b>	<b>1.9427</b>	<b>7.11</b>	<b>7.11</b>	<b>-259</b>	<b>0.011211</b>	<b>N/A</b>	<b>N/A</b>	<b>N/A</b>

Wire was slightly discolored after the test, but not nearly as significantly as the MP35N® and 35N LT®. There was no pitting. The saline solution looked clear as it did before the test. The material did not show a breakdown potential, although, the surface evaluation showed a slight difference between the appearances of the “as received” and the tested samples in discoloration. The average corrosion rate was found to be 0.011211 mpy.

### 3.1.1.11. Nitinol Light Oxide Results



*Figure 35. Nitinol Light Oxide As Drawn Surface*

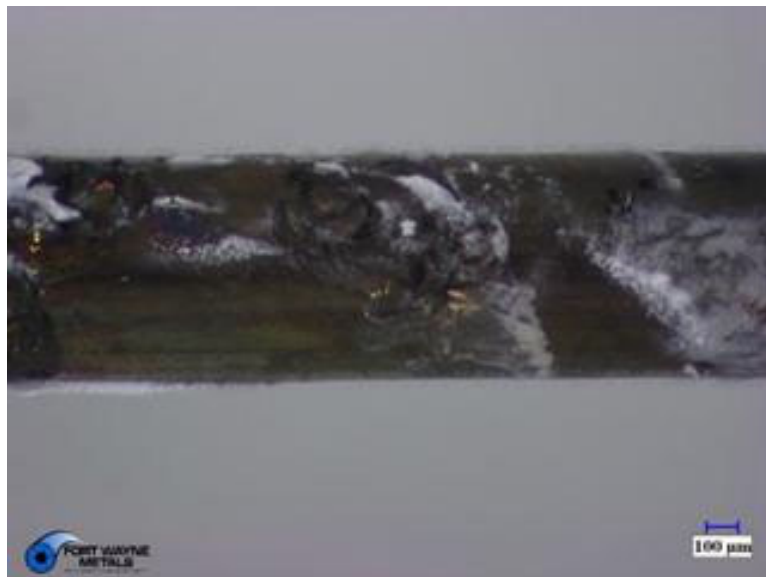


*Figure 36. Nitinol Light Oxide Surface After Corrosion Test*

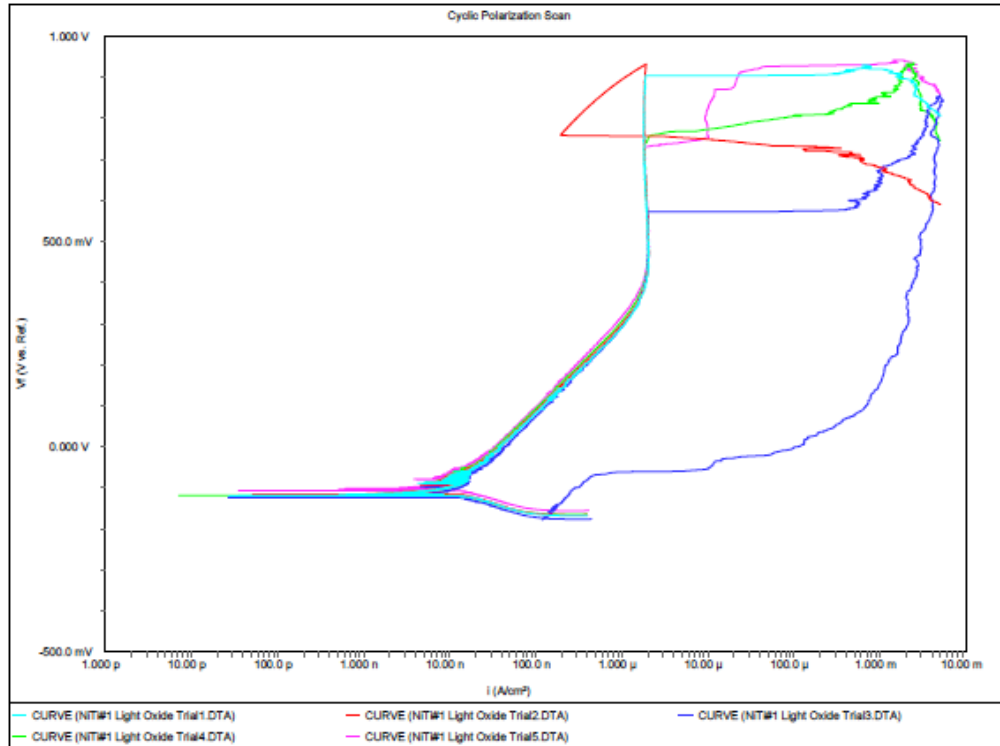


Figure 37. Nitinol Light Oxide Cyclic Polarization Curve

Table 18. Nitinol Light Oxide Cyclic Polarization Results

Trial	Surface Area (cm <sup>2</sup> )	Average pH Before Testing	Average pH After Testing	Final Open Circuit Potential E <sub>r</sub> (mV vs. SCE)	Corrosion Rate (mpy)	Breakdown Potential E <sub>b</sub> (mV vs. SCE)	Protection Potential E <sub>p</sub> (mV vs. SCE)	E <sub>b</sub> -E <sub>r</sub> (mV vs SCE)
1	1.8804	7.10	7.11	-69	0.012810	904	N/A	973
2	1.9980	7.15	7.13	-68	0.013200	759	N/A	827
3	1.8898	7.16	7.18	-78	0.013250	572	-175	650
4	1.8743	7.16	7.16	-66	0.012470	739	N/A	805
5	1.9032	7.12	7.14	-57	0.012150	731	N/A	788
<b>Average</b>	<b>1.9091</b>	<b>7.14</b>	<b>7.14</b>	<b>-68</b>	<b>0.012776</b>	<b>737</b>	<b>-175</b>	<b>809</b>

Wire had small pits upon removal from the cell. There was a substance at the location of the pitting. The saline solution appeared clear with particles in it at the end of the test. The particles that were in the saline solution were similar in color and consistency as the substance found on the pitting sites of the samples.

The severity of the pitting is dependent on the amount of time the sample is exposed to the corrosion cell. Trial 2 showed a breakdown potential in the reverse scan. The wire resisted corrosion in order to surpass the vertex potential but eventually broke down in the reverse scan. Trial 3 is the only test that ran to completion. The other trials reached a current that exceeded the capability of the corrosion cell, and therefore were terminated by the Gamry software. This does not affect the breakdown potential or the corrosion rate.

The corrosion rates of the trials were consistent, with an average corrosion rate of 0.012776 mpy. All trials show a breakdown potential, although there is a large variation, which is known to be typical for Nitinol. The average breakdown potential was found to be 737 mV vs. SCE. The surface evaluation shows a difference between the surface appearances of the “as received” and the tested samples in a substance, pitting, and slight discoloration.

#### 3.1.1.12. Nitinol Dark Oxide Results



*Figure 38. Nitinol Dark Oxide As Drawn Surface*

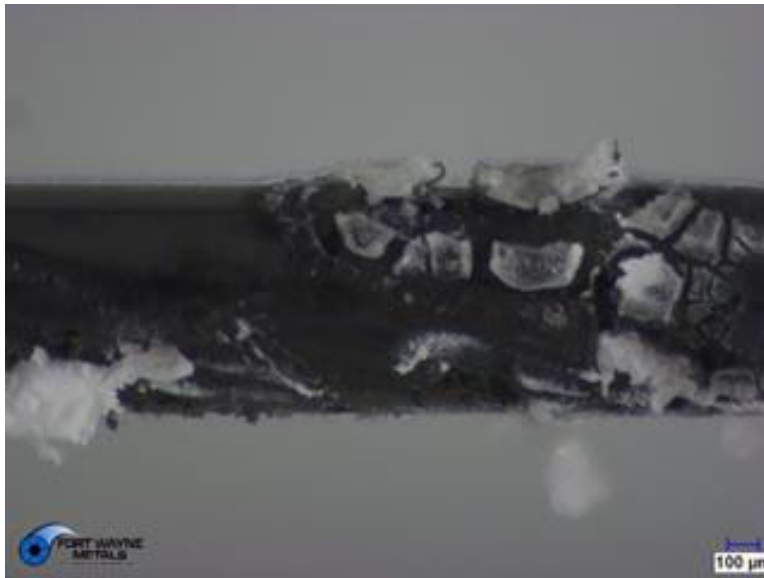


Figure 39. Nitinol Dark Oxide Surface After Corrosion Test

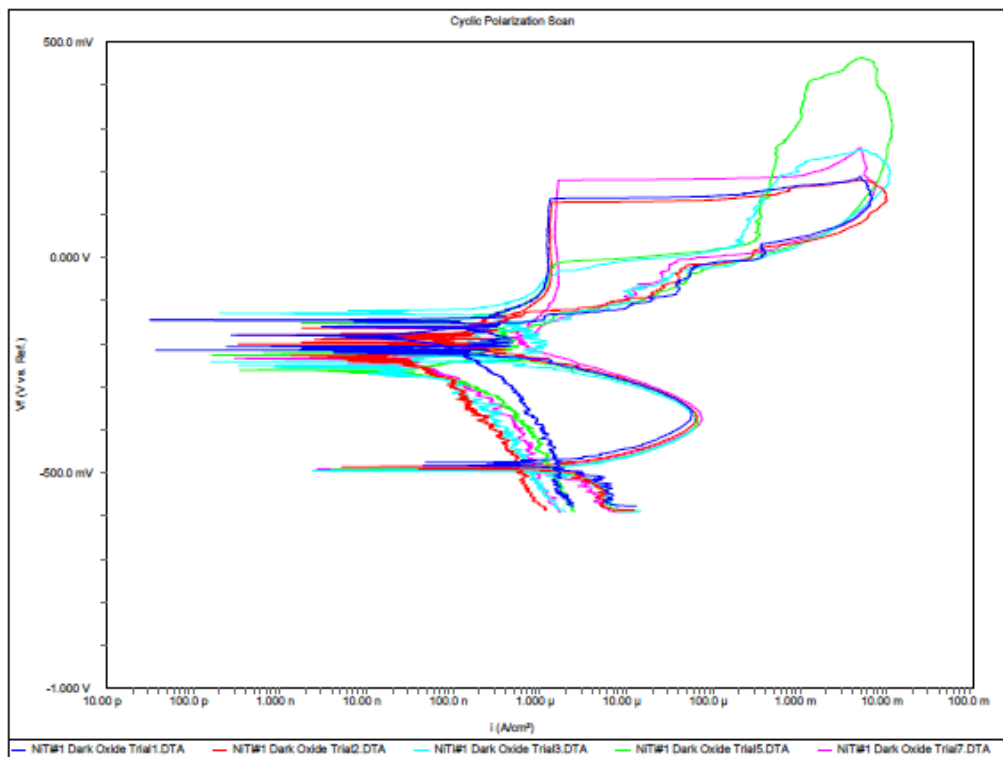


Figure 40. Nitinol Dark Oxide Cyclic Polarization Curve

*Table 19. Nitinol Dark Oxide Cyclic Polarization Results*

Trial	Surface Area (cm <sup>2</sup> )	Average pH Before Testing	Average pH After Testing	Final Open Circuit Potential E <sub>r</sub> (mV vs. SCE)	Corrosion Rate (mpy)	Breakdown Potential E <sub>b</sub> (mV vs. SCE)	Protection Potential E <sub>p</sub> (mV vs. SCE)	E <sub>b</sub> -E <sub>r</sub> (mV vs. SCE)
<b>1</b>	1.8324	7.13	7.14	-477	1.03686	136	-156	613
<b>2</b>	1.8725	7.14	7.14	-487	1.49662	127	-134	614
<b>3</b>	1.8421	7.15	7.15	-489	1.35562	-31	-152	458
<b>5</b>	1.9008	7.11	7.14	-490	2.54007	-13	-173	477
<b>7</b>	1.9502	7.19	7.21	-492	2.56359	179	-199	671
<b>Average</b>	<b>1.8796</b>	<b>7.14</b>	<b>7.16</b>	<b>-487</b>	<b>1.79855</b>	<b>80</b>	<b>-163</b>	<b>567</b>

Wire had small pits upon removal from the cell. There was a substance at the location of the pitting. The saline solution appeared clear with particles in it at the end of the test. The particles that were in the saline solution were similar in color and consistency as the substance found on the pitting sites of the samples.

The corrosion rates of the trials were inconsistent, with an average corrosion rate of 1.79855 mpy. All of the trials show a breakdown potential, although there is a large variation, which is known to be typical for Nitinol. The average breakdown potential was found to be 80 mV vs. SCE. The surface evaluation shows a difference between the surface appearances of the “as received” and the tested samples in a substance and pitting.

### 3.1.1.13. Nitinol Etched Surface Results

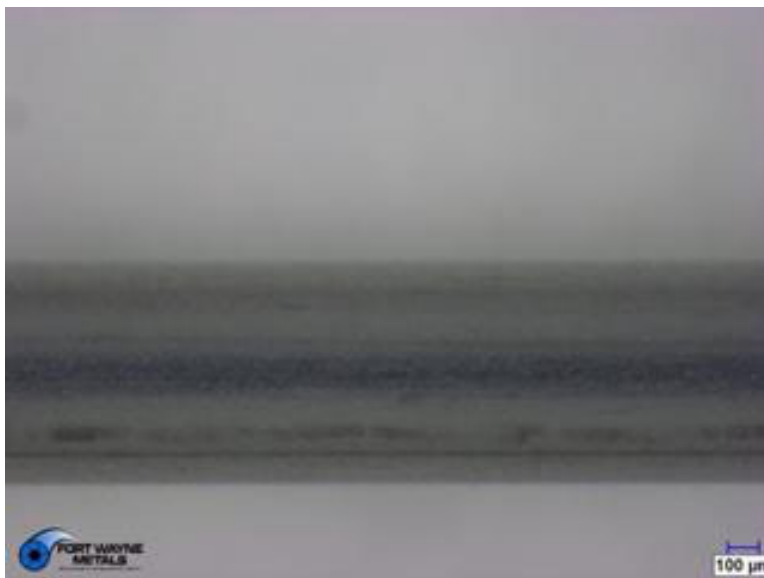


*Figure 41. Nitinol Etched As Drawn Surface*

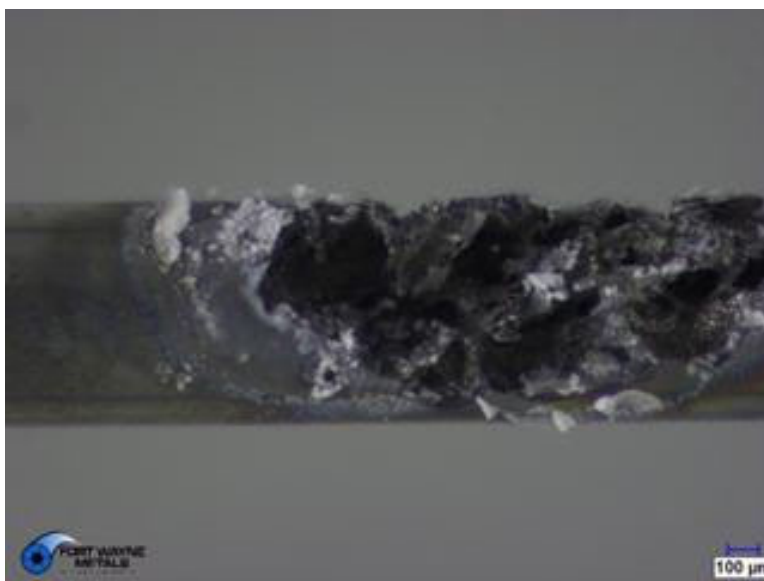


*Figure 42. Nitinol Etched Surface After Corrosion Test*

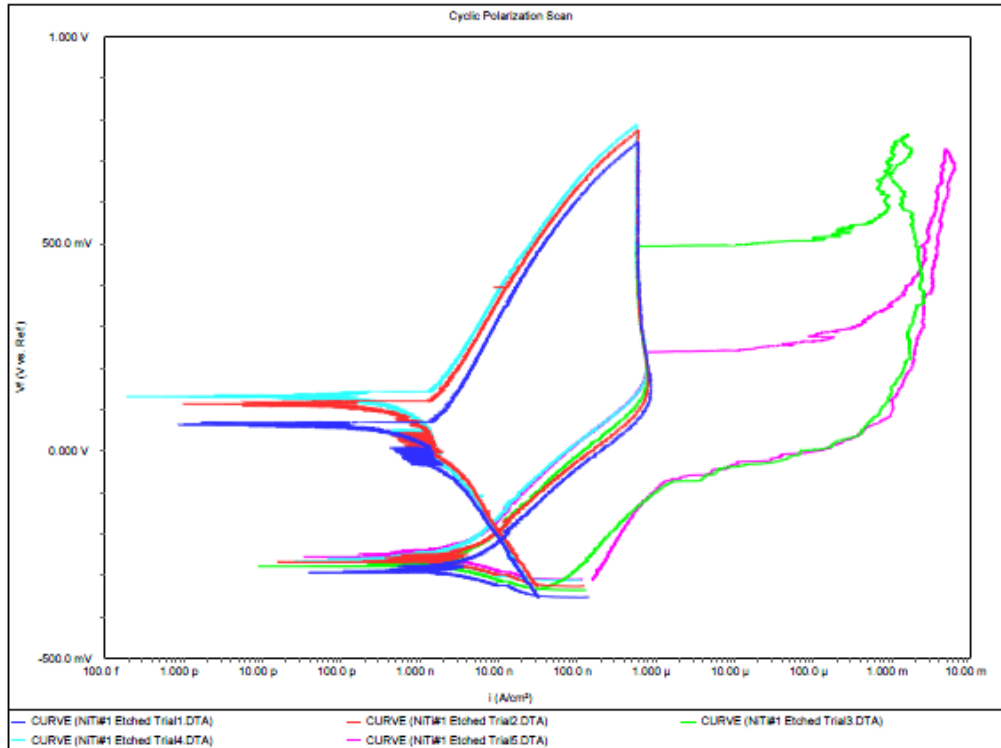


Figure 43. Nitinol Etched Cyclic Polarization Curve

Table 20. Nitinol Etched Cyclic Polarization Results

Trial	Surface Area (cm <sup>2</sup> )	Average pH Before Testing	Average pH After Testing	Final Open Circuit Potential E <sub>r</sub> (mV vs. SCE)	Corrosion Rate (mpy)	Breakdown Potential E <sub>b</sub> (mV vs. SCE)	Protection Potential E <sub>p</sub> (mV vs. SCE)	E <sub>b</sub> -E <sub>r</sub> (mV vs. SCE)
1	1.9382	7.15	7.14	-254	0.002445	N/A	N/A	N/A
2	1.9360	7.13	7.12	-227	0.002266	N/A	N/A	N/A
3	1.9637	7.14	7.14	-236	0.002074	494	-333	730
4	1.9491	7.16	7.15	-212	0.001656	N/A	N/A	N/A
5	1.9306	7.18	7.23	-211	0.001884	239	N/A	450
<b>Average</b>	<b>1.9435</b>	<b>7.15</b>	<b>7.16</b>	<b>-228</b>	<b>0.002065</b>	<b>367</b>	<b>-333</b>	<b>590</b>

Trials 1, 2 and 4 did not show any evidence of a breakdown potential, these trials also showed no signs of pitting or discoloration. The surface evaluation supported this observation by showing no change in appearance of the “as received” and the tested samples, in either pitting or discoloration. The solution also appeared clear and free of particles, similar to the appearance before the tests.



Trials 3 and 5 exhibited breakdown potentials. The average breakdown potential was found to be 367 mV. The surface evaluation shows a difference between the surface appearances of the “as received” and the tested samples in a substance, pitting, and slight discoloration. Trial 3 had one localized area of pitting. Trial 5 had two localized areas of pitting, one of which was very severe. The pitting corroded completely through the sample. The areas with pitting had a substance on the wire upon removal from the cell. For both Trials 3 and 5, the saline solution was clear with some dark particles, similar to the substance found on the areas with pitting, upon removal from the cell. The corrosion rates of the trials were consistent, with an average corrosion rate of 0.002065 mpy.

The severity and localization of the pitting on the samples that displayed a breakdown potential suggest that there was a surface anomaly in that area prior to being exposed to the corrosion cell. This would explain why they were more vulnerable to corrosion and the variation between the breakdown potentials.

### 3.1.1.14. Nitinol Etched, Mechanically Polished Results



*Figure 44. Nitinol Etched, Mechanically Polished As Drawn Surface*

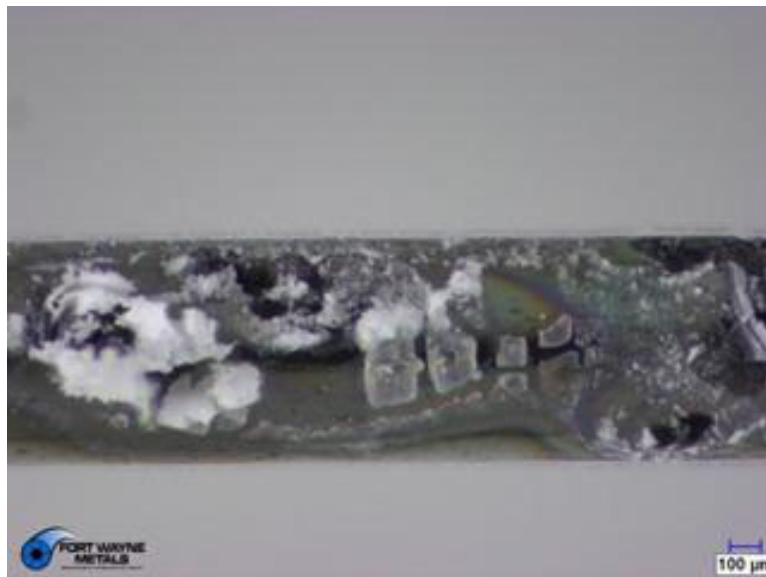


*Figure 45. Nitinol Etched, Mechanically Polished Surface After Corrosion Test*

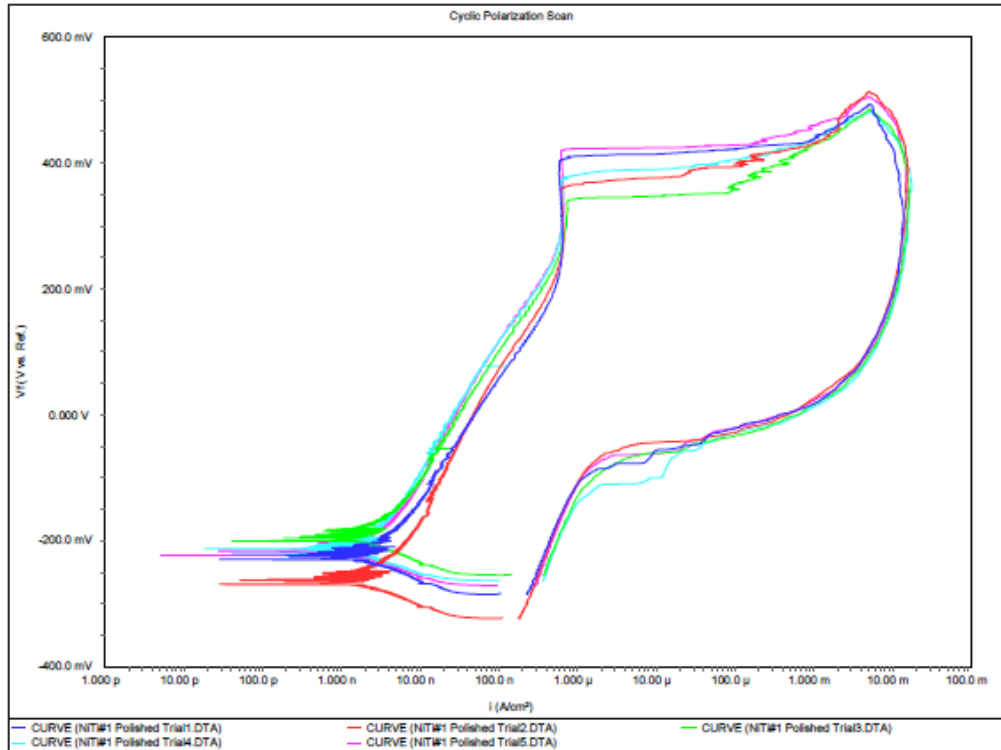


Figure 46. Nitinol Etched, Mechanically Polished Cyclic Polarization Curve

Table 21. Nitinol Etched, Mechanically Polished Cyclic Polarization Results

Trial	Surface Area (cm <sup>2</sup> )	Average pH Before Testing	Average pH After Testing	Final Open Circuit Potential E <sub>r</sub> (mV vs. SCE)	Corrosion Rate (mpy)	Breakdown Potential E <sub>b</sub> (mV vs. SCE)	Protection Potential E <sub>p</sub> (mV vs. SCE)	E <sub>b</sub> -E <sub>r</sub> (mV vs. SCE)
1	1.8506	7.15	7.20	-185	0.001946	406	N/A	591
2	1.8758	7.14	7.19	-224	0.001855	362	N/A	586
3	1.8293	7.19	7.23	-155	0.001788	341	N/A	496
4	1.8977	7.19	7.25	-164	0.001339	374	N/A	538
5	2.0063	7.16	7.22	-171	0.001520	420	N/A	591
<b>Average</b>	<b>1.8919</b>	<b>7.17</b>	<b>7.22</b>	<b>-180</b>	<b>0.001690</b>	<b>381</b>	<b>N/A</b>	<b>560</b>

The wire had small pits on the surface upon removal from the cell. There was a substance at the location of the pitting. The saline solution appeared clear with particles in it at the end of the test. The particles in the saline solution were similar in color and consistency to the substance found on the pitting sites of the samples.

The corrosion rates of the trials were consistent, with an average corrosion rate of 0.001690 mpy. All trials show a breakdown potential. The average breakdown potential was found to be 381 mV vs. SCE. The surface evaluation shows a difference between the surface appearances of the “as received” and the tested samples in a substance, pitting, and slight discoloration.

The deposits on the wire were likely a mixture of nonmetallic compounds including titanium oxides, titanium chlorides, sodium chlorides and phosphates. The deposits were likely a mixture of corrosion products and phosphate buffered saline residue. The deposits had a rough cracked morphology consistent with corrosion products.

The precipitate particles from the PBS solution consisted of the same elements as the deposits on the wire, likely as a mixture of corrosion products and PBS residue.

### 3.1.1.15. Commercially Pure Titanium Grade 1 Results



*Figure 47. Commercially Pure Titanium Grade 1 As Drawn Surface*

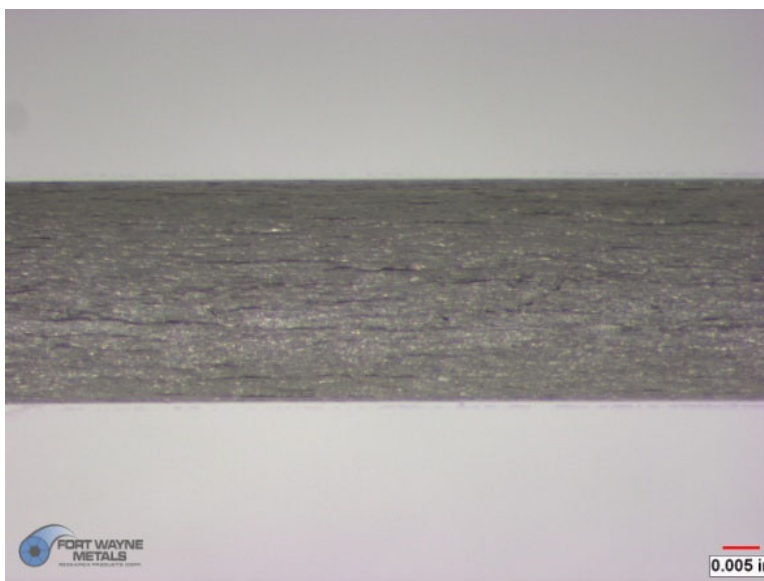


*Figure 48. Commercially Pure Titanium Grade 1 Surface After Corrosion Test*

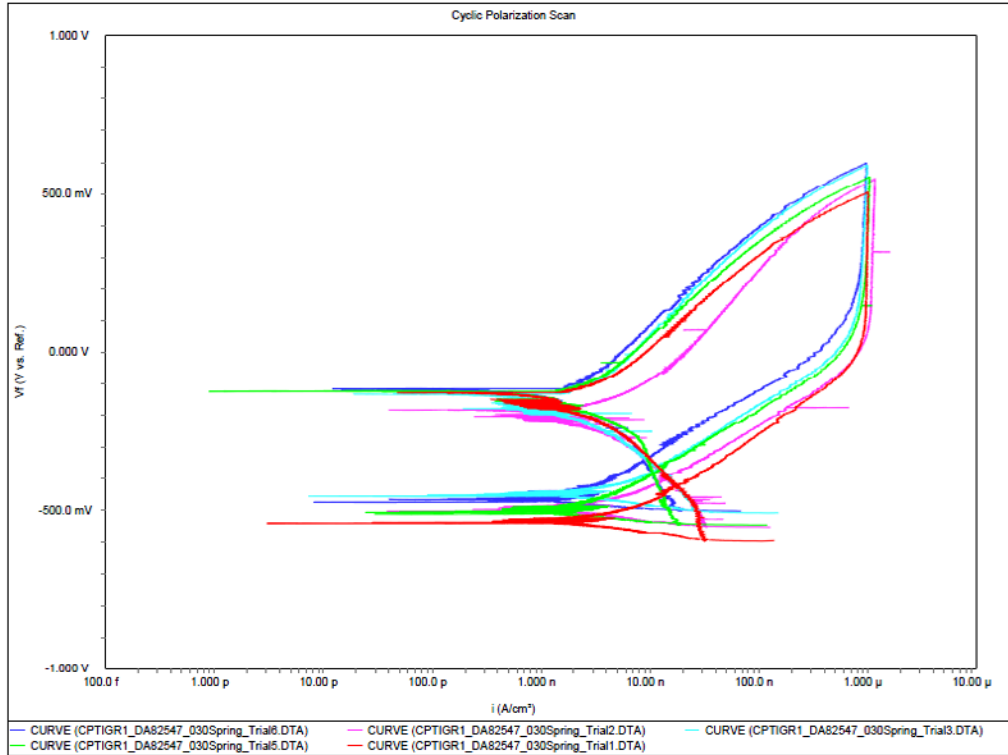


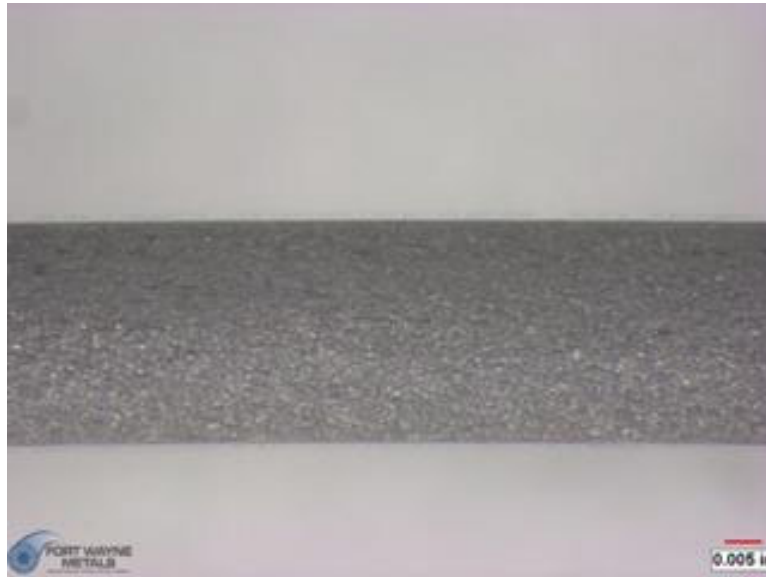
Figure 49. Commercially Pure Titanium Grade 1 Cyclic Polarization Curve

Table 22. Commercially Pure Titanium Grade 1 Cyclic Polarization Results

Trial	Surface Area (cm <sup>2</sup> )	Average pH Before Testing	Average pH After Testing	Final Open Circuit Potential E <sub>r</sub> (mV)	Corrosion Rate (mpy)	Breakdown Potential E <sub>b</sub> (mV vs. SCE)	Protection Potential E <sub>p</sub> (mV vs. SCE)	E <sub>b</sub> -E <sub>r</sub> (mV vs SCE)
1	0.9242	7.11	7.11	-495	0.002641	N/A	N/A	N/A
2	1.9345	7.08	7.07	-452	0.002356	N/A	N/A	N/A
3	1.9029	7.06	7.06	-408	0.002655	N/A	N/A	N/A
5	1.9099	7.08	7.08	-445	0.001336	N/A	N/A	N/A
6	1.8594	7.11	7.08	-401	0.001292	N/A	N/A	N/A
<b>Average</b>	<b>1.7062</b>	<b>7.09</b>	<b>7.08</b>	<b>-440</b>	<b>0.002247</b>	<b>N/A</b>	<b>N/A</b>	<b>N/A</b>

The wire appeared the same before and after the test. There was no pitting. The saline solution looked clear as it did before the test. The material did not show a breakdown potential. The surface evaluation maintained this conclusion by showing no difference between the appearances, in either pitting or discoloration. The average corrosion rate was found to be 0.002247 mpy.

### 3.1.1.16. Titanium 6Aluminum 4Vanadium ELI Results



*Figure 50. Titanium 6Aluminum 4Vanadium ELI As Drawn Surface*

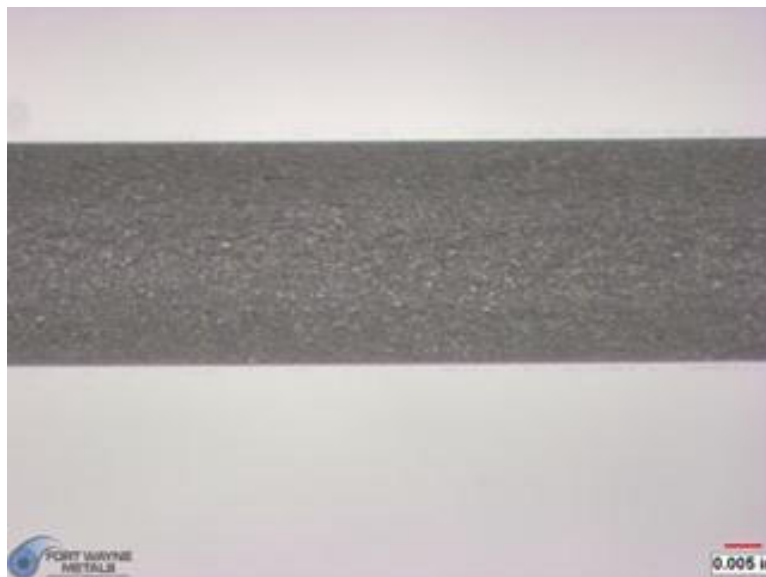


*Figure 51. Titanium 6Aluminum 4Vanadium ELI Surface After Corrosion Test*

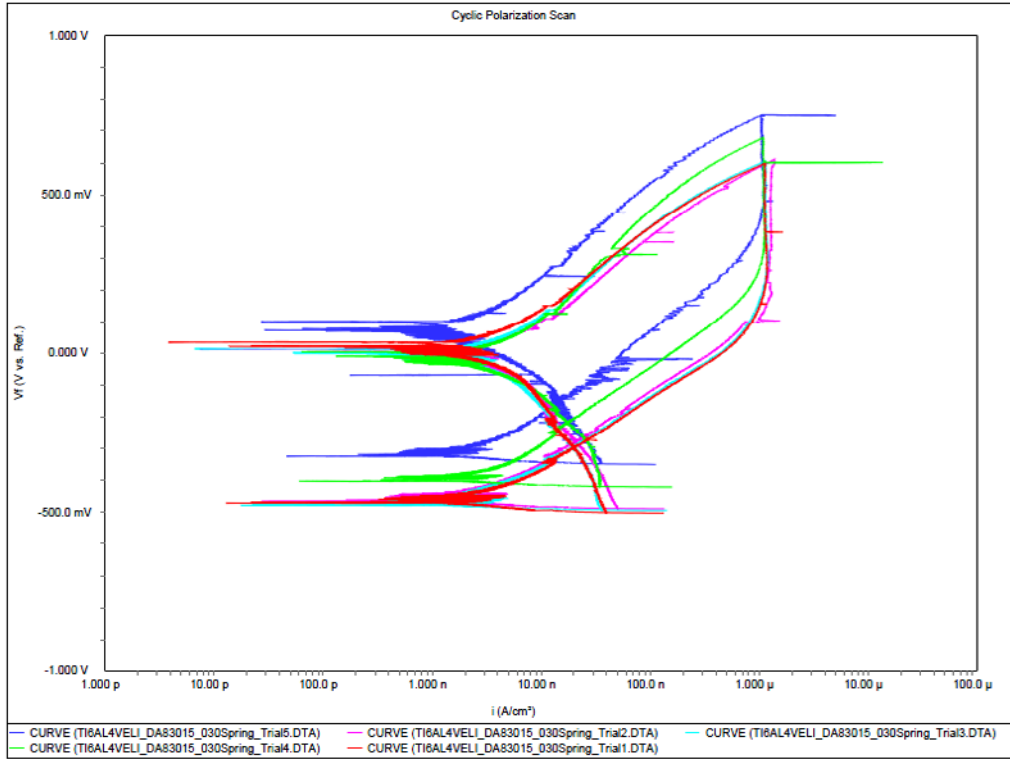


Figure 52. Titanium 6Aluminum 4Vanadium ELI Cyclic Polarization Curve

Table 23. Titanium 6Aluminum 4Vanadium ELI Cyclic Polarization Results

Trial	Surface Area (cm <sup>2</sup> )	Average pH Before Testing	Average pH After Testing	Final Open Circuit Potential (mV)	Corrosion Rate (mpy)	Breakdown Potential E <sub>b</sub> (mV vs. SCE)	Protection Potential E <sub>p</sub> (mV vs. SCE)	E <sub>b</sub> -E <sub>r</sub> (mV vs SCE)
1	1.9759	7.11	7.11	-401	0.001287	N/A	N/A	N/A
2	1.9880	7.10	7.10	-388	0.001285	N/A	N/A	N/A
3	1.9391	7.10	7.11	-393	0.002091	N/A	N/A	N/A
4	1.8780	7.05	7.05	-320	0.003403	N/A	N/A	N/A
5	1.9491	7.07	7.14	-249	0.001392	N/A	N/A	N/A
<b>Average</b>	<b>1.9460</b>	<b>7.09</b>	<b>7.10</b>	<b>-350</b>	<b>0.001892</b>	<b>N/A</b>	<b>N/A</b>	<b>N/A</b>

Wire appeared the same before and after the test. There was no pitting. The saline solution looked clear as it did before the test. The material did not show a breakdown potential. The surface evaluation maintained this conclusion by showing no difference between the appearances, in either pitting or discoloration. The average corrosion rate was found to be 0.001892 mpy.



### 3.1.1.17. 35N LT® DFT®-41Ag Masked Results

Ten [10] samples were prepared to be tested in separate trials. The ends of five [5] were left unmasked in order to expose the core to the corrosion cell. The ends of the other five [5] were masked to conceal the core. This was done to determine if any galvanic reaction occurred during the test between the sheath material and the core material.



*Figure 53. 35N LT® DFT®-41Ag Masked As Drawn Surface*

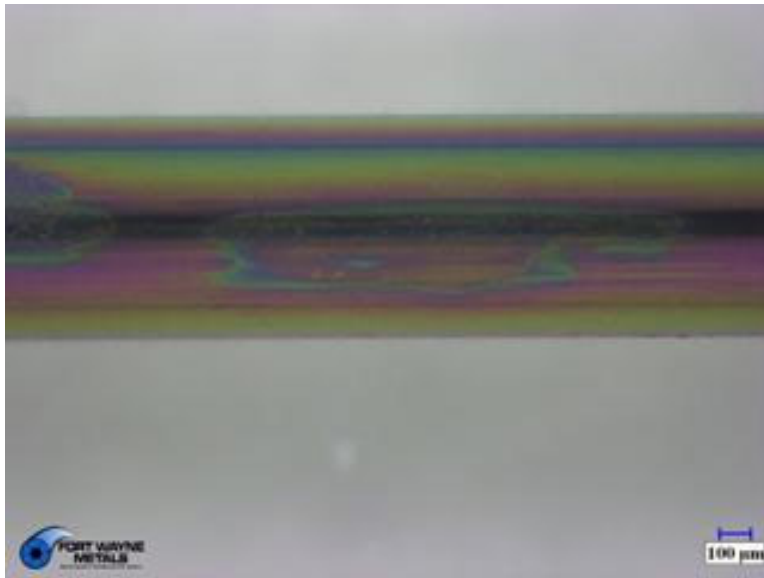


Figure 54. 35N LT® DFT®-41Ag Masked Surface After Corrosion Test

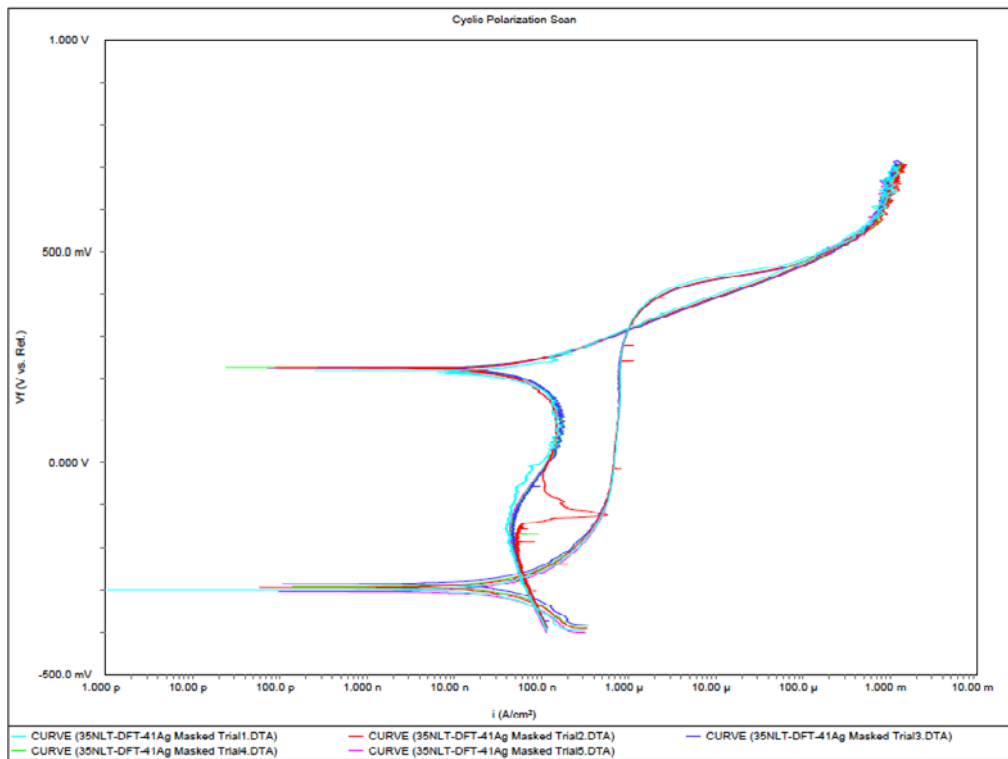


Figure 55. 35N LT® DFT®-41Ag Masked Cyclic Polarization Curve

Table 24. 35N LT® DFT®-41Ag Masked Cyclic Polarization Results

Sample	Surface Area (cm <sup>2</sup> )	Average pH Before Testing	Average pH After Testing	Final Open Circuit Potential E <sub>r</sub> (mV vs SCE)	Corrosion Rate (mpy)	Breakdown Potential E <sub>b</sub> (mV vs. SCE)	Protection Potential E <sub>p</sub> (mV vs. SCE)	E <sub>b</sub> -E <sub>r</sub> (mV vs SCE)
<b>Trial 1</b>	2.0084	7.14	7.15	-297	0.12158	N/A	N/A	N/A
<b>Trial 2</b>	1.8950	7.15	7.14	-292	0.08536	N/A	N/A	N/A
<b>Trial 3</b>	1.9832	7.15	7.14	-283	0.07844	N/A	N/A	N/A
<b>Trial 4</b>	2.0446	7.15	7.15	-290	0.07986	N/A	N/A	N/A
<b>Trial 5</b>	2.0774	7.13	7.13	-301	0.07794	N/A	N/A	N/A
<b>Masked Average</b>	<b>2.0017</b>	<b>7.14</b>	<b>7.14</b>	<b>-293</b>	<b>0.08864</b>	<b>N/A</b>	<b>N/A</b>	<b>N/A</b>

3.1.1.18. 35N LT®-DFT®-41Ag - Unmasked



Figure 56. 35N LT® DFT®-41Ag Unmasked As Drawn Surface

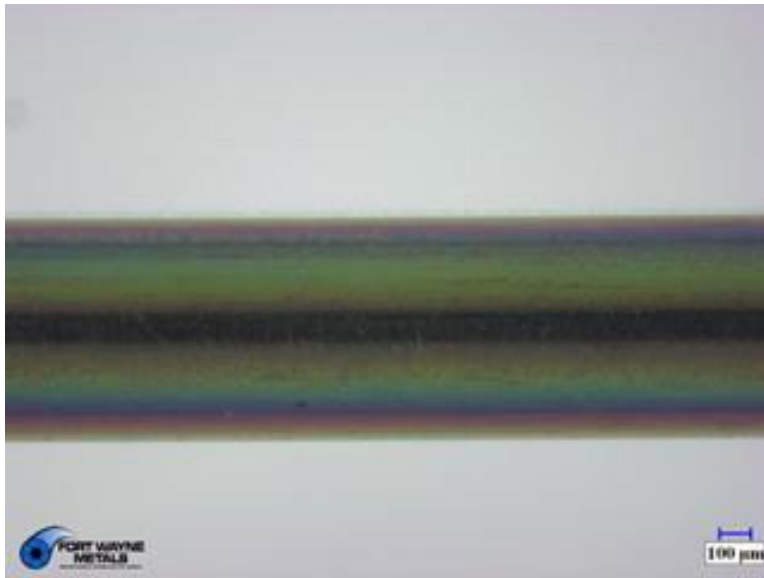


Figure 57. 35N LT® DFT®-41Ag Unmasked Surface After Corrosion Test

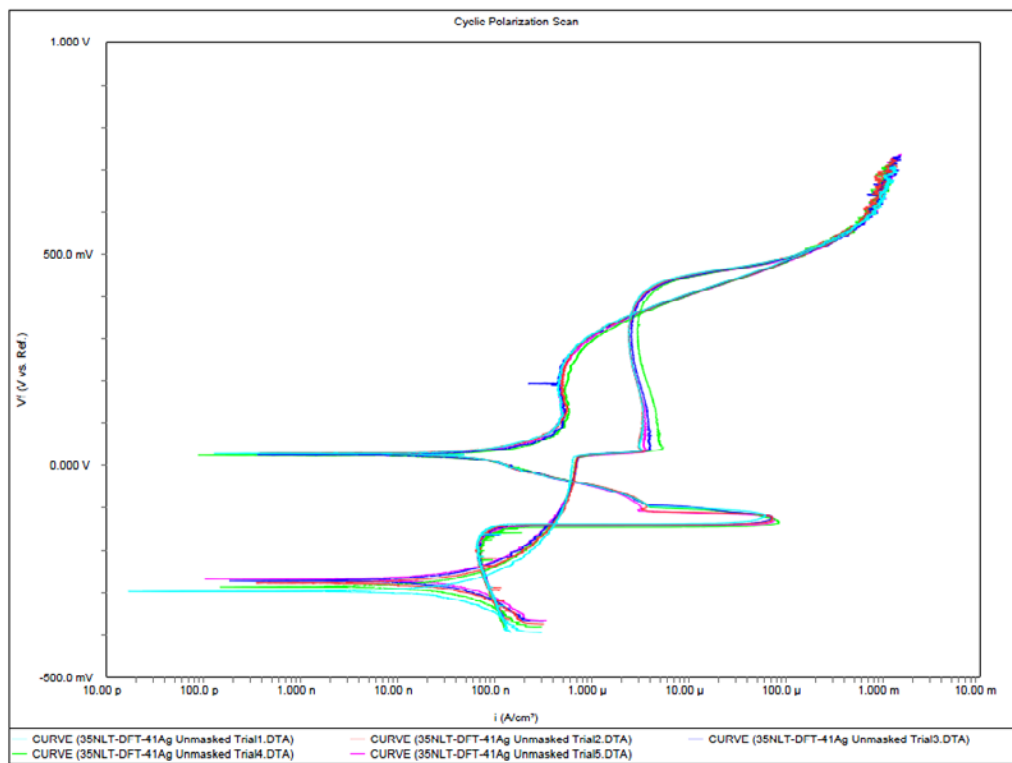


Figure 58. 35N LT® DFT®-41Ag Unmasked Cyclic Polarization Curve

Table 25. 35N LT® DFT®-41Ag Unmasked Cyclic Polarization Results

Sample	Surface Area (cm <sup>2</sup> )	Average pH Before Testing	Average pH After Testing	Final Open Circuit Potential E <sub>r</sub> (mV vs SCE)	Corrosion Rate (mpy)	Breakdown Potential E <sub>b</sub> (mV vs SCE)	Protection Potential E <sub>p</sub> (mV vs. SCE)	E <sub>b</sub> -E <sub>r</sub> (mV vs SCE)
<b>Trial 1</b>	1.9819	7.06	7.06	-266	0.07721	23	N/A	289
<b>Trial 2</b>	1.9151	7.12	7.12	-282	0.07071	23	N/A	305
<b>Trial 3</b>	1.9980	7.13	7.12	-269	0.05849	23	N/A	292
<b>Trial 4</b>	1.7202	7.13	7.12	-275	0.05960	21	N/A	296
<b>Trial 5</b>	1.8685	7.15	7.14	-294	0.07377	21	N/A	315
<b>Unmasked Average</b>	<b>1.8967</b>	<b>7.12</b>	<b>7.11</b>	<b>-277</b>	<b>0.06796</b>	<b>22</b>	<b>N/A</b>	<b>299</b>

The surface evaluation showed a difference between the surface appearances of the “as received” and the tested samples in discoloration. These are the second lowest breakdown potentials measured, only greater than the Alloy 420 material. The average corrosion rate was found to be 0.07830 mpy.

There is not a difference in surface appearance comparing the masked and unmasked material. Also, there is an insignificant difference between the average corrosion rates of the masked (0.08864 mpy) and unmasked (0.06796 mpy) material, considering the amount of variation between trials of the same material.

There is, however, a difference in the cyclic polarization scans of the masked and unmasked material. The unmasked material shows an average breakdown potential of 22mV, where the masked material shows no breakdown.

There also seems to be a corrosion of the material on the exposed end. The coarseness and jagged areas seen on the cut edge of the “as received” material as well as the cut edge of the unexposed core do not appear on the core exposed to the corrosion cell.

There is not a difference in the cross section of the “as received” material and the tested material.

### 3.2. Findings: Converging and Conflicting Evidence

The difference in the cyclic polarization scans of the masked and unmasked DFT material was suspected, but had not been documented. The unmasked material shows an average breakdown potential of 22mV, where the masked material shows no breakdown.

Because the only substantial, continuous variation in the samples is the exposure of the silver core, it is believed that this breakdown potential is of the silver material exposed to the corrosion cell and the galvanic couple established between the 35N LT sheath and the silver core.

This breakdown is revealed in the difference between the unexposed core of the sample prior to the test, Figure 59, and the exposed core of the unmasked sample after the test, Figure 60. There is a discoloration of the silver core that is exposed to the cell that does not appear if the core is not exposed.

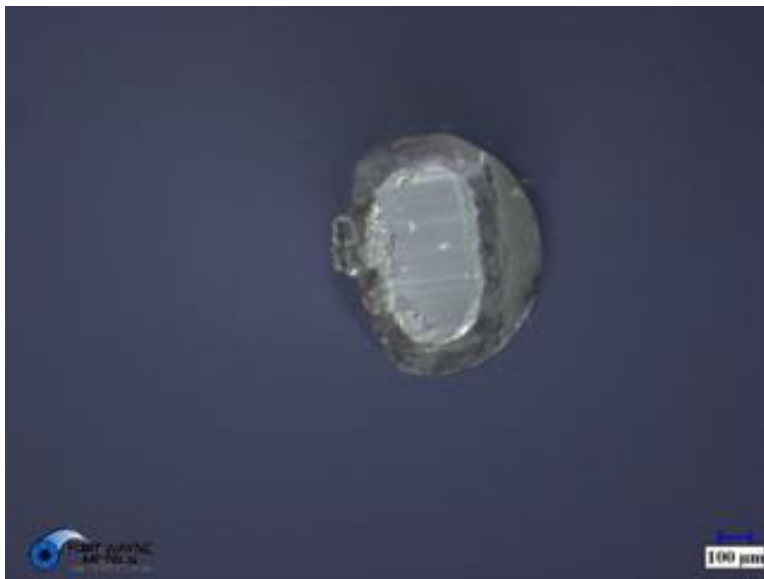


*Figure 59. 35N LT® DFT®-41Ag Cut End PRIOR TO Corrosion Test*

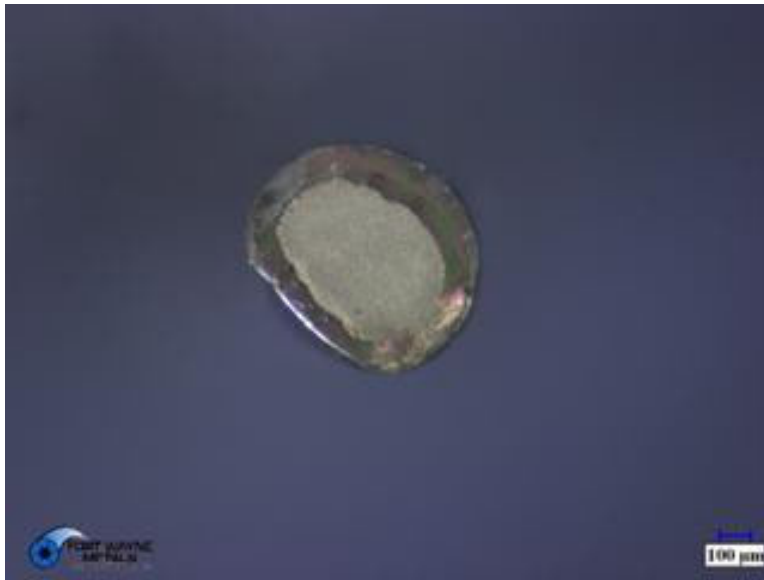


Figure 60. 35N LT® DFT®-41Ag Cut End AFTER Corrosion Test

Figure 61 plots the cyclic polarization curve of both the masked and the unmasked samples to show the differences.

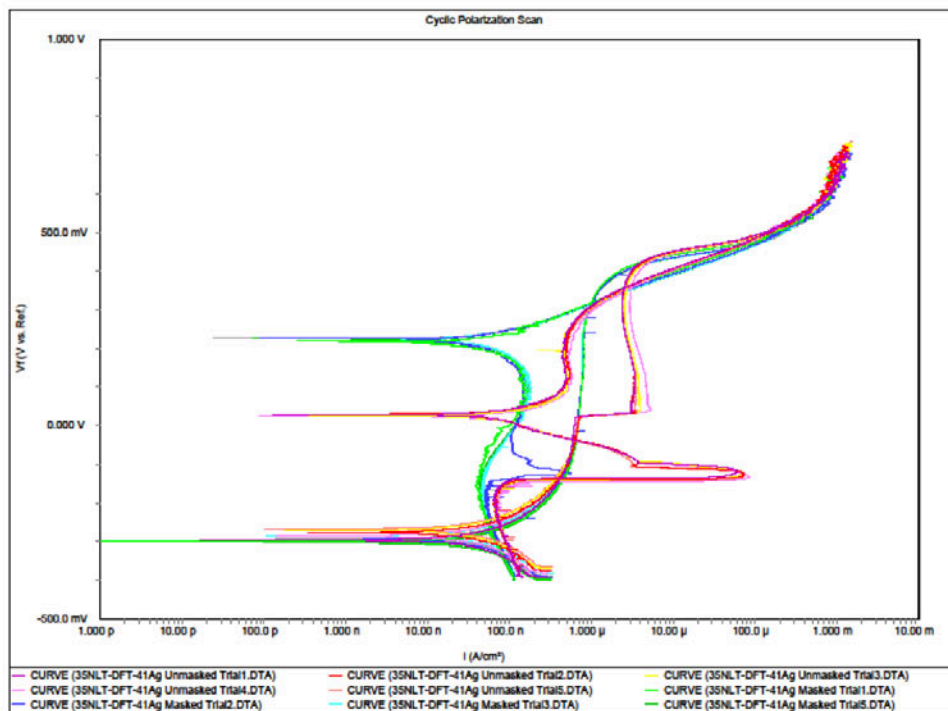


Figure 61. 35N LT® DFT®-41Ag Combined (Masked and Unmasked) Cyclic Polarization Curve

### 3.3. Further Directions and Experiments

Additional SEM analysis of the exposed ends of DFT® would be beneficial to demonstrate the theory that the breakdown is due to a galvanic couple.

Testing of samples in a passive condition to compare with the as drawn samples in this study would determine the amount of improvement that could be gained with the appropriate passivation solution treatment.

The original saltwater galvanic series provided in ASTM G82 indicated exposure times of “5 to 15 days”. A study of Corrosion Potentials over extended exposure study times of 1 Week, 1 Month, or 1 Year would be time consuming to conduct, but would provide further data.

As mentioned in Section 1.2 Gaps in Previous Knowledge, there are a number of alternative solutions which could be used to conduct the corrosion analysis. Using these alternate solutions could be used to quantify the results in the various mediums.

As with any in vitro test, there needs to be an analysis of the results with those obtained in vivo. As more implants are explanted and analyzed, the results need to be examined for areas of correlation and differences to help advance the understanding of the materials.

While this survey included a total of 17 materials, this is by no means the exhaustive list of materials with medical applications. Further studies of additional existing and proposed materials are suggested.

### 3.4. Discussion and Summary

Each of the corrosion test parameters collected is summarized in Appendix A.



Following the recommendation of Corbett, Confidence Interval graphs for each of the parameters collected were prepared using Minitab.

The rest potential ( $E_r$ ) values, Figure 62. *Interval Plot of  $E_r$* , for the L605 alloy and both Titanium materials were the only materials to have a confidence interval exceeding 100mV. It is also interesting to note that the Nitinol Dark Oxide is at the low end of the observed values, while the Nitinol Light Oxide is at the high end of the range of values. Typically a lower  $E_r$  value is desirable. See further discussion below.

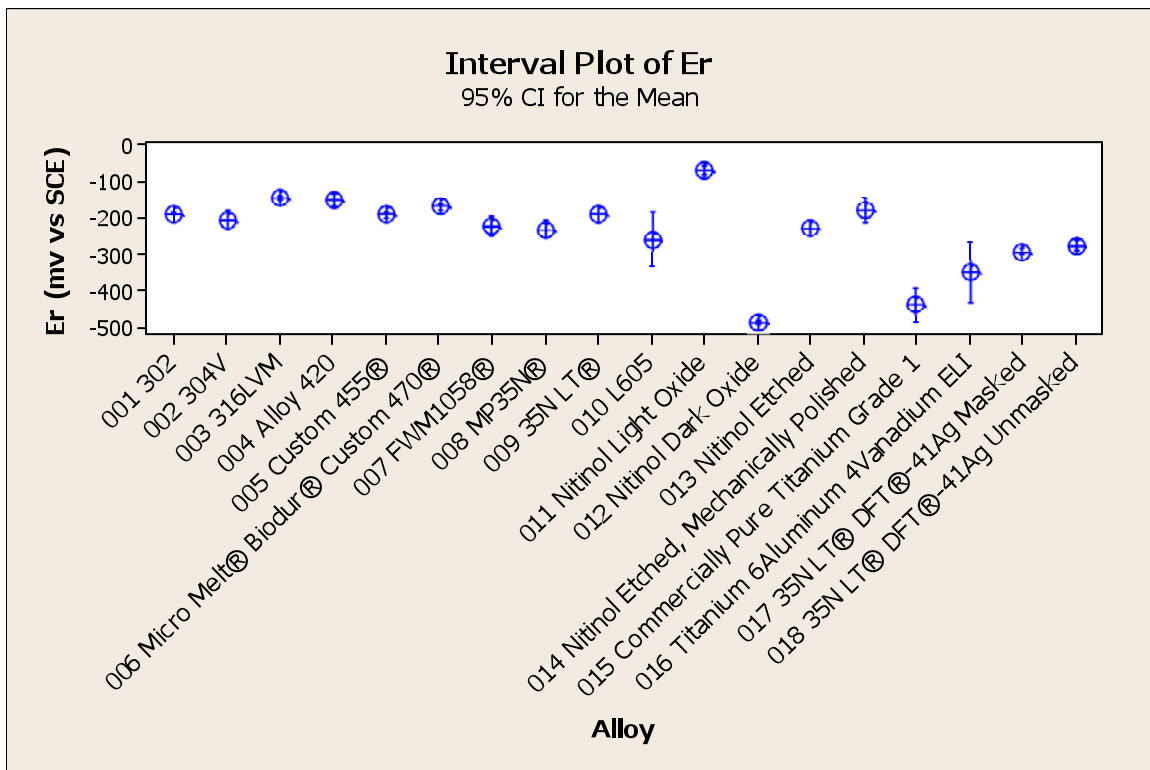


Figure 62. *Interval Plot of  $E_r$ , Rest Potential*

A low uniform corrosion rate is desired. The confidence interval plot for uniform corrosion rate, Figure 63. *Interval Plot of Uniform Corrosion Rate*, is the most consistent of the plots. The only material for which the confidence interval exceeded 0.5 mpy was the Nitinol Dark Oxide set of samples. The MP35N and the 35N LT materials had the highest uniform corrosion rates of the materials that did not experience breakdown.

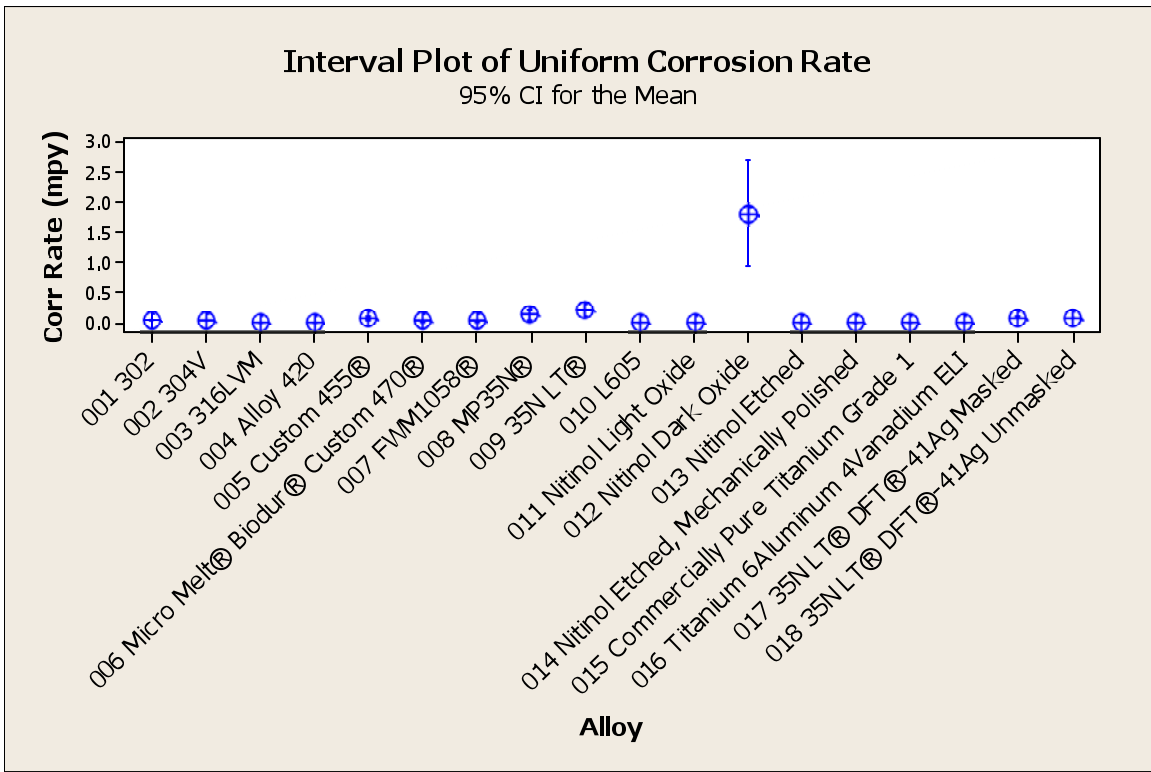


Figure 63. *Interval Plot of Uniform Corrosion Rate*

The interval plot for breakdown potential ( $E_b$ ) has values only for those alloys that experienced the breakdown phenomenon, Figure 64. The corrosion resistant alloys do not have a value for  $E_b$ . These values were very consistent with the exception of the Nitinol Etched material. This is due to three samples surviving without breakdown and the statistic being calculated on two values with a spread of 255mv creating a very large standard deviation. Shabalovskaya [24] reported that chemically etched Nitinol corrosion resistance is superior to the mechanically polished surface. This is confirmed in the three tests that did not experience breakdown, however this confidence interval is not to be considered accurate, other than the confirmation of inconsistent results for Nitinol.

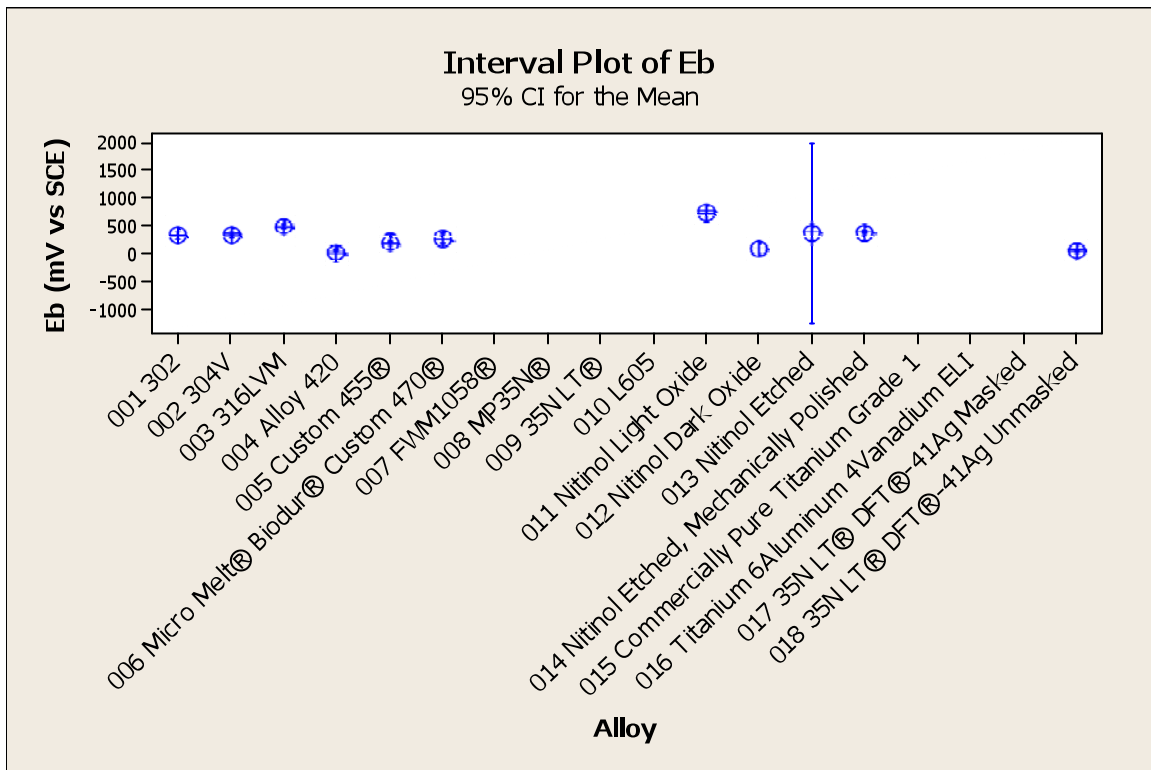


Figure 64. Interval Plot of  $E_b$ , Breakdown Potential

The protection potential,  $E_p$ , Figure 65. *Interval Plot of  $E_p$* , is a parameter that is achieved only after the material has experienced breakdown, although not every material reaches this condition where pitting will not propagate. Both the Nitinol Light Oxide and Nitinol Etched materials had only one sample reach protection potential, resulting in no confidence interval. The alloy 420 material did not reach a protection potential, indicating the material never achieves ‘repassivation’.

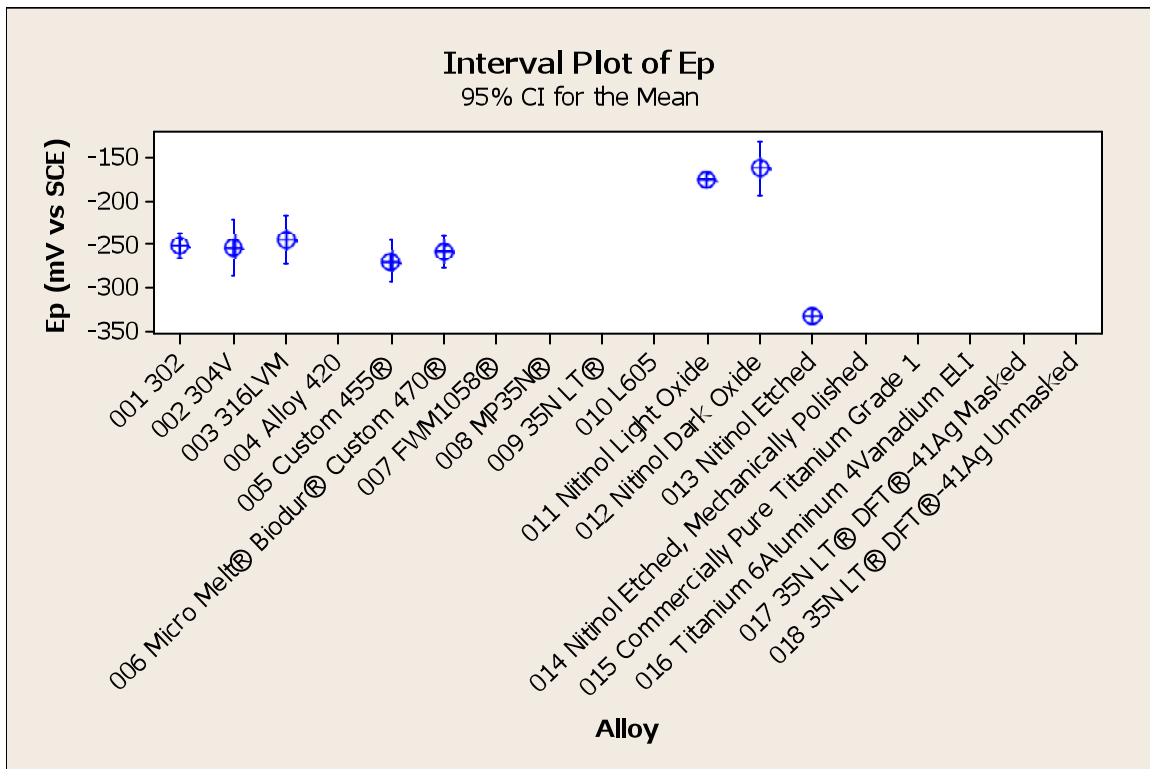


Figure 65. *Interval Plot of  $E_p$ , Protection Potential*

The DFT® interface should be sealed to reduce galvanic corrosion. This is the common practice for the use of the wire for both cardiac and neuro stimulation leads. These are typically jacketed with a dielectric coating, typically a fluoropolymer. The coated wires are then placed in the lumen of a silicone jacket for final product assembly.

The ASTM G82 standard publishes the well-known Galvanic Series which lists the metals of interest in order of their corrosion potentials, starting with the most active (electronegative) and proceeding in order to the most noble (electropositive). The potentials themselves (versus an appropriate reference half-cell) are listed so that the potential difference between metals in the series can be determined. This type of Galvanic Series has been put in graphical form as a series of bars displaying the range of potentials exhibited by the metal listed opposite each bar. Such a series is illustrated in Figure 66.

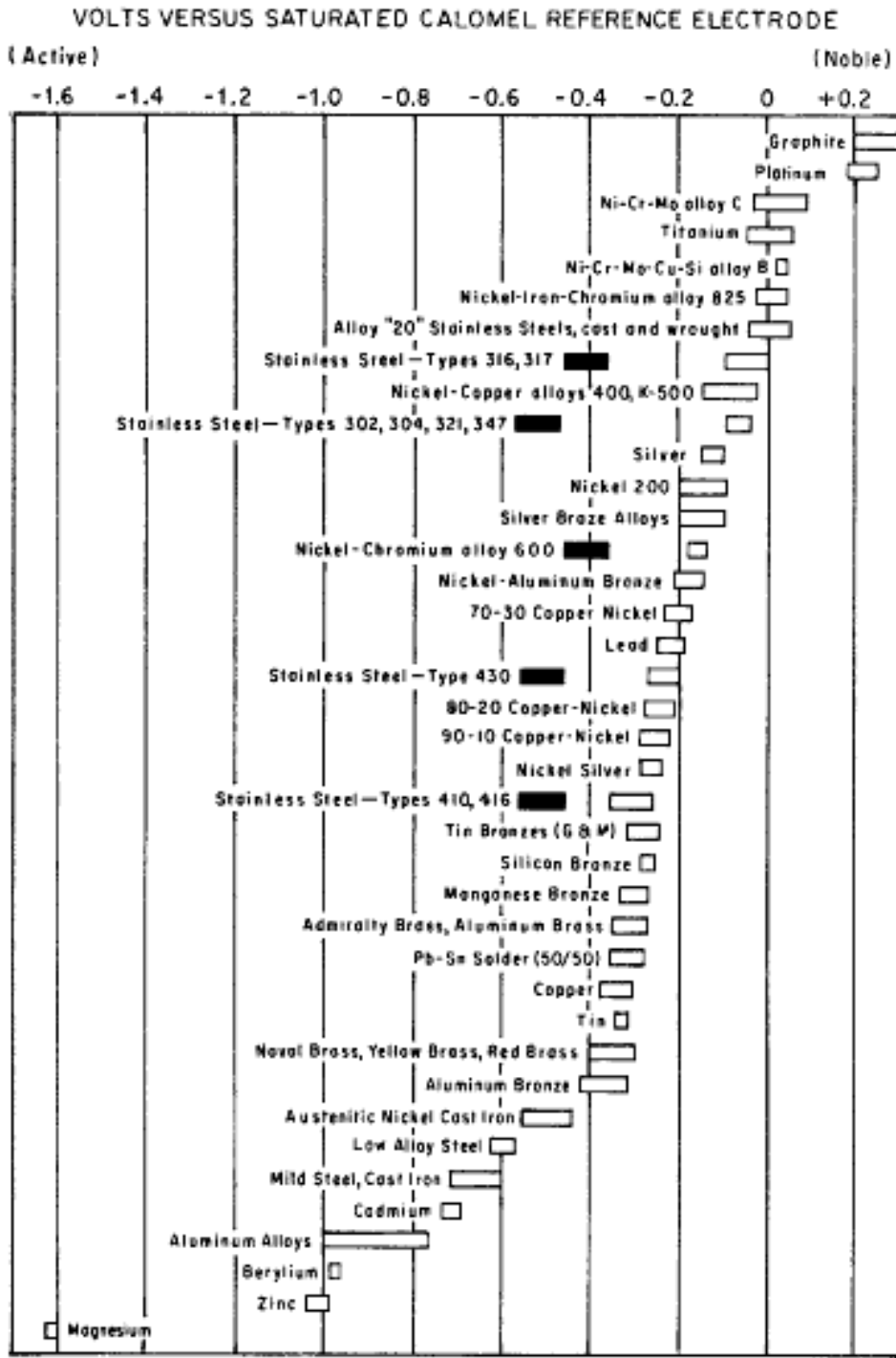


Figure 66. ASTM G82 Galvanic Series<sup>9</sup>

<sup>9</sup> From LaQue, F. L., Marine Corrosion, Causes and Prevention, John Wiley and Sons, New York, NY, 1975

Table 26 lists the Corrosion Potential,  $E_{corr}$ , results for each trial of the samples tested in this study. The data is graphed in Figure 67.

*Table 26. Corrosion Potential,  $E_{corr}$ , Results*

Corrosion Potential $E_{corr}$ (mV vs. SCE)										
Alloy	Trial 1	Trial 2	Trial 3	Trial 4	Trial 5	Average	Range	Standard Deviation	Min	Max
302	-235	-226	-230	-223	-227	-228	12	4.55	-235	-223
304-V	-225	-216	-220	-262	-262	-237	46	23.04	-262	-216
316-LVM	-187	-194	-195	-205	-185	-193	20	7.89	-205	-185
420	-211	-209	-195	-183	-178	-195	33	14.87	-211	-178
Custom 455®	-239	-239	-226	-234	-236	-235	13	5.36	-239	-226
MicroMelt® Biodur® Custom 470®	-232	-224	-218	-222	-219	-223	14	5.57	-232	-218
FWM1058®	-246	-253	-192	-268	-233	-238	76	28.85	-268	-192
MP35N®	-243	-246	-220	-262	-214	-237	48	19.75	-262	-214
35N LT®	-194	-199	-163	-201	-199	-191	38	15.97	-201	-163
L605	-232	-236	-199	-304	-361	-266	162	65.22	-361	-199
Nitinol Light Oxide	-120	-117	-124	-119	-108	-118	16	5.94	-124	-108
Nitinol Dark Oxide	-484	-486	-495	-493	-491	-490	11	4.66	-495	-484
Nitinol Etched	-293	-268	-278	-267	-256	-272	37	13.90	-293	-256
Nitinol Polished	-230	-269	-200	-213	-223	-227	69	26.05	-269	-200
CP Ti Gr1	-474	-502	-456	-506	-540	-496	84	32.23	-540	-456
Ti-6Al-4V ELI	-471	-464	-477	-402	-324	-428	153	65.26	-477	-324
35NLT®-DFT®-41%Ag Masked	-300	-295	-286	-293	-304	-296	18	6.88	-304	-286
35NLT®-DFT®-41%Ag Unmasked	-298	-278	-273	-287	-268	-281	30	11.90	-298	-268

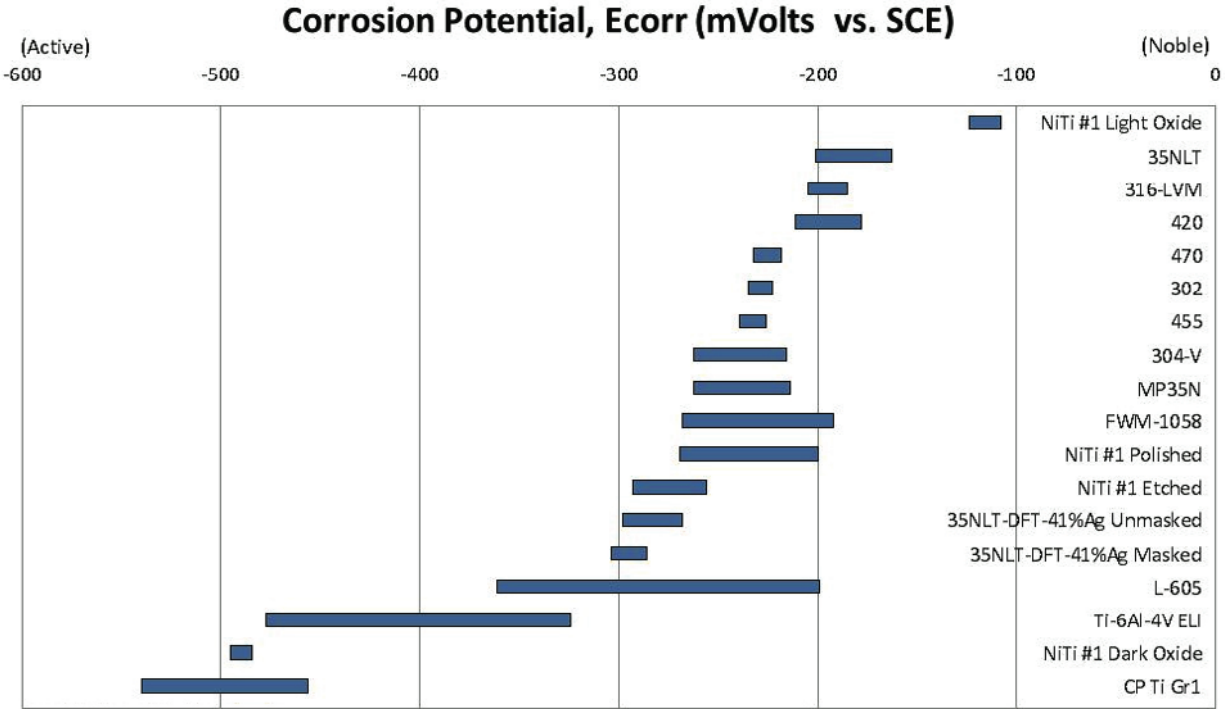


Figure 67. Galvanic Series of Data Generated in this Study

Comparing the data from this study to the chart from ASTM G82 shows some inconsistent results. For example the 1975 study showed a range of -100mV to 0mV for Stainless Steel Type 316. This is relatively similar to the results obtained for this study of -205mV to -185mV. However, the results for Titanium in particular do not agree with the published graph. The graph shows values of -50mV to +100mV, whereas the values measured in the study range from -540mV to -456 mV for CP Ti Gr 1, and -477mV to -324mV for Ti 6Al 4V.

Rosenbloom and Corbett [4] reported that the solution can have a substantial effect on the results and this may explain what would be perceived as a poor performance of some of the materials in this test. The ASTM G82 study was performed using saltwater as the electrolyte solution, whereas this study used buffered Phosphate solution. The solution was described as ‘Flowing Seawater’ with exposure of 5 to 15 days at temperatures from 5 to 30°C. Exposure



times of this study were for only 1 hour prior to the start of the test. Additionally the Titanium grade is not specified in the G82 graph.

Rondelli [17] tested materials in artificial physiological solution at a temperature of 40°C.

The authors reported E<sub>corr</sub> values of:

316L - ~-350mV vs SCE

Ti 6Al 4V ~ -425mV vs SCE

These values, particularly for the Titanium alloy, closely agree with the measurements obtained in this study. The differences between the previously reported Titanium values and those gathered in this study can be explained by these differences in electrolyte solution and exposure time.

Figure 68 plots the two studies for direct comparison.

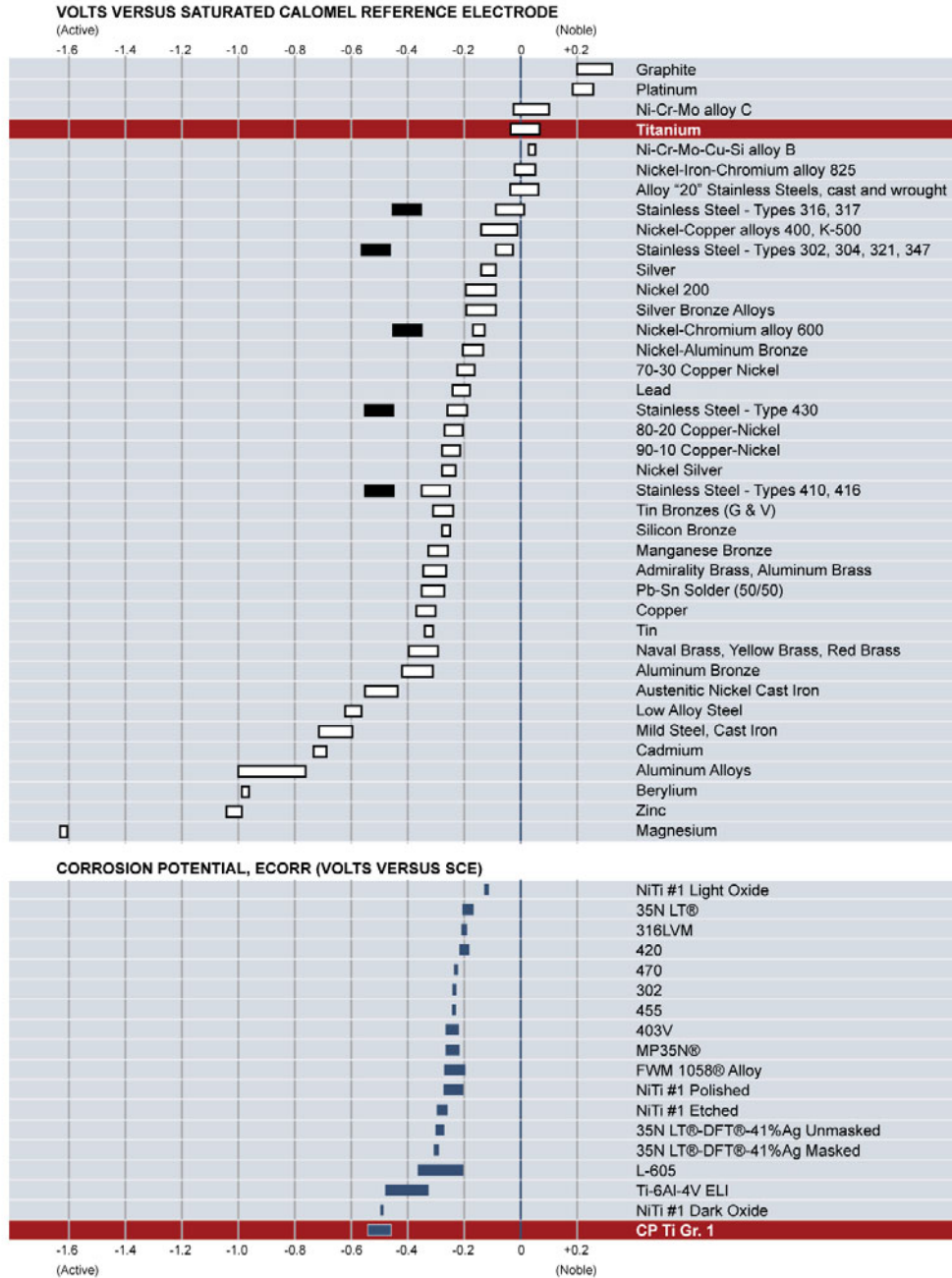


Figure 68. Current Study E<sub>corr</sub> Series vs. ASTM G82 Galvanic Series

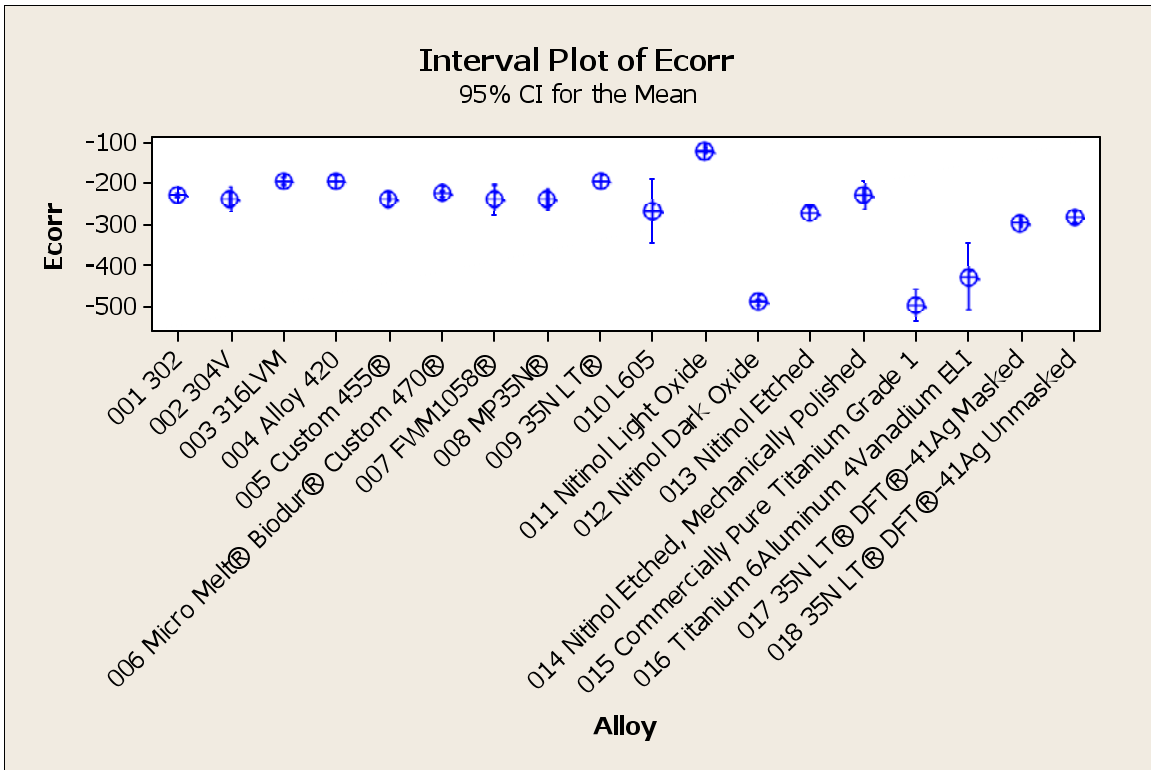


Figure 69. Interval Plot of E<sub>corr</sub>, Corrosion Potential

Figure 69 plots the confidence intervals for the corrosion potential (E<sub>corr</sub>) parameter. In particular the L605 and both Titanium materials demonstrated greater variation than desired and further testing is suggested to increase the confidence of the data for these materials.

### 3.5. Conclusions and Key Points

Following Corbett’s [10] recommendation for evaluation of the breakdown potential ( $E_b$ ), Table 27. *Evaluation of Breakdown Potential Results* presents the recommendations from this study. Corbett did not provide a rating suggestion for materials that do not experience breakdown. This category is added for additional clarity. The alloys that did not experience breakdown are listed in the order the samples are presented in this report, i.e. no specific ranking is intended. The balance of the alloys are ranked based on  $E_b$  average within the sub-categories.

*Table 27. Evaluation of Breakdown Potential Results*

<b>Alloy [<math>E_b</math> average, if applicable]</b>	<b>Breakdown Potential, <math>E_b</math> (mV vs SCE)</b>	<b>Corrosion Resistant Condition</b>
FWM1058® MP35N® 35N LT® L605 Cp Ti Gr 1 Ti 6Al 4V ELI 35N LT® DFT® 41Ag Masked Nitinol Etched <sup>10</sup>	No Breakdown observed	Most Desirable
Nitinol Light Oxide [737]	> +600	Optimum
316LVM [482] Nitinol Etched Mechanically Polished [381] 304V [329] 302 [324]	+300 to +600	Marginal
Micro Melt® Biodur® Custom 470® [253] Custom 455® [186] Nitinol Dark Oxide [80] 35N LT® DFT® 41Ag Un-Masked [22] Alloy 420 [14]	< +300	Not Optimum

<sup>10</sup> The Nitinol Etched material did not experience breakdown on three of the five samples.

Corlett [11] has proposed an evaluation based on the parameter  $E_b-E_r$ . This data is presented in Table 28. As accomplished above, if the material did not experience breakdown, this is considered optimal performance. These alloys are listed in the order the samples are presented in this report, i.e. no specific ranking is intended. The balance of the alloys are ranked based on the parameter  $E_b-E_r$  average within the sub-categories

*Table 28. Evaluation of  $E_b-E_r$*

Alloy [ $E_b$ average, if applicable]	$E_b-E_r$ (mV vs SCE)	
FWM1058®	No Breakdown observed	
MP35N®		
35N LT®		
L605		
Cp Ti Gr 1		
Ti 6Al 4V ELI		
35N LT® DFT® 41Ag Masked		
Nitinol Etched <sup>11</sup>		
Nitinol Light Oxide		809
316LVM	628	
Nitinol Dark Oxide	567	
Nitinol Etched Mechanically Polished	560	
304V	533	
302	521	
Micro Melt® Biodur® Custom 470®	423	
Custom 455®	378	
35N LT® DFT® 41Ag Un-Masked	299	
Alloy 420	163	

A close analysis of the data in Tables 27 and 28 indicates the ranking of only the Nitinol Dark Oxide material differs between the two tables. This indicates both parameters may be of interest to the device designer. The movement of the Nitinol Dark Oxide indicates one of the reasons there is much debate about the corrosion performance of this alloy system.

<sup>11</sup> The Nitinol Etched material did not experience breakdown on three of the five samples.

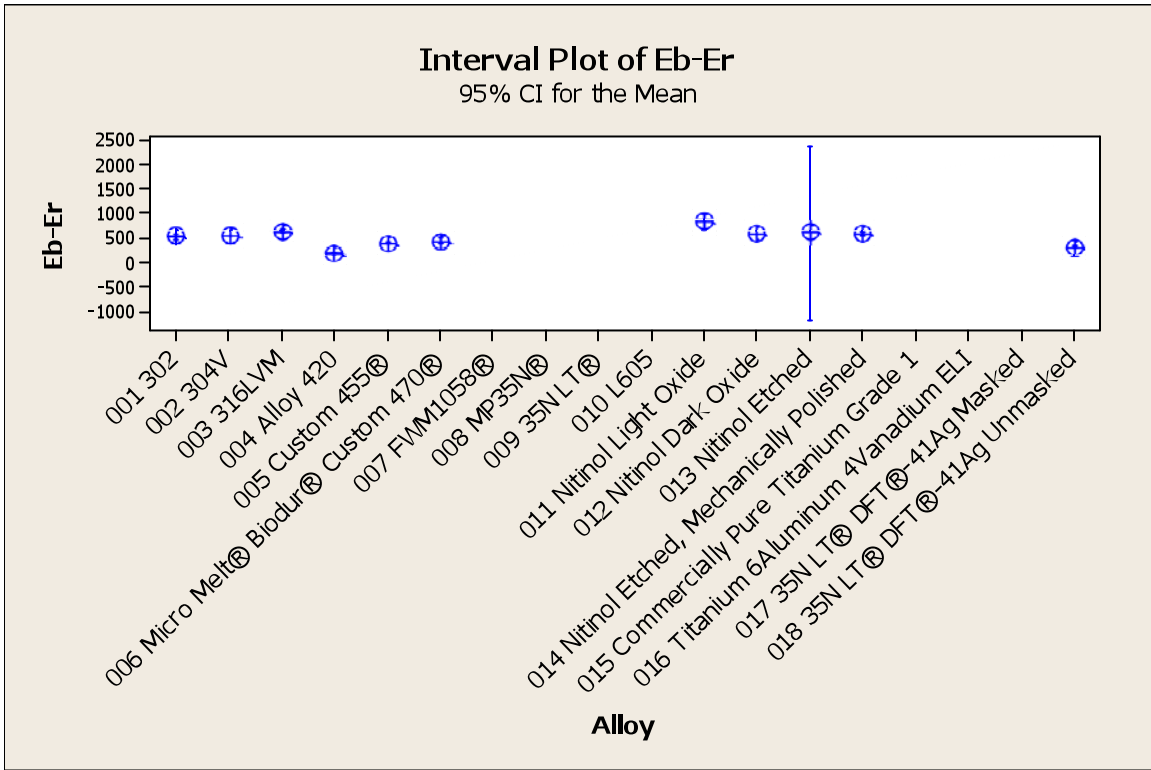


Figure 70. Interval Plot of Eb-Er

The interval plot of Eb-Er, Figure 70, shows excellent performance with the exception of the Nitinol Etched material. As noted earlier, three of the samples did not breakdown during testing. The average and confidence interval are calculated on the two samples that did experience breakdown and only serve to highlight the inconsistency of Nitinol performance in corrosion testing.

Table 29 summarizes the averages values for the eighteen tests completed in this study.

*Table 29. Corrosion Testing Results Summary*

Alloy	Surface Area (cm <sup>2</sup> )	Ave. pH Before Testing	Ave. pH After Testing	E <sub>corr</sub> Average Corrosion Potential (mV vs. SCE)	E <sub>r</sub> Final Open Circuit Potential (mV vs. SCE)	Corrosion Rate (mpy)	E <sub>b</sub> - Breakdown Potential (mV vs. SCE)	E <sub>p</sub> - Protection Potential (mV vs. SCE)	E <sub>b</sub> -E <sub>r</sub> (mV vs. SCE)
<b>302</b>	1.891	7.19	7.20	-228	-188	0.0252	324	-252	521
<b>304V</b>	1.905	7.12	7.14	-237	-204	0.0333	329	-254	533
<b>316LVM</b>	1.894	7.10	7.14	-193	-146	0.0126	482	-245	628
<b>Alloy 420</b>	1.892	7.19	7.19	-195	-150	0.0152	14	N/A	163
<b>Alloy Custom 455®</b>	1.962	7.11	7.13	-235	-192	0.0773	186	-270	378
<b>Micro Melt® Biodur® Custom 470®<sup>12</sup></b>	1.938	7.09	7.11	-223	-170	0.0265	253	-258	423
<b>FWM1058®</b>	1.924	7.13	7.14	-238	-223	0.0228	N/A	N/A	N/A
<b>MP35N®</b>	2.011	7.08	7.09	-237	-232	0.1332	N/A	N/A	N/A
<b>35N LT®</b>	1.912	7.06	7.07	-191	-191	0.2178	N/A	N/A	N/A
<b>L-605</b>	1.943	7.11	7.11	-266	-259	0.0112	N/A	N/A	N/A
<b>Nitinol Light Oxide<sup>13</sup></b>	1.909	7.14	7.14	-118	-68	0.0128	737	-175	809
<b>Nitinol Dark Oxide</b>	1.880	7.14	7.16	-490	-487	1.7986	80	-163	567
<b>Nitinol Etched<sup>14</sup></b>	1.944	7.15	7.16	-272	-228	0.0021	367	-333	590
<b>Nitinol Etched, Polished</b>	1.892	7.17	7.22	-227	-180	0.0017	381	N/A	560
<b>CP Ti Gr1</b>	1.706	7.09	7.08	-496	-440	0.0022	N/A	N/A	N/A
<b>Ti 6Al 4V ELI</b>	1.946	7.09	7.10	-428	-350	0.0019	N/A	N/A	N/A
<b>35N LT®-DFT®-41%Ag - Masked</b>	2.002	7.14	7.14	-296	-293	0.0886	N/A	N/A	N/A
<b>35N LT®-DFT®-41%Ag - Unmasked</b>	1.897	7.12	7.11	-281	-277	0.0680	22	N/A	299

<sup>12</sup> Only three of the five samples of the Custom 470 material achieved the E<sub>p</sub> parameter.

<sup>13</sup> Only one of the five samples of the Nitinol Light Oxide material achieved the E<sub>p</sub> parameter.

<sup>14</sup> The Nitinol Etched material did not experience breakdown on three of the five samples. The E<sub>b</sub>, E<sub>p</sub> and E<sub>b</sub>-E<sub>r</sub> values are the result of the two samples that did experience corrosion breakdown.

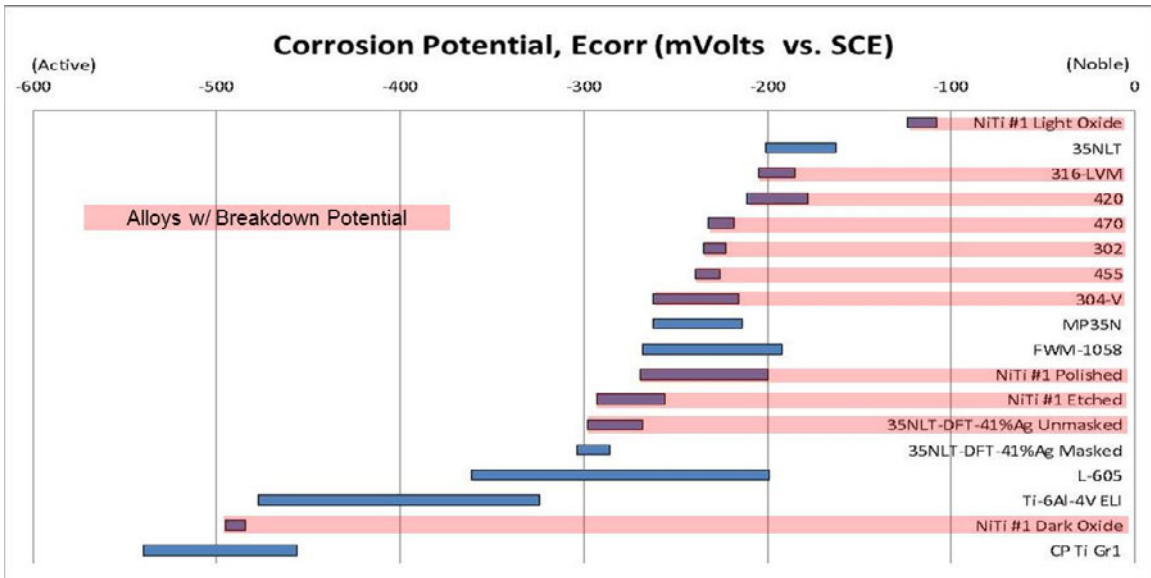


Figure 71. Study Ecorr Series vs. Breakdown Potentials

Figure 71 combines the Ecorr results with the Eb results. By contrasting the sample Ecorr ranking with the result of whether the alloy experienced breakdown or not shows that Ecorr Corrosion Potential values and Eb Breakdown Potentials are not directly related. Figure 72 is a scatterplot of Ecorr vs. Eb confirming that there is not a strong correlation between the two parameters.

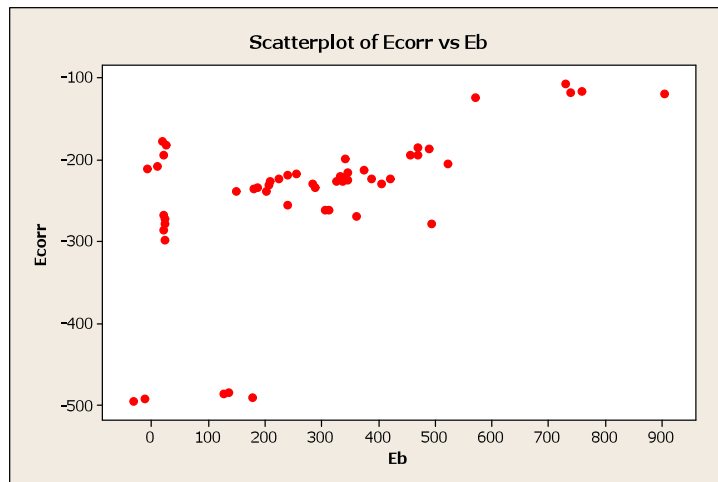


Figure 72. Scatterplot of Ecorr vs Eb.



## References

- [ 1] ASTM F2129. *Standard Test Method for Conducting Cyclic Potentiodynamic Polarization Measurement to Determine the Corrosion Susceptibility of Small Implant Devices*. 2008, Vol. 13.01.
- [ 2] ASTM G82. *Standard Guide for Development and Use of a Galvanic Series for Predicting Galvanic Corrosion Performance*. 1998 (Reapproved 2009), Vol. 03.02.
- [ 3] **Clarke, E. G. and Hickman, J.** Galvanic Series in Equine Serum. *Journal of Bone and Joint Surgery*. 1977, Vol. 35B, p. 467.
- [ 4] **Rosenbloom, S. N. and Corbett, R. A.** An Assessment of ASTM F2129 Electrochemical Testing of Small Medical Implants - Lessons Learned. *NACE Corrosion Conference and Expo*. 2007.
- [ 5] *Assessment of Wrought ASTM F1058 Cobalt Alloy Properties for Permanent Surgical Implants*. **Clerc, C. O., et al., et al.** 1997, John Wiley & Sons, Inc.
- [ 6] *Corrosion Resistance, Chemical Passivation, and Metal Release of 35N LT and MP35N for Biomedical Material Application*. **Ornberg, A., et al., et al.** 9, 2007, Journal of the Electrochemical Society, Vol. 154, pp. C546-C551.
- [ 7] **Pound, Bruce G.** *Corrosion Behaviour of Nitinol in Blood Serum and PBS Containing Amino Acids*. [prod.] Wiley InterScience. s.l. : [www.interscience.wiley.com](http://www.interscience.wiley.com), June 1, 2010.
- [ 8] **Perez, L. M., et al., et al.** *Effect of Nitinol Surface Treatments on Its Physico-chemical Properties*. [prod.] Wiley InterScience. s.l. : [www.interscience.wiley.com](http://www.interscience.wiley.com), 2009.
- [ 9] **Shabalovskaya, S. A.** Surface, Corrosion and Biocompatibility Aspects of Nitinol as an Implant Material. *Bio-Medical Materials and Engineering*. 12 2002, pp. 69-109.
- [ 10] *Laboratory Corrosion Testing of Medical Implants*. **Corbett, R. A.** s.l. : ASM International.
- [ 11] **Corlett, Nigel.** *Corrosion Testing & Performance of Materials for Implantable Medical Devices*. Exponent International Limited. s.l. : White Rose Health Innovation Partnership, 2008.
- [ 12] *Use of Stainless Steels in Medical Applications*. **Murty, Y. V.** Boston : ASM International, 2004. Medical Device Materials: Proceedings of the Materials and Processes for Medical Devices Conference. pp. 287-292.
- [ 13] **Davis, J. R.** *Handbook of Materials for Medical Devices*. Materials Park : ASM International, 2003.
- [ 14] ASTM F899. *Standard Specification for Wrought Stainless Steels for Surgical Instruments*. 2009e1, Vol. 13.01.

- [ 15] ASTM F138. *Standard Specification for Wrought 18Chromium-14Nickel-2.5Molybdenum Stainless Steel Bar and Wire for Surgical Implants (UNS S31673)*. 2008, Vol. 13.01.
- [ 16] ASTM A564/A564M. *Standard Specification for Hot-Rolled and Cold-Finished Age-Hardening Stainless Steel Bars and Shapes*. 2010, Vol. 01.03.
- [ 17] ASTM F1058. *Standard Specificaiton for Wrought 40Cobalt-20Chromium-16Iron-15Nickel-7Molybdenum Alloy Wire and Strip for Surgical Implant Applications (UNS R30003 and UNS R30008)*. 2008, Vol. 13.01.
- [ 18] ASTM F562. *Standard Specification for Wrought 35Cobalt-35Nickel-20Chromium-10Molybdenum Alloy for Surgical Implant Applications (UNS R30035)*. 2007, Vol. 13.01.
- [ 19] ASTM F90. *Standard Specification for Wrought Cobalt-20Chromium-15Tungsten-10Nickel Alloy for Surgical Implant Applications (UNS R30605)*. 2007, Vol. 13.01.
- [ 20] ASTM F2063. *Standard Specification for rought Nickel-Titanium Shape Memory Alloys for Medical Devices and Surgical Implants*. 2005, Vol. 13.01.
- [ 21] ASTM F67. *Standard Specification for Unalloyed Titanium, for Surgical Implant Applications (UNS50250, UNS R50400, UNS R50550, UNS R50700)*. 2006, Vol. 13.01.
- [ 22] ASTM F136. *Standard Specification for Wrought Titanium-6Aluminum-4Vanadium ELI (Extra Low Interstitial) Alloy for Surgical Implant Applications (UNS R56401)*. 2008e1, Vol. 13.01.
- [ 23] ASTM G3. *Standard Practice for Conventions Applicable to Electrochemical Measurements in Corrosion Testing*. 1989 (Reapproved 2010), Vol. 03.02.
- [ 24] Corrosion Montoring Basics. *NACE Resource Center*. [Online] [Cited: Nov 28, 2010.] <http://events.nace.org/library/corrosion/MonitorBasics/corripot.asp>.
- [ 25] *Comparative in vitro performances of bare Nitinol surfaces*. **Shabablovskaya, S., et al., et al.** s.l. : IOS Press, 2008, Bio-Medical Materials and Engineering, Vol. 18, pp. 1-14.
- [ 26] *The Corrosion Behaviour of Nickel Titanium Shape Memory Alloys*. **Rondelli, G., Vicentini, B. and Cigada, A.** 8/9, 1990, Corrosion Science, Vol. 30, pp. 805-812.
- [ 27] *Electrochemical Corrosion Nomenclature*. **Heusler, K. E., Landolt, D. and Trasatti, S.** 1, 1989, Pure and Applied Chemistry, Vol. 61, pp. 19-22.
- [ 28] NACE/ASTM G193. *Standard Terminology Relating to Corrosion and Corrosion Testing*. 2010b, Vol. 03.02.

## ACKNOWLEDGEMENTS

Where to begin.....

I thank the good Lord for an inquisitive mind, still active after all these years.

I thank my dear wife, Katrina, for the patience to endure the pursuit of education goals placed on hold and re-started.

I thank the many staff of Fort Wayne Metals who participated/tolerated this project: Scott Glaze, Mark Michael, Shawn Chaney, Anna Henry, Jeremy Schaffer, among others.

The good folks at IPFW who have been very encouraging, particularly Prof. Paul Lin, Dr. Barry Dupen, Prof. Ramesh Narang and former advisor Dr. Bimal Nepal.

## APPENDICES

### Appendix A. Complete Data Table of Corrosion Measurements

Alloy	Sample No	Surf Area	Avg pH before	Avg pH After	Er	Corr Rate	Eb	Ep	Eb-Er	Ecorr
302	1	1.8442	7.19	7.2	-193	0.026669	288	-247	481	-235
302	2	1.9248	7.2	7.22	-185	0.025492	336	-271	521	-226
302	3	1.8637	7.2	7.21	-187	0.026583	284	-248	471	-230
302	4	1.9631	7.18	7.19	-186	0.023306	388	-248	574	-223
302	5	1.8603	7.19	7.19	-188	0.023975	325	-246	513	-227
304V	1	1.9752	7.15	7.19	-186	0.02483	346	-249	532	-225
304V	2	1.8117	7.18	7.21	-190	0.03509	345	-237	535	-216
304V	3	1.8351	7.12	7.14	-192	0.03271	333	-231	525	-220
304V	4	1.9439	7.08	7.1	-228	0.04077	312	-260	540	-262
304V	5	1.9591	7.06	7.08	-225	0.03296	307	-295	532	-262
316LVM	1	1.8968	7.1	7.15	-141	0.009484	490	-231	631	-187
316LVM	2	1.9442	7.13	7.14	-146	0.01392	457	-227	603	-194
316LVM	3	1.9205	7.14	7.19	-148	0.01446	470	-284	618	-195
316LVM	4	1.8863	7.08	7.12	-154	0.01286	523	-244	677	-205
316LVM	5	1.8217	7.07	7.11	-141	0.01203	470	-240	611	-185
Alloy 420	2	1.8828	7.18	7.18	-163	0.018525	-8		155	-211
Alloy 420	3	1.9111	7.19	7.2	-165	0.017004	10		175	-209
Alloy 420	4	1.9132	7.22	7.21	-150	0.013456	21		171	-195
Alloy 420	5	1.8618	7.19	7.18	-137	0.011694	25		162	-183
Alloy 420	6	1.9561	7.15	7.17	-134	0.010638	20		154	-178
Custom 455®	1	1.9941	7.11	7.13	-201	0.08902	150	-299	351	-239
Custom 455®	2	2.0038	7.1	7.15	-196	0.1016	203	-258	399	-239
Custom 455®	3	1.9765	7.12	7.12	-189	0.08996	209	-245	398	-226
Custom 455®	4	1.933	7.1	7.12	-185	0.04538	187	-275	372	-234
Custom 455®	5	1.9021	7.11	7.12	-187	0.06038	181	-272	368	-236
Micro Melt® Biodur® Custom 470®	1	1.8637	7.07	7.09	-181	0.03528	206		387	-232
Micro Melt® Biodur® Custom 470®	2	1.9895	7.06	7.12	-169	0.03154	225	-255	394	-224
Micro Melt® Biodur® Custom 470®	3	1.9485	7.1	7.12	-165	0.03005	255	-253	420	-218
Micro Melt® Biodur® Custom 470®	4	1.9643	7.07	7.1	-167	0.01916	340	-267	507	-222
Micro Melt® Biodur® Custom 470®	5	1.9257	7.13	7.14	-168	0.01631	239		407	-219

Alloy	Sample No	Surf Area	Avg pH before	Avg pH After	Er	Corr Rate	Eb	Ep	Eb-Er	Ecorr
FWM1058®	1	1.9467	7.18	7.18	-232	0.02411				-246
FWM1058®	2	1.9409	7.12	7.19	-231	0.0126				-253
FWM1058®	3	1.8512	7.11	7.11	-185	0.0519				-192
FWM1058®	4	1.9105	7.11	7.09	-250	0.01228				-268
FWM1058®	5	1.9713	7.13	7.12	-216	0.01315				-233
MP35N®	1	1.947	7.07	7.08	-240	0.08907				-243
MP35N®	2	1.9138	7.1	7.1	-231	0.2525				-246
MP35N®	3	1.996	7.09	7.13	-218	0.1007				-220
MP35N®	4	2.0199	7.07	7.1	-259	0.142				-262
MP35N®	5	2.1765	7.07	7.06	-210	0.08197				-214
35N LT®	1	1.8664	7.09	7.09	-192	0.1252				-194
35N LT®	2	1.9284	7.07	7.09	-199	0.1829				-199
35N LT®	3	1.9172	7.03	7.05	-162	0.1391				-163
35N LT®	4	1.9296	7.06	7.05	-202	0.3228				-201
35N LT®	5	1.919	7.05	7.09	-201	0.3191				-199
L605	1	1.9762	7.08	7.08	-228	0.01484				-232
L605	2	1.8974	7.09	7.12	-229	0.01241				-236
L605	3	1.9278	7.11	7.11	-193	0.01651				-199
L605	4	1.8941	7.14	7.12	-299	0.005992				-304
L605	6	2.0178	7.13	7.11	-345	0.006302				-361
Nitinol Light Oxide	1	1.8804	7.1	7.11	-69	0.01281	904		973	-120
Nitinol Light Oxide	2	1.998	7.15	7.13	-68	0.0132	759		827	-117
Nitinol Light Oxide	3	1.8898	7.16	7.18	-78	0.01325	572	-175	650	-124
Nitinol Light Oxide	4	1.8743	7.16	7.16	-66	0.01247	739		805	-119
Nitinol Light Oxide	5	1.9032	7.12	7.14	-57	0.01215	731		788	-108
Nitinol Dark Oxide	1	1.8324	7.13	7.14	-477	1.03686	136	-156	613	-484
Nitinol Dark Oxide	2	1.8725	7.14	7.14	-487	1.49662	127	-134	614	-486
Nitinol Dark Oxide	3	1.8421	7.15	7.15	-489	1.35562	-31	-152	458	-495
Nitinol Dark Oxide	5	1.9008	7.11	7.14	-490	2.54007	-13	-173	477	-493
Nitinol Dark Oxide	7	1.9502	7.19	7.21	-492	2.56359	179	-199	671	-491
Nitinol Etched	1	1.9382	7.15	7.14	-254	0.002445				-293
Nitinol Etched	2	1.936	7.13	7.12	-227	0.002266				-268
Nitinol Etched	3	1.9637	7.14	7.14	-236	0.002074	494	-333	730	-278
Nitinol Etched	4	1.9491	7.16	7.15	-212	0.001656				-267

Nitinol Etched	5	1.9306	7.18	7.23	- 211	0.001884	239		450	-256
----------------	---	--------	------	------	----------	----------	-----	--	-----	------

Alloy	Sample No	Surf Area	Avg pH before	Avg pH After	Er	Corr Rate	Eb	Ep	Eb-Er	Ecorr
Nitinol Etched, Mechanically Polished	1	1.8506	7.15	7.2	-185	0.001946	406		591	-230
Nitinol Etched, Mechanically Polished	2	1.8758	7.14	7.19	-224	0.001855	362		586	-269
Nitinol Etched, Mechanically Polished	3	1.8293	7.19	7.23	-155	0.001788	341		496	-200
Nitinol Etched, Mechanically Polished	4	1.8977	7.19	7.25	-164	0.001339	374		538	-213
Nitinol Etched, Mechanically Polished	5	2.0063	7.16	7.22	-171	0.00152	420		591	-223
Commercially Pure Titanium Grade 1	1	0.9242	7.11	7.11	-495	0.002641				-474
Commercially Pure Titanium Grade 1	2	1.9345	7.08	7.07	-452	0.002356				-502
Commercially Pure Titanium Grade 1	3	1.9029	7.06	7.06	-408	0.002655				-456
Commercially Pure Titanium Grade 1	5	1.9099	7.08	7.08	-445	0.001336				-506
Commercially Pure Titanium Grade 1	6	1.8594	7.11	7.08	-401	0.001292				-540
Titanium 6Aluminum 4Vanadium ELI	1	1.9759	7.11	7.11	-401	0.001287				-471
Titanium 6Aluminum 4Vanadium ELI	2	1.988	7.1	7.1	-388	0.001285				-464
Titanium 6Aluminum 4Vanadium ELI	3	1.9391	7.1	7.11	-393	0.002091				-477
Titanium 6Aluminum 4Vanadium ELI	4	1.878	7.05	7.05	-320	0.003403				-402
Titanium 6Aluminum 4Vanadium ELI	5	1.9491	7.07	7.14	-249	0.001392				-324
35N LT® DFT®-41Ag Masked	1	2.0084	7.14	7.15	-297	0.12158				-300
35N LT® DFT®-41Ag Masked	2	1.895	7.15	7.14	-292	0.08536				-295
35N LT® DFT®-41Ag Masked	3	1.9832	7.15	7.14	-283	0.07844				-286
35N LT® DFT®-41Ag Masked	4	2.0446	7.15	7.15	-290	0.07986				-293
35N LT® DFT®-41Ag Masked	5	2.0774	7.13	7.13	-301	0.07794				-304
35N LT® DFT®-41Ag Unmasked	1	1.9819	7.06	7.06	-266	0.07721	23		289	-298
35N LT® DFT®-41Ag Unmasked	2	1.9151	7.12	7.12	-282	0.07071	23		305	-278
35N LT® DFT®-41Ag Unmasked	3	1.998	7.13	7.12	-269	0.05849	23		292	-273
35N LT® DFT®-41Ag Unmasked	4	1.7202	7.13	7.12	-275	0.0596	21		296	-287
35N LT® DFT®-41Ag Unmasked	5	1.8685	7.15	7.14	-294	0.07377	21		315	-268

Appendix B. – Wire Mechanical Properties (Imperial Units)

Alloy	Specimen	Ultimate Tensile Strength (psi)	Yield Strength (psi)	Elongation (%)	Modulus (Mpsi)
302	1	300,141	248,358	2.6	20.369
	2	299,654	243,790	2.6	20.729
	3	300,323	245,174	2.6	20.886
	Average	300,039	245,774	2.6	20.661
304V	1	313,728	271,290	2.7	20.793
	2	313,473	256,162	2.9	20.072
	3	312,584	246,030	3.1	20.342
	Average	313,262	257,827	2.9	20.402
316LVM	1	262,784	216,539	3.2	20.470
	2	262,733	217,415	3.1	20.525
	3	262,579	221,250	3.0	20.222
	Average	262,698	218,401	3.1	20.405
420	1	153,446	138,984	3.1	21.562
	2	153,318	140,401	3.4	20.252
	3	153,284	137,909	3.3	20.934
	Average	153,349	139,098	3.3	20.916
Custom 455®	1	207,703	186,510	3.2	21.622
	2	207,460	190,158	2.7	20.495
	3	207,670	187,268	2.7	21.122
	Average	207,611	187,979	2.9	21.080
MicroMelt® Biodur® Custom 470®	1	217,854	200,507	2.3	20.390
	2	217,966	201,833	2.6	20.016
	3	218,114	200,866	2.5	19.806
	Average	217,978	201,069	2.4	20.071



Appendix B. Continued

Alloy	Specimen	Ultimate Tensile Strength (psi)	Yield Strength (psi)	Elongation (%)	Modulus (Mpsi)
FWM 1058®	1	314,563	247,676	3.5	20.346
	2	314,468	244,525	3.5	20.124
	3	314,064	248,942	3.4	19.919
	Average	314,365	247,048	3.5	20.130
MP35N®	1	308,567	264,810	2.9	23.404
	2	308,299	259,632	2.8	23.332
	3	308,209	262,237	2.9	23.413
	Average	308,358	262,226	2.9	23.383
35N LT®	1	305,227	261,914	2.7	21.892
	2	305,405	263,524	3.0	22.274
	3	305,290	260,387	3.2	22.442
	Average	305,307	261,942	2.9	22.203
L605	1	308,987	238,379	4.3	23.353
	2	309,510	242,118	4.7	23.423
	3	309,595	246,929	4.3	23.436
	Average	309,364	242,475	4.4	23.404
CP Ti Gr1	1	109,867	83,832	5.3	11.818
	2	110,035	88,237	5.8	10.974
	3	110,113	84,845	5.3	11.785
	Average	110,005	85,638	5.5	11.526
Ti 6Al 4V ELI	1	186,618	139,140	3.4	12.022
	2	186,520	140,172	4.5	12.063
	3	186,472	139,031	4.1	12.075
	Average	186,537	139,448	4.0	12.053
35N LT®-DFT®-41%Ag	1	185,902	165,795	1.9	16.049
	2	187,070	165,051	2.4	16.776
	3	187,107	166,075	2.3	16.623
	Average	186,693	165,641	2.2	16.483

Appendix C. – Wire Mechanical Properties (SI Units)

Alloy	Specimen	Ultimate Tensile Strength (Mpa)	Yield Strength (Mpa)	Elongation (%)	Modulus (Gpa)
302	1	2,069	1,712	2.6	140.439
	2	2,066	1,681	2.6	142.919
	3	2,071	1,690	2.6	144.005
	Average	2,069	1,695	2.6	142.454
304V	1	2,163	1,870	2.7	143.365
	2	2,161	1,766	2.9	138.388
	3	2,155	1,696	3.1	140.252
	Average	2,160	1,778	2.9	140.668
316LVM	1	1,812	1,493	3.2	141.132
	2	1,811	1,499	3.1	141.514
	3	1,810	1,525	3.0	139.424
	Average	1,811	1,506	3.1	140.690
420	1	1,058	958	3.1	148.663
	2	1,057	968	3.4	139.635
	3	1,057	951	3.3	144.331
	Average	1,057	959	3.3	144.210
Custom 455®	1	1,432	1,286	3.2	149.075
	2	1,430	1,311	2.7	141.309
	3	1,432	1,291	2.7	145.633
	Average	1,431	1,296	2.9	145.339
MicroMelt® Biodur® Custom 470®	1	1,502	1,382	2.3	140.587
	2	1,503	1,392	2.6	138.003
	3	1,504	1,385	2.5	136.556
	Average	1,503	1,386	2.4	138.382
FWM 1058®	1	2,169	1,708	3.5	140.280
	2	2,168	1,686	3.5	138.748
	3	2,165	1,716	3.4	137.339
	Average	2,167	1,703	3.5	138.789

Alloy	Specimen	Ultimate Tensile Strength (Mpa)	Yield Strength (Mpa)	Elongation (%)	Modulus (Gpa)
MP35N®	1	2,127	1,826	2.9	161.364
	2	2,126	1,790	2.8	160.871
	3	2,125	1,808	2.9	161.427
	Average	2,126	1,808	2.9	161.221
35N LT®	1	2,104	1,806	2.7	150.938
	2	2,106	1,817	3.0	153.575
	3	2,105	1,795	3.2	154.733
	Average	2,105	1,806	2.9	153.082
L605	1	2,130	1,644	4.3	161.011
	2	2,134	1,669	4.7	161.495
	3	2,135	1,703	4.3	161.588
	Average	2,133	1,672	4.4	161.365
CP Ti Gr1	1	758	578	5.3	81.485
	2	759	608	5.8	75.663
	3	759	585	5.3	81.256
	Average	758	590	5.5	79.468
Ti 6Al 4V ELI	1	1,287	959	3.4	82.891
	2	1,286	966	4.5	83.168
	3	1,286	959	4.1	83.251
	Average	1,286	961	4.0	83.104
35N LT®-DFT®-41%Ag	1	1,282	1,143	1.9	110.657
	2	1,290	1,138	2.4	115.669
	3	1,290	1,145	2.3	114.613
	Average	1,287	1,142	2.2	113.646

Appendix D. – Nitinol Wire Mechanical Properties (Imperial Units)

Alloy	Specimen	Ultimate Tensile Strength (psi)	Upper Plateau Strength (psi)	Lower Plateau Strength (psi)	Elongation (%)	Modulus (Mpsi)
NiTi#1 Dark	1	219,768	84,586	26,615	16.2	6.905
	2	219,546	80,676	26,067	16.1	6.763
	3	219,620	85,215	28,331	16.2	7.337
	Average	219,644	83,492	27,004	16.2	7.002
NiTi#1 Etched	1	216,269	81,666	26,838	15.9	7.415
	2	216,194	83,398	27,485	16.0	7.961
	3	216,118	86,033	28,406	15.9	8.187
	Average	216,194	83,699	27,576	15.9	7.854
NiTi#1 Light	1	212,405	82,346	24,753	15.6	8.296
	2	212,344	83,834	25,228	15.6	8.775
	3	212,619	78,745	24,297	15.4	8.631
	Average	212,456	81,642	24,759	15.5	8.567
NiTi#1 Polished	1	220,699	80,576	24,696	16.2	7.493
	2	220,548	81,489	23,617	16.1	7.678
	3	220,548	84,350	27,103	16.2	7.406
	Average	220,599	82,138	25,138	16.2	7.526

Appendix E. – Nitinol Wire Mechanical Properties (SI Units)

Alloy	Specimen	Ultimate Tensile Strength (Mpa)	Upper Plateau Strength (Mpa)	Lower Plateau Strength (Mpa)	Elongation (%)	Modulus (Gpa)
NiTi#1 Dark	1	1,515	583	184	16.2	47.608
	2	1,514	556	180	16.1	46.629
	3	1,514	588	195	16.2	50.587
	Average	1,514	576	186	16.2	48.277
NiTi#1 Etched	1	1,491	563	185	15.9	51.125
	2	1,491	575	190	16.0	54.889
	3	1,490	593	196	15.9	56.447
	Average	1,491	577	190	15.9	54.151
NiTi#1 Light	1	1,464	568	171	15.6	57.199
	2	1,464	578	174	15.6	60.501
	3	1,466	543	168	15.4	59.509
	Average	1,465	563	171	15.5	59.067
NiTi#1 Polished	1	1,522	556	170	16.2	51.662
	2	1,521	562	163	16.1	52.938
	3	1,521	582	187	16.2	51.063
	Average	1,521	566	173	16.2	51.890